UNIVERSITY OF HAWAII
LIBRARY
FEB 19 '53

ADVANCES IN PHYSICS

A QUARTERLY SUPPLEMENT of the PHILOSOPHICAL MAGAZINE

EDITOR
PROFESSOR N. F. MOTT, M.A., D.Sc., F.R.S.

EDITORIAL BOARD
SIR GEORGE THOMSON, M.A., D.Sc., F.R.S.
PROFESSOR A. M. TYNDALL, C.B.E., D.Sc., F.R.S.
SIR LAWRENCE BRAGG, O.B.E., M.C., M.A., D.Sc., F.R.S.

VOLUME 2 JANUARY 1953 NUMBER 5

PRICE per part 15*s.* 0*d.*
PRICE per annum £2 15*s.* 0*d.* post free

PRINTED AND PUBLISHED BY TAYLOR & FRANCIS LTD.
RED LION COURT, FLEET ST., LONDON E.C.4

QC1
A36

MONOGRAPHS ON THE PHYSICS AND CHEMISTRY OF MATERIALS

General Editors

WILLIS JACKSON, H. FRÖHLICH, N. F. MOTT

This series is intended to summarize the recent results of academic or long-range research in materials and allied subjects, in a form that should be useful to physicists in Universities and in Government and industrial laboratories

Already Published

DETONATION IN CONDENSED EXPLOSIVES
By J. TAYLOR 25*s. net*

FERROMAGNETIC PROPERTIES OF METALS AND ALLOYS
By K. HOSELITZ 40*s. net*

THE HARDNESS OF METALS
By D. TABOR 15*s. net*

THE PHOTOGRAPHIC STUDY OF RAPID EVENTS
By W. D. CHESTERMAN 25*s. net*

DIELECTRIC BREAKDOWN OF SOLIDS
By S. WHITEHEAD 25*s. net*

WAVE THEORY OF ABERRATIONS
By H. H. HOPKINS 17*s.* 6*d. net*

PHYSICAL PROPERTIES OF GLASS
By J. E. STANWORTH 21*s. net*

MULTIPLE-BEAM INTERFEROMETRY OF SURFACES AND FILMS
By S. TOLANSKY 21*s. net*

METAL RECTIFIERS
By H. K. HENISCH 18*s. net*

THE PHYSICS OF RUBBER ELASTICITY
By L. R. G. TRELOAR 30*s. net*

THEORY OF DIELECTRICS:
DIELECTRIC CONSTANT AND DIELECTRIC LOSS
By H. FRÖHLICH 25*s. net*

LUMINESCENT MATERIALS
By G. F. J. GARLICK 30*s. net*

OTHER VOLUMES ARE IN ACTIVE PREPARATION

OXFORD UNIVERSITY PRESS

CONTENTS

5807-22

ADVANCES IN PHYSICS

A QUARTERLY SUPPLEMENT

of the

PHILOSOPHICAL MAGAZINE

VOLUME 2 JANUARY 1953 NUMBER 5

The Unsaturated Helium Film

By EARL LONG and LOTHAR MEYER
Institute for the Study of Metals, The University of Chicago,
Chicago, Illinois, U.S.A.

§1. INTRODUCTION

LIQUID helium at the temperature 2·19° K, denoted by T_λ, undergoes a remarkable transformation, usually called the λ-transformation, owing to the form of the specific heat curve. Above T_λ, the modification He I behaves like an ordinary condensed rare gas, as would be expected, except for the pronounced influence of the zero-point energy, especially on the density and heat of vaporization. Below T_λ, however, the modification He II shows an enormous heat conductivity, its viscosity is under certain conditions immeasurably small, it shows the 'fountain effect', i.e., hydrostatic pressure differences caused by temperature gradients, the so-called second sound, or temperature waves within the liquid, and the phenomenon of the 'film', an unusually thick layer covering all surfaces in contact with saturated vapour, and displaying an amazing mobility. These properties are all treated in detail in the recent review articles of Dingle (1952) and Atkins (1952).

The purpose of this discussion is to survey the investigations of surface layers of helium which are thinner than the 'film', in that such thin layers are in contact, not with saturated vapour at P_0, the vapour pressure of the bulk liquid, but rather with vapour at a pressure P which is smaller than P_0. There arises the interesting question whether or not He II properties appear also in these unsaturated films, and if such properties do appear, how they compare with those of the bulk liquid.

It was hoped that knowledge of the behaviour of these thin films would throw light on the problem of the influence of the wall on the condensed He II phase, but, as will be seen from the subsequent discussions, the experiments have yielded results which, though in themselves quite interesting, are at present somewhat inexplicable in terms of the present state of knowledge of the He II problem.

§2. The Adsorption Process

Such thin films cannot of course be obtained without adsorption, which is merely the condensation of He atoms from the gas phase onto a wall, due to the attractive forces of the wall. In this discussion we consider only physical adsorption on non-porous substrates, at temperatures in the liquid helium range, and thus ignore a considerable literature on the adsorption of helium on charcoal and similar porous adsorbents ; in such cases the adsorbed helium cannot be expected to exist in a state similar to that of the saturated film on a surface, but probably rather more like that of liquid helium in very fine capillaries.

The adsorption of gases on solids has been treated in detail by Brunauer (1945). It is customary to describe the process in terms of adsorption isotherms, in which v, the volume of gas adsorbed per unit surface area, is plotted against the *saturation* P/P_0, where P is the pressure of the gas in equilibrium with the adsorbed phase, and P_0 is the saturated vapour pressure at the same temperature.

For non-porous adsorbents and gases such as the rare gases or nitrogen, the isotherm has the sigmoid form shown in fig. 1. At very low saturations, the forces of the wall cause a considerable amount of gas to be held, producing the steeply rising branch of the isotherm, starting at the origin. Then, when the wall is covered with one layer of adsorbate, any further adsorption is possible only in a second or higher layer. (There is, of course, no sharp distinction between these, since all layers are statistical, but it is convenient and qualitatively correct to discuss the adsorbed film in this manner.) The forces of the wall, being van der Waals in nature, decrease with the third power of the distance ; consequently, the second and higher layers are held by much weaker forces. The isotherm therefore bends over sharply, and becomes rather flat after completion of the first layer, since, in order to increase the coverage, the saturation P/P_0 must be increased considerably. The ' point ' at which the isotherm bends over on completion of the first adsorbed layer is customarily called point ' B ', and is usually estimated to lie around 10–15% saturation. The adsorption isotherm rises steeply again when the saturation P/P_0 approaches unity. Under these conditions, interactions between the adsorbed molecules themselves become dominant, and lead finally to ordinary condensation at $P/P_0=1$.

Of the numerous thermodynamic and statistical theories of physical adsorption, we mention here the early derivation of Langmuir (1918) which treated only coverages up to a mono-layer. Langmuir calculated the distribution of molecules between the gas phase and a given number of sites on the surface on which the molecules are held by an adsorption energy being the same for all available sites. This leads to an isotherm of the form :

$$\frac{v}{v_m}=\frac{bP}{1+bP}, \quad \ldots\ldots\ldots \quad (1a)$$

or

$$\frac{P}{v}=\frac{1}{v_m b}+\frac{P}{v_m}, \quad \ldots\ldots\ldots \quad (1b)$$

where b is a constant depending on the heat of adsorption, and v_m the amount adsorbed when all sites are occupied and the surface thus covered with just one layer.

Brunauer, Emmet and Teller (1938) treated the case that second and higher layers can be formed yielding the so-called BET isotherm,

$$\frac{P}{v(P_0-P)} = \frac{1}{v_m C} + \frac{C-1}{v_m C}\frac{P}{P_0}, \quad \ldots\ldots (2)$$

where the term C is related to the heat of adsorption, and v_m has the same significance as before. Equations (2) and (1 b) become identical

Fig. 1

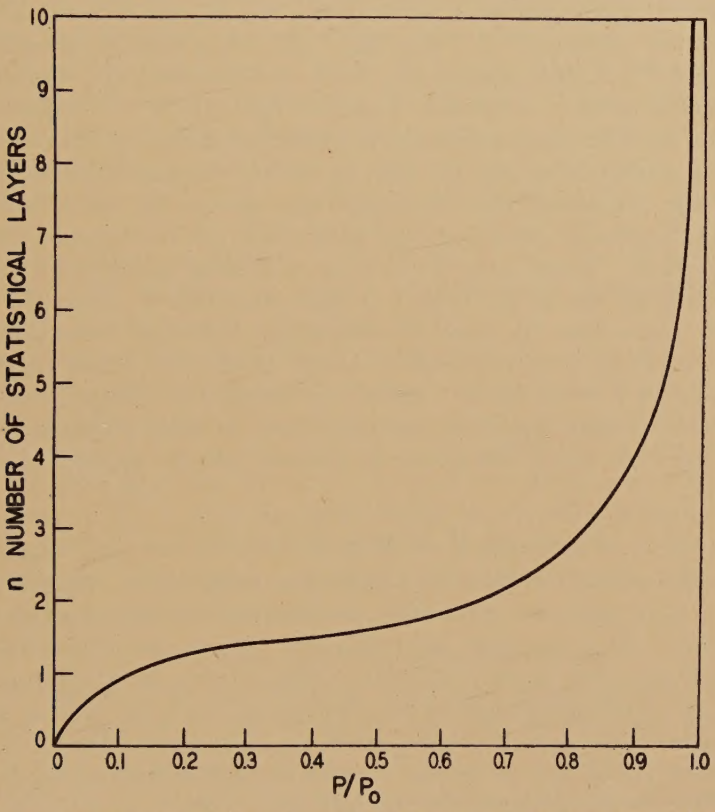

Typical adsorption isotherm for physical adsorption on non-porous adsorbents : Amount adsorbed in numbers of statistical layers as a function of the saturation P/P_0.

at low saturations, since $P_0-P \sim P_0$ under these conditions. Equation (2) has been extensively tested for various cases of non-porous adsorbents and a number of gases. In particular, the adsorption of nitrogen has been so carefully investigated that it may be used with some confidence to determine the surface areas of adsorbents by determining v_m for nitrogen from the BET equation, and then using the normal liquid density

of nitrogen to obtain a molecular spacing from which the surface area can be derived. Although there are deviations from the BET equation above 20 to 40% saturation, it may be used with some confidence at lower saturations to determine v_m, and thus deductions concerning spacings in the first adsorbed mono-layer can be made. (Compare P. H. Emmet 1948, and McMillan and Teller 1951.)

In order to have an understanding of the unsaturated helium film behaviour, particularly in the He II region, it will be necessary to consider the adsorption of helium in some detail.

(*a*) *The Adsorption of Helium at Low Saturations*

The early work on the adsorption of helium on solids (glass, and glass covered with condensed gases, such as H_2, Ne, N_2, and O_2) was performed at quite low pressures (<1 mm Hg), and consequently at saturations well below 1%. The preliminary work of Keesom and Schmidt (1933) was followed by that of Keesom and Schweers (1941). The data showed that even at these low saturations a considerable adsorption occurs.

The adsorption of a rare gas such as helium should, at low saturations, be the case nearest to the conditions assumed in the derivation of the Langmuir isotherm ; however, the data could not be fitted to the Langmuir equation. From later work, to be described in the next section, it was found that the v_m for helium is quite anomalous ; also, the data of Schweers show that the heat of adsorption decreases from almost 100 cal/mole at about 10% coverage to about 40 cal/mole when approaching completion of a mono-layer. Since the Langmuir equation assumes no interaction between adsorbed particles (heat of adsorption independent of coverage) obviously the isotherm cannot then be applied to the case of helium.

(*b*) *Multi-layer Adsorption*

Later work was devoted to multi-layer adsorption. Frederikse and Gorter (1950) measured isotherms on jeweller's rouge (Fe_2O_3) and on steel from 1·39° K to 2·26° K ; Schaeffer, Smith and Wendell (1949) measured isotherms on two different carbon adsorbents at the bp ; Long and Meyer (1949) investigated adsorption on Fe_2O_3 at 1·53 to 2·45° K ; Mastrangelo and Aston (1951) reported an isotherm on TiO_2 at 2·41° K ; and Strauss (1952) has measured a series of eight isotherms on Fe_2O_3, at temperatures ranging from 1·59° to 4·21° K.

Schaeffer, Smith and Wendell were the first to derive v_m, the quantity adsorbed in the first layer. They determined the surface areas of their carbon adsorbents from adsorption isotherms of nitrogen, for which v_m is well known. Using this as a comparison, they found that v_m for helium at the bp is far greater than that calculated from their surface area and the cross-section of the helium atom, as derived from the density of liquid helium. In almost all other cases, these two values differ for spherical molecules by only a few per cent.

The subsequent data of Frederikse and Gorter (1950) and of Long and Meyer (1949) for adsorption on Fe_2O_3 confirmed these results. The density of adsorbed helium in the first mono-layer is much higher than that of the liquid at the same temperature. At temperatures below 2° K, values up to four times the liquid density were observed ; in liquid helium the spacing of helium atoms is approximately 4 Å, whereas in the first adsorbed layer it is reduced to values as low as 2 Å, corresponding roughly to the gas kinetic diameter of 2·1 Å. The various values of v_m and their corresponding atomic spacings are shown in table 1, expanded from a similar table by Frederikse (1950).

The abnormally large atomic spacing in liquid helium is due to the zero-point energy.* In the adsorbed film, interaction with the wall, much stronger than the van der Waals forces of helium–helium interaction, overcomes the repulsive action of the zero-point energy, so that the first film layer is compressed to about the gas-kinetic diameter, i.e., the diameter of the electronic shell of the helium atom.† As a consequence on filling up the first layer, the repulsive action of the zero-point energy must counteract more and more the atttractive forces of the wall, and thus the effective heat of adsorption should drop strongly as the first layer becomes occupied. This argument is borne out by the data of Schweers, previously mentioned. Evidently in the case of helium, the zero-point energy provides an energy of interaction of the same order of magnitude as the heat of adsorption itself.

On completion of the first layer, the forces of the wall are to a great extent balanced by the zero-point energy, and the heat of adsorption is then only slightly higher than the heat of vaporization of bulk liquid. It is not surprising that v_m appears to be dependent on temperature, in spite of the fact that the forces of the wall are great compared to kT. This is shown in fig. 2, from the data of Strauss, for adsorption on Fe_2O_3.

Mastrangelo and Aston (1951) propose an interpretation of the adsorption data which is based on the assumption that several solid layers are formed instead of one very dense mono-layer.

(c) *Adsorption at Intermediate Saturations*

It was evident from the data of Long and Meyer (1949) that the adsorption of helium in the He II region, and between 15 and 80%

---

* See discussion by Dingle (1952).

† The BET theory assumes that the site of an adsorbed atom in the first layer is a potential site for atoms in the higher layers. If, however, the first layer is of much higher density than the liquid, and therefore than that of higher layers (which must rapidly approach liquid density, provided the attractive forces are van der Waals in origin) then it contains more atoms per unit surface area than the next higher layer can accomodate. Band (1949, 1951) showed, however, that even in this case it is justified to use the formalism of the BET theory in deriving v_m. Compare also O. Theimer, 1952, *Trans. Faraday Soc.* **48,** 326.

Application of the BET theory to the original data of Keesom and Schweers (1941) leads also to the same qualitative result for v_m. See table 1.

saturation, was only slightly temperature-dependent. They concluded, therefore, that the heat of adsorption for these coverages cannot differ much from the heat of vaporization, and since the adsorbed film is in equilibrium with a gas phase at a pressure $P<P_0$, the entropy of the adsorbed film must in consequence be higher than that of the bulk liquid (see eqn. 7, below).

Let μ be the chemical potential, let the subscript g denote the gas phase, f the adsorbed film, and l the bulk liquid. S is the molar entropy, H the molar heat content, and T the temperature. A bar above S or H

Table 1

T (° K)	v_m (c.c. $(SPT)/m^2$)	d (Å)	Adsorbent	Author
4·2	0·48	2·9	Glass	Keesom and Schweers (1941)
1·6	0·97	2·0		
1·2	1·06	1·9		
4.2	0·49	2·8	Carbon	Schaeffer, Smith, and Wendell (1949)
below 2.2	1·0–0·71	2·0–2·4	Steel	Frederikse (1950)
below 2.2	0·83	2·2	Jeweller's rouge pressed	
below 2·2	0·83	2·2	Jeweller's rouge pressed	Long and Meyer (1949)
4·2	0·58	2·6	Jeweller's rouge hand-packed	Strauss (1952)
2·1	0·74	2·3		
1·6	0·78	2·2		
4·2	(0·24)*	4·2	(Bulk liquid)	W. H. Keesom (1942)
below 2·2	(0·25)*	4·0		

* Monolayer with density of liquid.

means a differential molar value. Then we have, assuming the gas to be ideal (justified below the lambda-point, since P is less than 4 cm Hg) :

$$\mu_f=\overline{H}_f-T\overline{S}_f=\mu_g{}^P=H_g-TS_g{}^P, \quad . \quad . \quad . \quad . \quad . \quad (3a)$$

$$\mu_l=H_l-TS_l=\mu_g=H_g-TS_g{}^0, \quad . \quad . \quad . \quad . \quad . \quad (3b)$$

or

$$T(S_l-S_g{}^0)=\Delta H^0, \quad . \quad . \quad . \quad . \quad . \quad . \quad (4a)$$

$$T(S_f-S_g{}^P)=\overline{\Delta H}_f, \quad . \quad . \quad . \quad . \quad . \quad . \quad (4b)$$

or

$$S_f-S_l=\frac{1}{T}(\overline{\Delta H}_f-\Delta H_0)+S_g{}^P-S_g{}^0. \quad . \quad . \quad . \quad . \quad (5)$$

Since

$$S_g{}^0-S_g{}^P=R\log\frac{P}{P_0}, \quad . \quad . \quad . \quad . \quad . \quad . \quad . \quad (6)$$

we get

$$\overline{S}_f-S_l=\frac{1}{T}(\overline{\Delta H}_f-\Delta H_0)-R\log\frac{P}{P_0}. \quad . \quad . \quad . \quad . \quad . \quad (7)$$

Using the Clausius–Clapeyron equation

$$\Delta H = RT^2 \frac{\partial \log P}{\partial T}$$

yields

$$\overline{S}_f - S_l = -RT \frac{\partial \log (P/P_0)}{\partial T} - R \log \left(\frac{P}{P_0}\right)$$

$$= -\frac{\partial}{\partial T}\left\{RT \log \left(\frac{P}{P_0}\right)\right\}. \quad \ldots\ldots \quad (8)$$

In order to properly estimate the film behaviour from such a thermodynamic treatment, a number of carefully measured isotherms is needed. The most extensive investigations is that of Strauss (1952)* whose isotherms are shown in fig. 3. Figure 4 shows plots of $\log P$ *vs* $1/T$ for a

Fig. 2

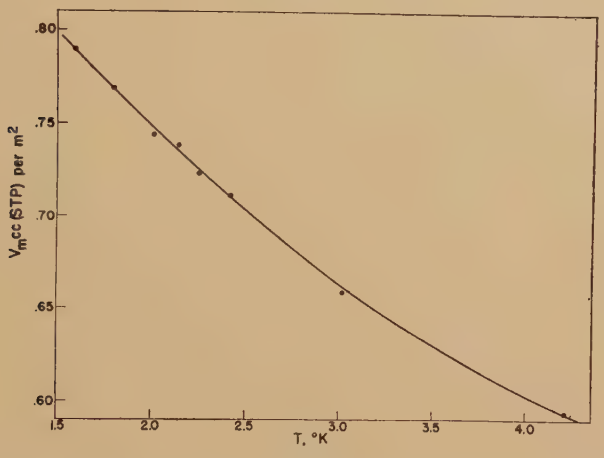

v_m=the amount of helium adsorbed on jeweller's rouge in the first statistical layer as a function of temperature (Strauss 1952).

number of constant coverages. Figure 5 shows some of the heats of adsorption derived therefrom, plotted against temperature at various constant coverages. Figure 6 shows the variation of heat of adsorption with coverage, at two different temperatures. In fig. 7 is shown the entropy difference $\overline{S}_f - S_l$, as defined by eqn. (8). It will be noted that above the λ-point the entropies and heats of adsorption are 'normal', while in the He II region they show anomalous values. Above the λ-point, the differential entropy of the adsorbed film is, as usual, lower than that of the bulk liquid, because the adsorbate attains a higher

* The absolute values of the adsorption data of Strauss differ from those of Frederikse and Gorter (1950) and of Long and Meyer (1949) despite the fact that he used the same jeweller's rouge as did Long and Meyer. This difference seems to be due to the fact that Long and Meyer, and also Frederikse, compressed the rouge, whereas Strauss worked with hand-packed adsorbent.

degree of order than does the liquid.* Below the λ-point, however, the entropy of the adsorbed film shows values distinctly higher than that of

Fig. 3

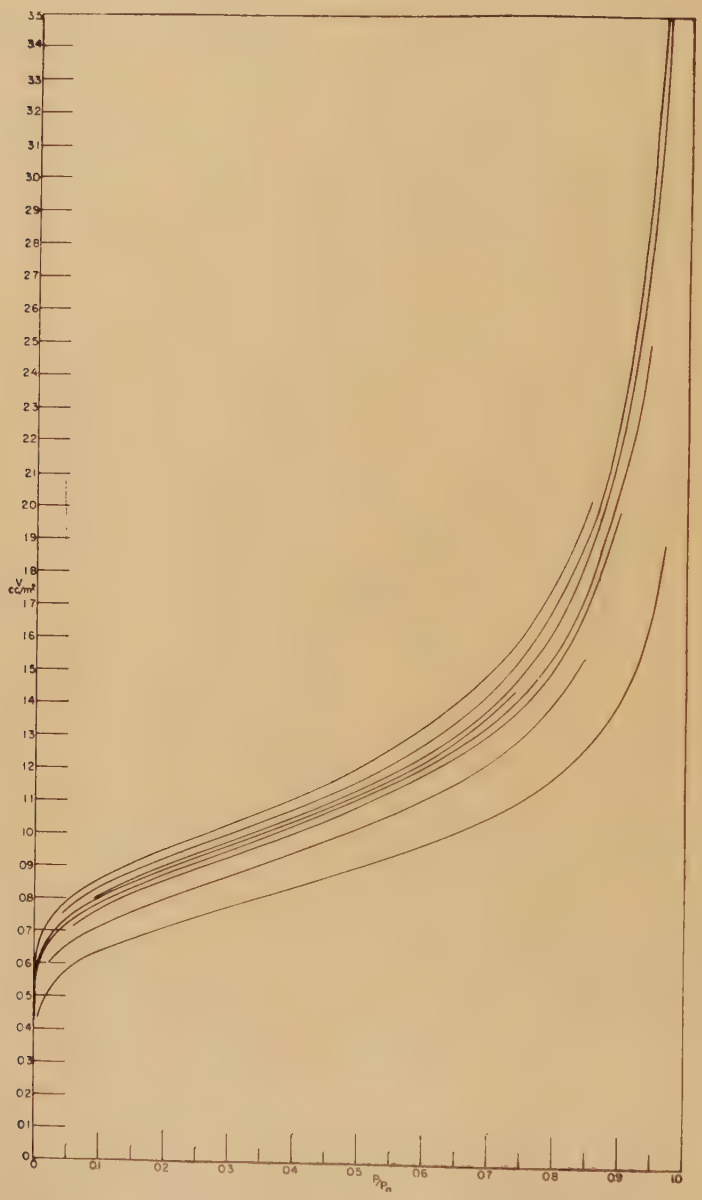

Adsorption isotherms of helium on jeweller's rouge in c.c.$(SPT)/m^2$ as a function of saturation at 4·21° K—lowest curve; 3·02°, 2·42°, 2·25°, 2·14°, 2·01° 1·80°, and 1·59°—top curve (Strauss 1952).

* Compare C. Kemball, 1950, Entropy of Adsorption, in *Advances in Catalysis*, Vol. II (New York: Academic Press).

the bulk liquid. The peculiar ordering process which occurs in He II below T_λ appears therefore to be less developed in the adsorbed layers than in bulk liquid helium.*

Fig. 4

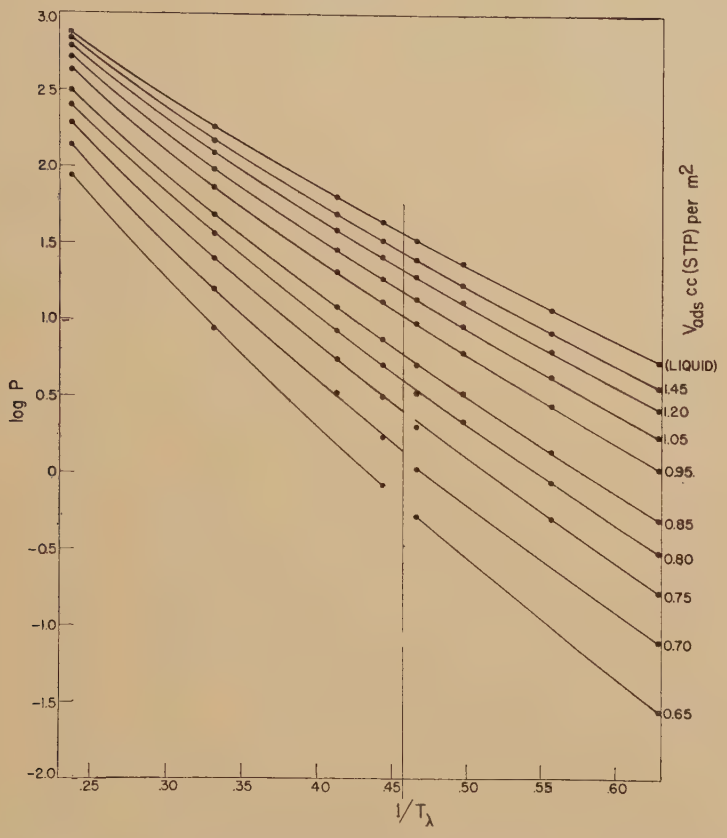

Log P at constant amount adsorbed as function of $1/T$ derived from the isotherms of fig. 3 (Strauss 1952).

---

* Gorter and Frederikse (1949) derived the relatively high entropy of the adsorbate by combining the BET isotherm with eqn. (8). But, in the derivation of the BET equation, it was assumed (in order to simplify the mathematical treatment) that the heat of adsorption of the second and all higher layers is equal to the heat of vaporization of the bulk liquid. The first term on the right-hand side of eqn. (7) is therefore *a priori* zero, and $\overline{S}_f - S_l$ positive, since $P < P_0$; this result is purely a consequence of the simplifying assumption of the theory. In reality, the heat of adsorption of the second and higher layers must always be higher than the heat of vaporization; this usually overcompensates the positive contribution of the $R \log P/P_0$ term of eqn. (7). Note fig. 6, in which the heat of adsorption is plotted against the coverage; the values start at about the completion of the first layer—a value of 0·4 cm³ represents approximately the volume adsorbed in the second layer, and 0·25 cm³ may be taken for each additional layer, in first approximation.

Frederikse and Gorter (1950) also derived $\overline{S}_f - S_l$ from their adsorption measurements. Their values agree well qualitatively with those of Strauss, showing in particular that the entropy of the adsorbed layers is higher than that of the bulk liquid in the He II region. However, the absolute values of $S_f - S_l$ (up to 4 cal/mol deg) seem to be rather high, considering that the destruction of the He II ordering process in bulk liquid produces only about $1\frac{1}{2}$ entropy units, which is the entropy of the bulk liquid at the λ-point.

Fig. 5

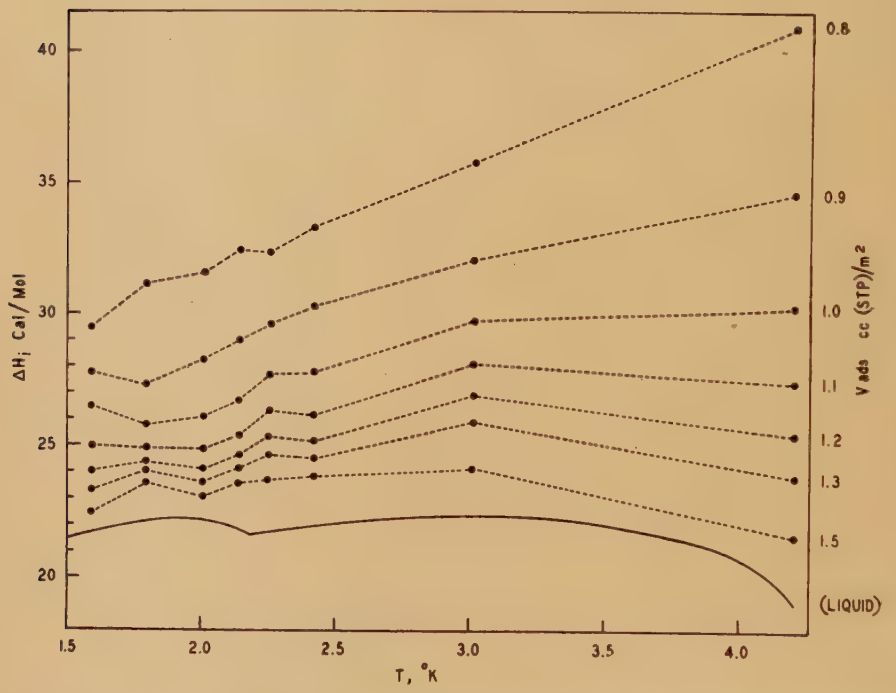

Heat of adsorption ΔH_f of helium on jeweller's rouge in cal/mol at constant amount adsorbed as a function of temperature for different amounts adsorbed (Strauss 1952).

Mastrangelo and Aston (1951) report a ' kink ' occurring at $P/P_0 \sim 0{\cdot}45$ in their measurements of the adsorption isotherm of helium on TiO_2 at 2·41° K, which they assume is due to the formation of an additional adsorbed layer. It is difficult to understand how such a kink could occur, unless it were due to a first-order transition in the adsorbed phase, not observed in any of the other measurements on adsorbed helium films. Also, the careful measurements of Strauss, including one isotherm at 2·42° K (on Fe_2O_3) fail to reveal any indication of similar behaviour.

(*d*) *The Adsorption at High Saturations*

The first attempt to measure the thickness of the helium film by adsorption measurements near saturation was made by Kistemaker (1947). He used a glass vessel with a number of sealed-in glass rods, designed in such a way that capillary condensation was practically prevented. His original conclusion, that the He II film is only about 30 atomic layers thick, was incorrect, due to an error in evaluation. A re-examination of his data by Frederikse and Kistemaker (see Frederikse 1950, p. 60) led to a value of about 150 atomic layers. In this evaluation, the slope of Kistemaker's adsorption isotherms had to be estimated,

Fig. 6

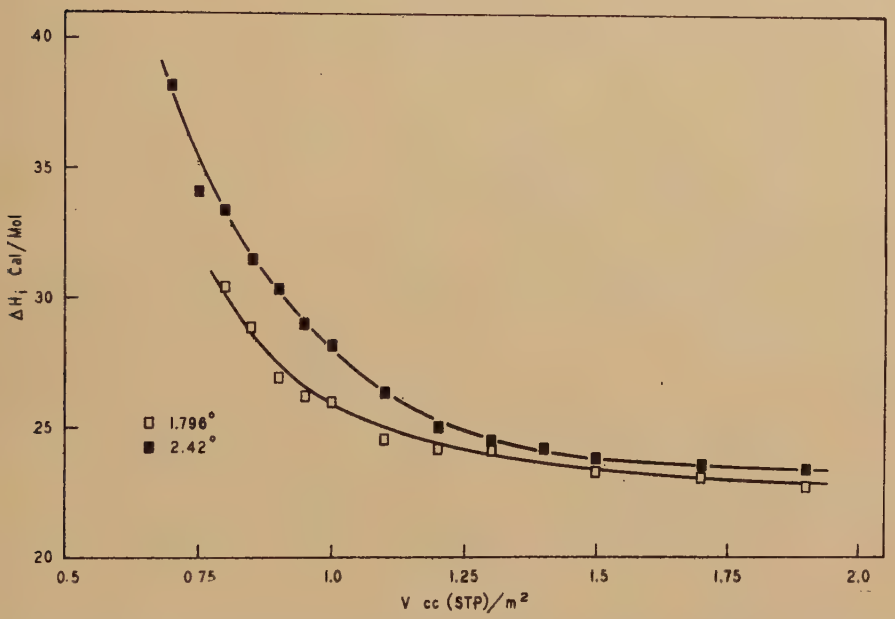

Heat of adsorption ΔH_f of helium adsorbed on jeweller's rouge in cal/mol as a function of the amount adsorbed, at constant temperature (Strauss 1952).

introducing, of course, a great uncertainty. However, it is easily derived from Kistemaker's original data on the pressures in the adsorption cell that the film must be several times the 30 atomic layers originally stated.

Long and Meyer (1949) followed the adsorption of helium on Fe_2O_3 to very high saturations in the He II region and reported about 150 atomic layers at pressures just below saturation. In this case, however, the possibility of capillary condensation cannot be ignored, so that the reported value should be somewhat less reliable than that derived from Kistemaker's work.

It seems from this evidence that the He II film, at pressures at or very near saturation, has a thickness not greatly different from that of the film in contact with bulk liquid. An accurate determination, however, has not yet been carried out.

§3. Specific Heat of the Unsaturated Film

Frederikse (1949, 1950) in a careful and exacting series of experiments, measured the specific heat of helium adsorbed on Fe_2O_3 at coverages between 6% and 80% saturation, corresponding to about $\frac{1}{2}$ to 8 atomic layers. The data are summarized in fig. 8.

Fig. 7

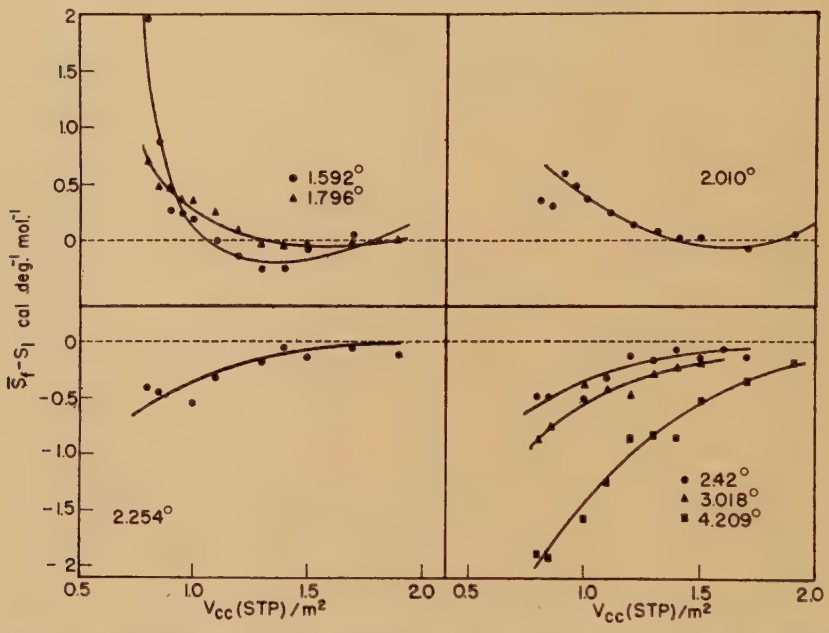

Difference between differential entropy $\bar{S}_f$ of helium adsorbed on jeweller's rouge and the entropy S_l of bulk liquid helium as a function of the amount adsorbed for different temperatures (Strauss 1952).

So long as the amount adsorbed does not exceed one statistical layer, the specific heat curve shows no anomalies, and follows roughly a T^2 law, suggesting that the first layer is like a two-dimensional Debye solid (Band 1949). At higher coverages, a more and more pronounced maximum appears, first at temperatures well below the λ-point of the bulk liquid, and rapidly approaching that temperature as the coverage is increased.

A direct quantitative comparison of these data with the entropy values derived from adsorption measurements is difficult. The adsorption data yield differential molar quantities, whereas the specific heat data of Frederikse represent integral or average values. The measurements,

although an achievement in themselves, are unfortunately not sufficiently accurate to allow the necessary differentiation for direct comparison with adsorption data.

Fig. 8

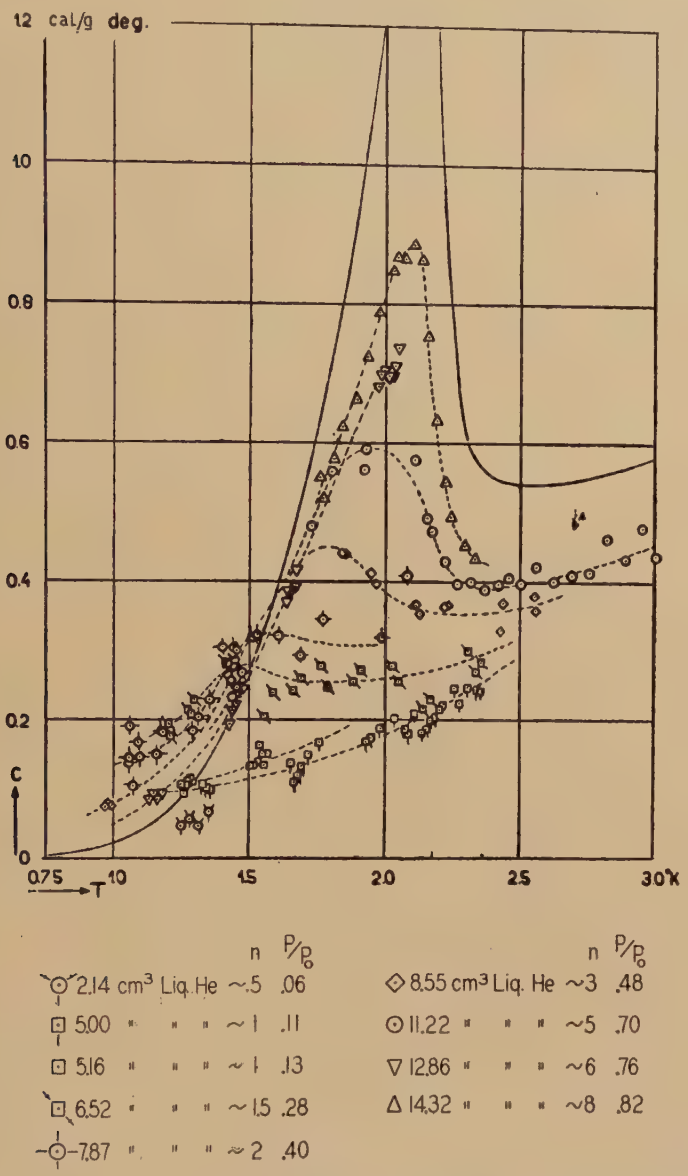

Average specific heat of helium adsorbed on jeweller's rouge in cal/g deg as a function of temperature for different amounts adsorbed. Number of statistical layers estimated as: 1st layer $= v_m$; 2nd layer $= \frac{1}{2} v_m$; 3rd and higher layer = liquid density $= \frac{1}{4} v_m$. Drawn line specific heat of bulk liquid helium (Frederikse 1950).

Qualitatively, the results agree very well. The specific heat curves for the adsorbed layers cross the specific heat curve of the bulk liquid, which requires, just as derived from the adsorption data, that the entropy of the adsorbed helium be higher than that of bulk liquid below T_λ. This is shown in fig. 9, in which the entropies of Frederikse's films have been calculated from his reported specific heat data, and are plotted

Fig. 9

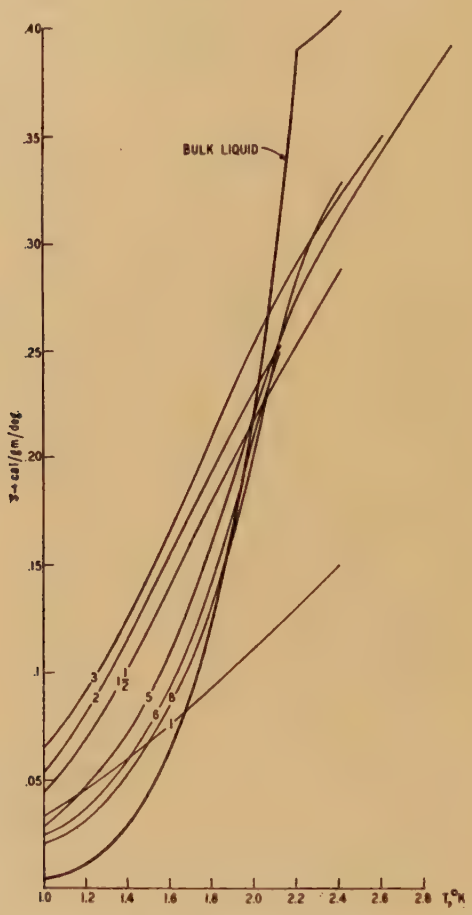

Average entropy in cal/g deg of helium adsorbed on jeweller's rouge as a function of temperature derived from fig. 8.

against temperature. Though the derived curves are subject to large errors in absolute value, comparison of the various coverages should be reasonably valid (Long and Meyer 1952 a).

These specific heat curves show one fact very clearly : even in very thin adsorbed films a phenomenon is taking place which is quite similar to that of the transition He I–He II.

Mastrangelo and Aston (1951) report some specific heat curves for helium adsorbed on TiO_2, with results in general agreement with those of Frederikse.

§4. Superfluidity in the Unsaturated Helium Film

(*a*) *Flow Experiments*

The fact that specific heat and adsorption data indicate an excitation process for the unsaturated film in the He II region, having some features similar to the thermal behaviour of bulk liquid helium, raises the possibility of the occurrence of superfluidity in the unsaturated film. Since in this case there is no reservoir of bulk liquid, and therefore no transition bulk liquid-film and vice versa involved in the flow, it is of interest to investigate the flow characteristics.

It is a common experience among workers using vacuum equipment immersed in liquid He II that the tiniest hole will result in superflow into the vacuum and also that residual helium gas causes excessive heat leak at temperatures below 2·19° K. Ganz (1940) was probably the first to report an experiment which showed the influence of superflow in the unsaturated film. In his work on heat propagation in He II he performed a qualitative experiment in which weak heat pulses were detected along a tube which contained an unknown amount of residual gas, thus showing that thermal energy can be transmitted through the film at considerable velocities.

In the work of Long and Meyer (1949) on adsorption of helium on Fe_2O_3, the approach to pressure equilibrium was quite different above and below 2·19° K, indicating the possibility of superflow.

The flow characteristics of the unsaturated film were then investigated by Long and Meyer (1950, 1952 a) in several different ways. In such experiments, in which direct measurements of the film flow are desired, the ordinary gas flow must be minimized, and so quite fine channels are required. Therefore, a technique similar to that used by Giauque, Stout, and Barieau (1939) was adopted. In this method, a series of ' superleaks ', either fine platinum wires sealed into Pyrex glass, or optically ground stainless steel plates pressed together, were sealed to a chamber which contained an adsorbent, in this case Fe_2O_3. The exit of any given superleak was connected to a measuring system, so that flow through the leak could be investigated under a range of condition of the saturation P/P_0 in the adsorption system, the temperature, and the pressure gradient across the superleak. The system does not quite permit direct measurement of the film flow itself, since it depends on flow through the leak, evaporation of the film in the system just outside the leak (or perhaps in the leak itself) and subsequent measurement of a gas pressure in a measuring system at room temperature.

In Method I of these experiments, the measuring system and the exit of the superleak were initially pumped to high vacuum, with the leak and the adsorption system at a given temperature T and saturation P/P_0 (the

saturation of course determines the film coverage). Once these conditions had been attained, the pumping was stopped, and the pressure rise in a known volume was measured over a period of time.

Superfluidity in the unsaturated film was detected, and was observed to occur in a quite striking and reproducible way. The results of measurements on eleven different film coverages, from ~ 2 to ~ 18 atomic layers (as determined by the values of P/P_0) are shown in fig. 10, in which the flow

Fig. 10

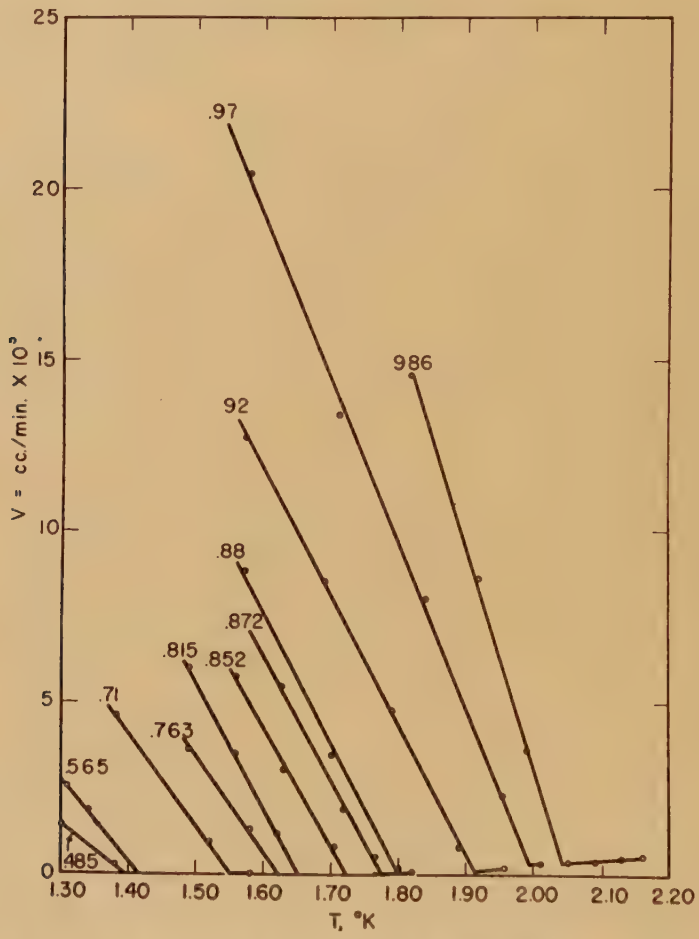

Flow rate through superleaks as a function of temparature for different saturations (Long and Meyer 1952).

rate in c.c. (STP)/min is plotted against the temperature T. It was found that for any given saturation P/P_0 (and, therefore, for any given film thickness, over the range investigated) in the adsorption chamber, there exists a sharply-defined temperature below which superflow occurs, the flow increasing from the very small gas flow rate to a rate which can only be due to superfluid behaviour in the unsaturated film,

Control experiments using a superleak with no adsorbent present gave exactly the same result, as is to be expected, since the adsorbent merely serves as a reservoir to provide a source of reasonably constant pressure during the flow measurements.

It will be noted that the temperature below which superflow occurs is greatly dependent on film coverage, being 1·39° K at ~2 layers and 2·04° at ~18 layers. The ' onset ' temperature for superflow is, under these conditions, independent of the geometry of the channel.

Also, the flow in the superfluid region, under conditions of constant temperature, is not a linear function of the pressure difference across the leak. Recent experiments by J. Landauer (1952) show that the flow rate follows roughly the third root of the pressure difference, a behaviour somewhat similar to that of the heat current in liquid He II (Keesom, Saris, and Meyer 1940).

Long and Meyer (1952 a) investigated flow in this system in another manner, designated Method II. Instead of initial high vacuum in the measuring system and at the exit of the superleak, helium gas was admitted to a given pressure p, such that a small pressure gradient was established across the leak, instead of the pressure gradient being initially the maximum possible gradient of Method I. Measurements made in this way gave results in direct disagreement with those of Method I, and somewhat confusing in themselves. Superflow was again observed, as was to be expected, but the superflow always started at the normal λ-point, 2·186° K, for all coverages above ~$1\frac{1}{2}$ layers ($P/P_0=0{\cdot}15$). The flow, however, was extremely sensitive to slight fluctuations of the bath temperature, and could even be reversed in direction by variations of a few ten-thousands of a degree. The results were discussed by Long and Meyer in terms of the effect of temperature gradients across the superleak, but no really satisfactory explanation has been given. It is clear, however, that under these conditions superflow does occur at the normal λ-point in thin films, and therefore that the film is behaving in a quite different manner from that of the conditions of Method I, previously described.

These direct flow measurements were followed by cooling experiments by Long and Meyer, in which two chambers, each filled with adsorbent, were connected by a short stainless steel capillary tube tightly packed with the same adsorbent (Fe_2O_3) designed to provide an effective superleak of considerable capacity. One chamber was in contact with the surrounding liquid He II bath, and the other was insulated by high vacuum. The temperature of each chamber could be measured by means of carbon thermometers. The insulated chamber was then heated to a temperature above the normal λ-point (say 2·5° K), the heating was stopped, and the temperatures and pressures in both chambers were followed as a function of time. Since the pressure in an adsorption system follows approximately a vapour pressure relation (except for dead-space corrections, minimized in this case) a plot of log P *vs* time for the cooling insulated chamber should be approximately a straight line, *provided* superflow from the other chamber does not occur, due either to a temperature gradient,

a pressure gradient, or both. Since both temperature and pressure gradients were created by heating the insulated chamber above the λ-point, observations of the temperatures and pressures should provide information as to the onset of superflow.

The results of these experiments again showed that superflow in the unsaturated film occurred at temperatures quite near the normal λ-point. In a series of measurements, with saturations varying from 40% to 85%, pronounced breaks in the log P *vs* time curves were observed to occur at $2{\cdot}19^{\circ} \pm 0{\cdot}01^{\circ}$ K, again in marked disagreement with the results of Method I of the direct flow measurements.

Fig. 11

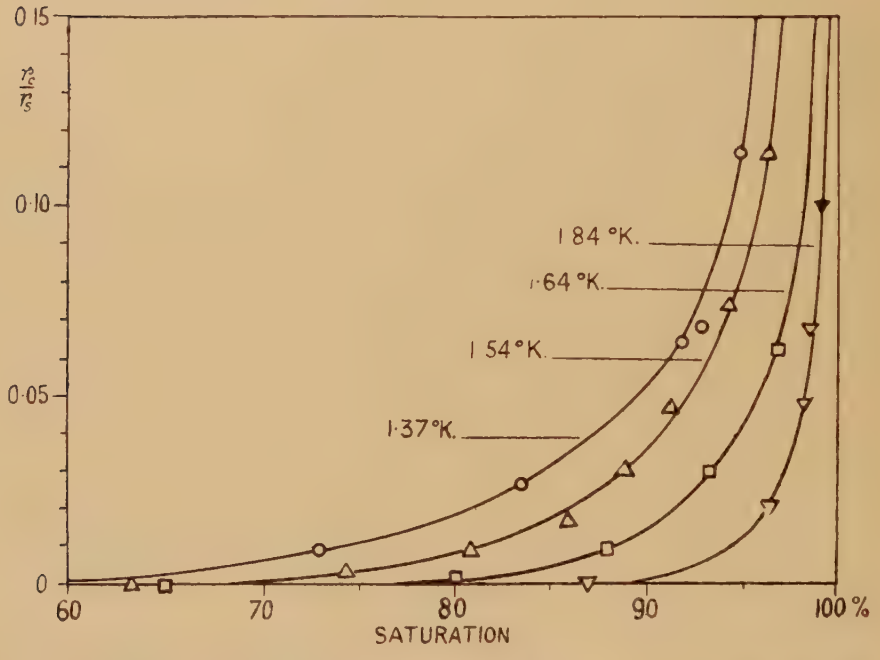

Heat conductance of helium film on wall of metal tube, normalized to a conductance 1 at P_0, as a function of saturation for different temperatures (Bowers, Brewer, and Mendelssohn 1951).

(*b*) *Heat Transport Experiments*

Another method for the investigation of superfluidity in unsaturated films is the determination of their contribution to the heat transport. The simplest experimental arrangement is that of two chambers, each provided with sensitive thermometers, connected by a thin-walled tube, with one chamber in good thermal contact with a heat sink (the surrounding He II bath) and the other provided with a heater and insulated by high vacuum. If helium gas is then admitted to the system, adsorption occurs,

and the film coverage can be controlled by regulating the saturation, as usual, even though the total surface area is quite small. The thermal conductivities of the tube and the contained helium gas are so small that any heat transport due to superflow in the adsorbed film easily becomes the dominant effect. It is necessary, of course, to place the heated chamber above the chamber which constitutes the heat sink, in order to minimize convection effects in the gas phase.

This method was used by Bowers, Brewer, and Mendelssohn (1951). They found that at any given saturation the adsorbed film is able to transport heat with essentially zero temperature gradient, up to a critical value of the heat input. At the critical and higher values of the heating rate, a ' run-away ' phenomenon occurs, with the result that the temperature rises rapidly beyond the range of measurement in the experiments. The results of their experiments are shown in fig. 11, in which the critical heating rate is plotted against the saturation, for a number of temperatures.

Measurements of the critical heating rates under conditions of saturation ($P/P_0=1$) yielded heating rates which, when normalized with the flow rate of the saturated He II film at any given temperature of measurement, were proportional to the well-known transfer rate of helium films over surfaces (Daunt and Mendelssohn (1939), Mendelssohn and White (1950)).

Long and Meyer (1952 b) used essentially the same method, with somewhat higher accuracy, and with results which, though they agree in general with those of Bowers, Brewer, and Mendelssohn, show some effects not observed by them.

Again, as in Method I of the direct flow measurements of Long and Meyer, the contribution of the unsaturated film to the heat transport appears abruptly at a well-defined temperature, previously designated as the ' onset ' temperature for superflow (see fig. 10 in the discussion of the flow measurements). This is shown in fig. 12, in which the ' onset ' temperatures for superflow, as determined by Method I of the direct flow measurements, are plotted against film coverage, as determined by P/P_0. The circles designate heat transport measurements, a negative sign indicating no superfluid contribution to the heat transport, and a positive sign a definite superfluid contribution. The solid curve is obtained from the flow measurements of Method I (fig. 10). No attempt was made to re-determine accurately the curve from the heat transport experiments, which are experimentally not as precise for the determination of the ' onset ' temperatures.

In the heat transport experiments, superflow is easily observed. The heat transport cycle must consist of flow of superfluid film to some higher temperature (not necessarily that of the upper chamber during the measurement) evaporation at the higher temperature, return as gas to the heat sink, condensation at the heat sink, and a repetition of the flow. Thus, the heat of vapourization and an additional (approximately 10%) contribution due to the thermomechanical effect, amounting to $\sim 5\,\mu$W per layer, is carried by the film, more or less independent of the ΔT.

Since the thermal conductance of the system, excluding superflow, can be held to $\sim 15\,\mu$w/deg, the contribution of one superfluid layer can easily be determined, especially at small temperature gradients.

As regards the onset of superfluidity under these conditions, the data of Bowers, Brewer, and Mendelssohn (1951) and those of Long and Meyer (1952 b) are in agreement. The intersections of the curves of Bowers, Brewer, and Mendelssohn with the P/P_0 axis from the published data in fig. 11 are consistent with the ' onset ' temperatures of Long and Meyer, as shown by fig. 12.

Fig. 12

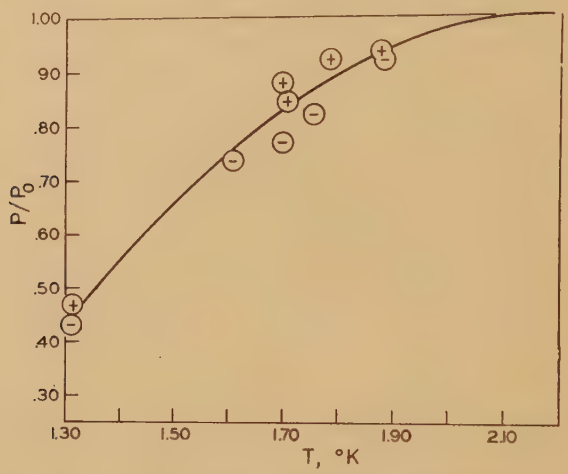

Onset of superfluidity as a function of saturation and temperature. Superflow observed in region above drawn line, but not below. Drawn line derived from the break-points of fig. 10, + and — from heat conductivity (Long and Meyer 1952).

The measurements of Long and Meyer on saturated films yielded critical heating rates which followed the transfer rate curve for the saturated film, again in agreement with Bowers, Brewer, and Mendelssohn. However, at heating rates below critical, Long and Meyer found that there was always a finite temperature gradient established for all except quite small heat inputs. The temperature gradient for a given heat input depended on the amount of excess liquid in the cell, whereas the critical heating rate was independent of this effect.

In preliminary measurements on unsaturated films in the superfluid region, Long and Meyer established that the heat transport occurs, not with zero temperature gradient, as reported by Bowers *et al.*, but always with a finite ΔT, which increases non-linearly with increasing heat current density. A typical experiment is shown in fig. 13, in which the heating rate in microwatts is plotted against the temperature difference, for the system containing a film at $P/P_0 = 0{\cdot}58$ at $1{\cdot}313^\circ$ K.

The temperature distribution along the tube, according to Long and Meyer, is such that the ΔT between centre and bottom is finite, but much smaller than that between centre and top. It appears that most of the temperature gradient occurs in a small region at the top of the tube, at least for all but the smallest temperature gradients. If so, then perhaps the film evaporates just below this region, and ordinary heat transport occurs across the region of maximum temperature gradient. This is quite possible because the temperature gradient becomes very steep in this region due to its short length, so that a considerable amount of heat can be conducted in spite of the low conductivity.

The small, but finite, temperature gradient between the centre and bottom of the tube during heat transport, observed in the preliminary work of Long and Meyer, is of greater interest. If this temperature gradient, in one case about 0·001°, as compared to the total ΔT of 0·016°

Fig. 13

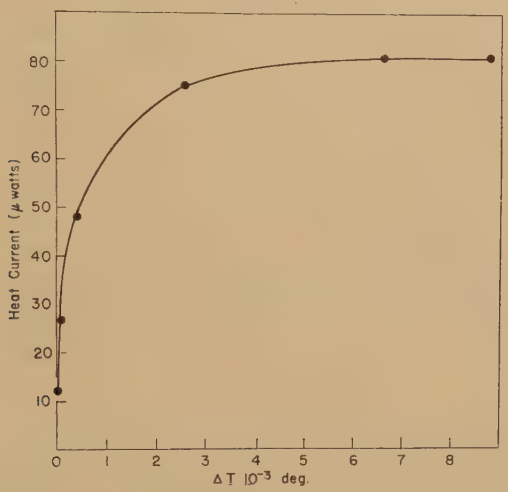

Temperature difference between upper and lower end of heat conduction tube as a function of the heat current for $P/P_0=0{\cdot}58$ and $T=1{\cdot}313$. Heat conduction due to film transport.

across the entire tube, is indeed a real ΔT in the unsaturated film, rather than being due to lack of equilibrium between the film and the wall, then the flow is probably not to be regarded as a pure superfluid process, but rather flow of very long mean free path. More experiments, under varying geometries, are needed to decide the question.

White, Chou and Johnston (1952) have recently reported some interesting experiments in which heat transport measurements were carried out in the same manner as those of Bowers, Brewer, and Mendelssohn and Long and Meyer, but with a metal tube packed with silica gel, instead of the ' empty ' tubes of the previous workers. No superfluid contribution to the heat flow was observed at saturations below 95–97%, while at 97% the usual high heat transport occurred. Subsequent measurements of adsorption

isotherms for helium on this adsorbent, above and below T_λ, showed adsorption behaviour typical of capillary condensation, rather than the sigmoid type of isotherm typical of ordinary physical adsorption (see Brunauer 1945).

The authors suggest that such a capillary-condensed adsorption system could account for the absence of superfluidity in the adsorbed layers, because the binding energy of the higher layers built up in the capillaries would be considerably larger than that corresponding to ordinary liquefaction. In this case, superflow could occur only when the capillaries are filled up, presumably the case in the measurement of 97%.

This argument may indeed be true, but another factor would seem to be of more importance in explaining the behaviour in such a powder-filled tube in which capillary condensation occurs. At *all* saturations, adsorption occurs, not only in the capillaries of the silica gel, but also on the walls of the tube and its connected chambers. Since layers on the tube should behave in the same way as in the experiments with an open tube, then some other factor must be responsible for the absence of high heat transport. The presence of packed powder in the tube will result in a very severe inhibition of the return gas flow in the heat transport cycle, and it is therefore suggested that this factor alone would probably explain the negative results. As previously mentioned, the direct flow measurements of Long and Meyer (1952 a) Method I, were independent of the presence of an adsorbent, since the walls of the experimental chamber provided sufficient adsorption area to replace the film at the entrance of the flow channel during the flow. This would not be the case in a heat transport experiment if the return gas flow rate were sharply limited.

§ 4. Discussion

A coherent picture of the behaviour of the unsaturated film is difficult to formulate from the information available at the present time.

The influence of the zero-point energy and the high compressibility of helium can be seen as resulting in the high packing density and rapidly changing heats of adsorption in the layers closest to the wall. That the attractive forces of the wall can counterbalance the zero-point energy to produce such effects is to be expected, although the magnitude of the interaction is large. Investigations on the adsorption of ^{3}He should reveal even greater effects.

The nature of the transition He I–He II in the film is not at all clear. The specific heat and adsorption data definitely show that an excitation process is taking place, while the flow and heat transport experiments show the great influence of superfluidity. But these experiments are inconsistent in themselves. The direct flow measurements of Method I of Long and Meyer are clearly confirmed by the open-tube heat transport experiments of Bowers, Brewer, and Mendelssohn and of Long and Meyer, in showing the rather startling occurrence of the ' onset ' temperatures for the start of superflow. But, on the other hand, the Method II flow

measurements and the cooling experiments described by Long and Meyer always gave the result that superflow occurred at all temperatures up to 2·186° K, for coverages above $\sim 1\frac{1}{2}$ layers. It is certainly true that the ' onset ' temperature phenomenon cannot be due to capillary condensation or other spurious effects in the direct flow investigations, because the heat transport experiments, with no small radii involved, show decisively the same effect.

Mass transport in unsaturated films due to a temperature difference across a fine channel would be a phenomenon corresponding to the fountain effect in bulk liquid He II. Meyer and Long (1951) derived that in the steady state the pressure difference ΔP over adsorbed layers, due to the fountain effect produced by a temperature difference ΔT, exceeds the change in vapour pressure by only about 10%, whereas in bulk liquid the fountain effect is about ten times greater than the change in vapour pressure. This does not exclude the possibility that transient temperature differences produce considerable mass flow under non-equilibrium conditions, which could be responsible for some of the flow phenomena observed in Method II ; but the fact that there is no heat transport by the film at temperatures between T_λ and the ' onset ' temperatures is hardly compatible with the argument.

All experiments showing the sharp ' onset ' temperature for superflow have one feature in common : all the superfluid moving in the process must evaporate completely to keep the process going. In the flow experiments, the film passing through the superleak must evaporate before being measured in a volume originally at high vacuum. In the heat transport, the cycle responsible for the flow of heat involves evaporation of the film at or near the warm end of the tube, with subsequent condensation and repetition of the cycle.

The films are too thin to allow normal fluid to move with the temperature gradient in order to compensate the superflow, as is assumed to occur for heat flow in bulk liquid. Thus, the rate of evaporation of the adsorbed film, and not its mobility, might be the rate-determining step, although it is difficult to correlate such a picture with the sharpness of the ' onset ' temperatures. New experiments are needed to decide the question.

The experiments have not answered adequately the question whether or not there exists in the unsaturated film a sharp transition point corresponding to the λ-point of the bulk liquid, and, if so, the effect of film thickness. The ' onset ' temperatures for superflow discussed above are sharp to about 0·001° and easily reproducible, but they are in complete disagreement with the maxima in the specific heat measurements of Frederikse. These maxima are up to 0·4° K higher than the ' onset ' temperatures (fig. 8).*

* Frederikse's data represent average specific heats, whereas the thermodynamic transition point would be characterized by an anomaly of the differential specific heats. Such a differentiation would shift the maxima only to higher temperatures and thus increase the discrepancy.

Meyer and Long (1952) investigated thermodynamically the pressure dependence of a transition point (such as a melting point or a λ-point in adsorbed films) when passing from pressures higher than the saturation vapour pressure P_0 to pressures below the vapour pressure line. It results that the slope of the dT_λ/dP curve changes strongly on crossing the vapour pressure curve, because below P_0 the two adsorbed phases involved in the transition must not only be in equilibrium with each other, but also with the vapour ; this introduces the gas density as a new factor. The slope of an ordinary melting curve is thus reduced to that of a vapour pressure curve ; however, its sign should not change, since the terms which determine the sign of a Clausius–Clapeyron type of equation (difference in specific volume and entropy differences of the two phases) remain unchanged.

Morrison and Drain (1950) have recently reported some interesting specific heat measurements on adsorbed argon films over a range of temperatures in the region of the argon melting point. Application of the above arguments to their data lead to rather good numerical agreement ; the experiments especially confirm the fact that the sign of the melting curve remains unchanged when crossing the vapour pressure line.

Unfortunately, it is not possible to treat the case of the helium films with the same accuracy, since the specific heat data do not permit the necessary differentiations. The behaviour may be treated qualitatively : the thermodynamic argument requires that the sign of the slope of the curve dT_λ/dP does not change on crossing the vapour pressure line. Since the λ-point of the bulk liquid is shifted by pressure to lower temperatures, then it should appear in unsaturated films, for which $P<P_0$, at temperatures *higher* than the normal λ-point, rather than lower. Since the pressure range available in the film case is at the most about 1/20 atmosphere, only a very small change in T_λ is to be expected at all.

This is not incompatible with the fact that the specific heat curves show maxima at temperatures considerably below T_λ. A maximum in the specific heat represents a transition of the second kind only if due to a kink in the entropy curve ; it may also be produced by a point of inflection in the entropy–temperature curve, as pointed out by Long and Meyer (1952 a). Integration of the Frederikse specific heat data (see fig. 9) actually suggests the latter case. If so, the first appearance of the low-temperature phase can occur at temperatures above that of the specific heat maximum. However, it seems at present there is no thermodynamic argument which could explain the first appearance of the low temperature phase at a temperature considerably below the specific heat maxima, as apparently suggested by the 'onset' temperatures. In bulk liquid helium the onset of superfluidity coincides exactly with the specific heat maximum (A. P. Keesom 1938).

Mastrangelo (1950) and Aston and Mastrangelo (1951) present an explanation of the specific heat data which correlates the specific heat maxima with the shift of the λ-temperature in bulk liquid with pressure.

In this treatment they use a three-dimensional analog of the surface pressure. It was pointed out by Meyer and Long (1952) that the only pressure entering thermodynamic relationships and determining uniquely the free energy is the pressure of the gas phase in equilibrium with the unsaturated film, and that the pressures assumed in such a treatment had no relationship to the thermodynamic pressure. The case has been treated by Guggenheim (1949, p. 37).

Morrison and Drain (1950) point out that application of the Mastrangelo argument to the case of adsorbed argon leads to a pressure dependence of the melting point which is opposite in sign to that found in their experiments.

Unfortunately it does not seem possible to derive the temperatures of a transition in the unsaturated films from the adsorption isotherms. It is true that in such a transition the log P–$1/T$ curve at constant amount adsorbed should show an anomaly similar to that exhibited by the vapour pressure curve of bulk liquid helium around the λ-point (Keesom 1942, p. 192). But even for bulk liquid the magnitude of the effect is within the error of the measurements. The case of the unsaturated film is much worse : one can only measure directly the pressure in equilibrium with the film in a ' closed-vessel ' experiment over a series of temperatures. At each temperature the amount adsorbed (and therefore the film thickness) will be different, because of the varying amounts of gas in the ' dead space '. The log P–$1/T$ curve has then to be derived from the measurements and the slopes of the adsorption isotherms, introducing another source of error.*

The scatter in the entropy values derived by Strauss (fig. 7) and by Frederikse and Gorter from the adsorption isotherms makes it hopeless to search for small changes in slopes due to an eventual λ-transition. The fact that $\bar{S}_f - S_l$ changes sign around T_λ does not in itself indicate a transition in the film at that temperature ; the change of sign could easily be caused by differences in the variation with temperature of the entropies of film and bulk liquid in the He II region. In particular, it can be due to the very steep drop of the entropy of the liquid below T_λ.

---

* Mastrangelo and Aston (1951) report that the log P—$1/T$ curve for helium adsorbed on TiO_2 in such a ' closed-vessel ' experiment, plotted directly without correcting to constant amount adsorbed, shows a break at the temperature of the maximum of the specific heat, the magnitude of the change in slope becoming smaller when the data are corrected to constant coverage. But the isotherms of Strauss and those of Frederikse and Gorter show no such effects. Long, Meyer, and Strauss (unpublished data) performed a series of very careful ' closed-vessel ' experiments with helium adsorbed on Fe_2O_3 (for which the ' dead-space ' corrections are much less serious than on TiO_2) over a range of temperatures and saturations from $T=1{\cdot}7^\circ$ to $T=2{\cdot}3^\circ$ K and P/P_0 from 0·31 to 0·99, without finding the slightest indication of a break in the He II region for the uncorrected log P -$1/T$ curve of the system. The only unusual effects observed were slight *discontinuities* in the plots at the bulk liquid λ-point, due to small errors in the hydrostatic corrections for the bath temperature above $2{\cdot}186^\circ$ K ; it was these effects which led Long and Meyer (1951) to a re-determination of the λ-point pressure of the bulk liquid, previously measured by Schmidt and Keesom (1937).

Though it is not possible at the present time to establish experimentally a ' λ-line ' for the unsaturated films, there is no doubt that typical properties of He II do appear in the films : specific heat anomalies, indicating the influence of an excitation process, and ' superfluid ' flow caused by pressure gradients and by temperature gradients, the latter causing an extremely high heat transport. The flow measurements and the heat transport experiments show that only $\sim\frac{1}{2}$ statistical layer on top of the densely packed first mono-layer is sufficient to produce He II phenomena. This is of some interest in connection with theoretical conclusions that a Bose–Einstein condensation cannot take place in a two-dimensional system (Osborne 1949).

Further experiments are needed to solve the questions raised, in particular whether or not the appearance of typical He II properties in the unsaturated film occurs in a transition similar to that of the bulk liquid, and whether the so-called two-fluid model can be applied to explain the observed properties of the adsorbed layers. A careful investigation of very dilute ^{3}He–^{4}He mixtures in adsorption systems should provide additional information on superfluid behaviour of these films in the He II region, because it can be expected that the distribution of ^{3}He between the gas and condensed phases is in this case as much influenced by the appearance of He II-like properties as in bulk liquid below the λ-point (compare Daunt 1952).

References

Aston, J. G., and Mastrangelo, S. V. R., 1951, *J. Chem. Phys.*, **19,** 1067.

Atkins, K. R., 1952, *Advances in Physics*, **1,** 169.

Band, W., 1949, *Phys. Rev.*, **76,** 441 ; 1951, *J. Chem. Phys.*, **19,** 435.

Bowers, R., Brewer, D. F., and Mendelssohn, K., 1951, *Phil. Mag.*, **42,** 1445.

Brunauer, St., 1945, *Adsorption of Gases and Vapors* (Princeton University Press).

Brunauer, St., Emmet, P. H., and Teller, E., 1938, *J. Amer. Chem. Soc.*, **60,** 309.

Daunt, J. G., 1952, *Advances in Physics*, **1,** 209.

Daunt, J. G., and Mendelssohn, K., 1939, *Proc. Roy. Soc.* A, **170** 439.

Dingle, R. B., 1952, *Advances in Physics*, **1,** 111.

Emmet, P. H., 1948, *Advances in Catalysis*, Vol. I (New York : Academic Press).

Frederikse, H. P. R., 1949, *Physica*, **15,** 860 ; 1950, *Thesis*, Leiden.

Frederikse, H. P. R., and Gorter, C. J., 1950, *Physica*, **16,** 403.

Ganz, E., 1940, *Proc. Camb. Phil. Soc.*, **36,** 127.

Giauque, W. F., Stout, J. W., and Barieu, R. E., 1939, *J. Amer. Chem. Soc.*, **61,** 654.

Gorter, C. J., and Frederikse, H. P. R., 1949, *Physica*, **15,** 891.

Guggenheim, E. A., 1949, *Thermodynamics*, Amsterdam.

Keesom, A. P., 1938, *Thesis*, Leiden.

Keesom, W. H., 1942, *Helium* (Amsterdam-New York : Elzevier).

Keesom, W. H., and Schmidt, G., 1933, Comm. Leiden, 226 b.

Keesom, W. H., and Schweers, J., 1941, *Physica*, **8,** 1020, 1032.

Keesom, W. H., Saris, B. F., and Meyer, L., 1940, *Physica*, **7,** 817.

Kistemaker, J., 1947, *Physica*, **13,** 81.

Landauer, J., 1952, to be published.
Langmuir, I., 1918, *J. Amer. Chem. Soc.*, **40,** 1361.
Long, E., and Meyer, L., 1949, *Phys. Rev.*, **76,** 440 ; 1950, *Ibid.*, **79,** 1031 ; 1951, *Ibid.*, **83,** 860 ; 1952 a, *Ibid.*, **85,** 1030 ; 1952 b, *Ibid.*, **87,** 153.
McMillan, W. G., and Teller, E., 1951, *J. Chem. Phys.*, **19,** 25 ; *J. Phys. and Colloid Chem.*, **55,** 17.
Mastrangelo, S. V. R., 1950, *J. Chem. Phys.*, **18,** 896.
Mastrangelo, S. V. R., and Aston, J. G., 1951, *J. Chem. Phys.*, **19,** 1370.
Mendelssohn, K., and White, G. K., 1950, *Proc. Phys. Soc.* A, **63,** 1328.
Meyer, L., and Long, E., 1951, *Phys. Rev.*, **84,** 551 ; 1952, *Ibid.*, **85,** 1035.
Morrison, J. A., and Drain, N. E., 1950, *J. Chem. Phys.*, **19,** 1063.
Osborne, M. F. M., 1949, *Phys. Rev.*, **76,** 396.
Schaeffer, W. D., Smith, W. R., and Wendell, C. B., 1949, *J. Chem Soc.*, **71,** 863.
Schmidt, G., and Keesom, W. H., 1937, *Physica*, **4,** 963.
Strauss, A. J., 1952, *Thesis*, Chicago.
White, D., Chou, C., and Johnston, H. L., 1952, *J. Chem. Phys.*, **20,** 1819.

The Thermal Conductivity of Metals at Low Temperatures

By J. L. Olsen* and H. M. Rosenberg
The Clarendon Laboratory, Oxford

CONTENTS

* Now at the Eidgenössische Technische Hochschule, Zürich,

§1. Introduction

The recent wide access to simple cryogenic equipment has produced a new interest in the thermal conductivity of metals at low temperatures and a very great deal of experimental work has been done in this field in the last few years. It is the aim of this article to provide a review of this work from an experimental point of view. The results must necessarily be compared with theory, but no effort is made to examine the basis of the theory critically or in any detail.

The situation in a metal is somewhat more complicated than in a non-conductor, since in a metal there are two mechanisms conducting the heat. As in non-conductors there is a transfer of heat by the lattice waves, but in metals there is in addition a transfer of heat by the electrons. The total heat conductivity is thus made up of two components: K_g the lattice conduction (with which another article in this volume is concerned), and K_e the electronic conduction. We may write

$$K = K_e + K_g . \qquad (1)$$

It is of course well known that the electronic thermal conductivity is closely connected with the electrical conductivity of the metal (Wiedemann–Franz law). As a not unexpected consequence such effects as magneto-resistance, anisotropies of various sorts, and superconductivity have their counterparts in K_e. The existence of free electrons in a metal also has an effect on the lattice conductivity by supplying a scattering mechanism which is not present in the non-conductors and which in the case of reasonably pure metals reduces the lattice conduction to an insignificant value compared with the electronic thermal conductivity.

In this article we shall deal first with the variation with temperature of K_e in normal metals and with the effect on it of a small impurity content, of a magnetic field and of crystalline anisotropy. When the impurity content is very large, K_g does become important and K_e and K_g in alloys are therefore dealt with together. The effects of superconductivity and the behaviour of the thermal conductivity below 1° K are dealt with in the last sections.

§2. The Theory of the Electronic Thermal Conductivity

2.1. *General Remarks*

The calculation of the thermal conductivity, like that of the electrical conductivity, depends upon the solution of the Boltzmann equation to give the velocity distribution function of the electrons in the presence of an external field. This solution is complicated in general, and has so far only been carried out for the simplest case: that of quasi-free electrons where the energy is of the form

$$E = \frac{\hbar^2}{8\pi^2 m} |\mathbf{k}|^2 . \qquad (2)$$

where $\mathbf{k}$ is the wave vector and m the effective mass of the electron. This is not such a rigid restriction as it seems, since by choosing a suitable value for m we can take account of quite complicated potential distributions.

It is also necessary to assume that the distribution function of the lattice waves is unaffected by the temperature gradient. This appears to be justified except in exceptional cases where the theory is in any case of very doubtful validity (e.g. bismuth: Makinson 1938, and Sondheimer 1952 a, b).

At high temperatures where $(\theta/T)^2$ may be neglected a solution may easily be obtained (Wilson 1936). The case of an impure metal at low temperatures may be dealt with by a method of successive approximations, but the higher order approximations become very complicated and the method cannot be applied to the ideally pure metal. Wilson (1937) has calculated the zero order approximation at low temperatures and gives an interpolation formula for intermediate temperatures. These formulae have been investigated in detail and evaluated by Makinson (1938).

2.2. *Makinson's Work*

Makinson quotes Wilson's result that the electronic heat resistance $1/K_e$ can be split into two parts (Matthiesen's rule) so that

$$1/K_e = 1/K_0 + 1/K_i \quad . \quad . \quad . \quad . \quad . \quad . \quad . \quad (3)$$

where $1/K_0$ is the resistance due to impurity scattering, and $1/K_i$ is the resistance due to the scattering of the electrons by the lattice waves. K_0 is connected with the residual electrical resistance ρ_0 by the equation

$$K_0 = \frac{1}{3}\left(\frac{\pi k}{\epsilon}\right)^2 \frac{T}{\rho_0} . \quad . \quad . \quad . \quad . \quad . \quad . \quad . \quad (4)$$

It will be noted that $\frac{1}{3}(\pi k/\epsilon)^2$ is the ordinary Lorenz number, L_0, valid for high temperatures where it is obtainable from fairly simple considerations. The ideal resistance $1/K_i$ is represented by the somewhat complicated expression:

$$\frac{1}{K_i} = \frac{27h}{8\pi^2 k^2 \zeta^2 A\theta}\left(\frac{T}{\theta}\right)^2 \left\{ \mathcal{J}_5\left(\frac{\theta}{T}\right) + \frac{D}{\zeta}\left(\frac{T}{\theta}\right)^2 \left(\frac{2\pi^2}{3}\mathcal{J}_5\left(\frac{\theta}{T}\right) - \tfrac{1}{3}\mathcal{J}_7\left(\frac{\theta}{T}\right)\right)\right\}, \quad (5)$$

where ζ is the Fermi energy of the electrons,

$$D = \frac{(6\pi^2)^{2/3}\hbar^2}{16\pi^2 m a^2} . \quad . \quad . \quad . \quad . \quad . \quad . \quad . \quad . \quad (6)$$

$$A = \left(\frac{4\pi}{3}\right)^{1/3} \frac{4Mak\,\theta}{3\hbar^2 C^2} , \quad . \quad . \quad . \quad . \quad . \quad . \quad . \quad (7)$$

a is the lattice constant and k is Boltzmann's constant. This should not cause any confusion with the use of **k** as the wave vector.

C is a constant which gives the absolute amount of the interaction between the electrons and the lattice. M is the mass of an atom. The function $\mathcal{J}_n$ is given by:

$$\mathcal{J}_n(x) = \int_0^x \frac{z^n dz}{(e^z - 1)(1 - e^{-z})} . \quad . \quad . \quad . \quad . \quad . \quad . \quad (8)$$

For high and low values of the argument this reduces to

$$\mathcal{J}_n\left(\frac{\theta}{T}\right)\sim n\,!\sum_{r=1}^{\infty}\frac{1}{r^n} \qquad \text{for } \left(\frac{T}{\theta}\right)\to 0 \quad . \quad . \quad . \quad . \quad . \quad (9)$$

and

$$\mathcal{J}_n\left(\frac{\theta}{T}\right)\sim \frac{1}{n-1}\left(\frac{\theta}{T}\right)^{n-1} \qquad \text{for } \left(\frac{T}{\theta}\right)\to\infty, \quad . \quad . \quad . \quad . \quad (10)$$

thus $\mathcal{J}_5=124{\cdot}3$ at $T=0°\text{K}$ falling to 100 at about $\theta/T=8$. Intermediate values of $\mathcal{J}_n$ may be found tabulated by Sondheimer (1950).

It will be seen by inspection of (5) that at low temperatures (below about $\theta/10$) it reduces to $1/K_i=\alpha T^2$ and hence (3) becomes

$$1/K=\beta/T+\alpha T^2 \quad . \quad . \quad . \quad . \quad . \quad . \quad . \quad . \quad . \quad (11)$$

where

$$\beta=\rho_0/L_0\,, \quad \alpha=\frac{95{\cdot}3\,N_a^{2/3}}{K_\infty\theta^2} \quad . \quad . \quad . \quad . \quad . \quad . \quad (12)$$

and K_∞ is the limiting thermal conductivity at very high temperatures. We may note that a simple calculation yields

$$D/\zeta=2^{-1/3}\,N_a^{-2/3} \quad . \quad . \quad . \quad . \quad . \quad . \quad . \quad (13)$$

where N_a is the number of free electrons per atom.

Makinson has examined the behaviour of eqn. (3) for the cases of copper and bismuth, for which he takes N_a to be 1 and $1{\cdot}8\times10^{-2}$ respectively. His curves for the variation of K in copper of various purities is shown in fig. 1. The relative amount of impurity is measured by the parameter $\rho_0/4A$ where

$$A=\frac{3\pi\hbar D}{16\epsilon^2\,\zeta^3 A}. \quad . \quad . \quad . \quad . \quad . \quad . \quad . \quad . \quad (14)$$

The theoretical calculation of A depends upon our ability to calculate the interaction constant C. This calculation may, however, be avoided, since for $T/\theta>0{\cdot}6$ we have accurately

$$1/\sigma_i=AT/\theta \quad . \quad . \quad . \quad . \quad . \quad . \quad . \quad . \quad (15)$$

where σ_i is effectively the electrical conductivity at high temperatures. There is a corresponding equation involving the thermal conductivity. A may thus be found by measurements at high temperatures on the electrical or thermal conductivity.

An examination of experimental data shows that for an extremely pure, unstrained specimen $\rho_0/4A$ might be of the order of 10^{-4} while in a specimen of lead containing 1/10% of bismuth $\rho_0/4A$ would be about 5×10^{-2}.

It is seen in fig. 1 that for all the fairly pure specimens of copper, K_e first rises linearly, then less steeply to a maximum which is higher and occurs at a lower temperature the greater the purity. It then falls to a minimum at about $\theta/5$ and then finally rises slowly to a constant value at high temperatures.

2.3. *The Lorenz Number*

A series of curves is also given for the Lorenz number $L_e=K_e/\sigma T$. These are shown in fig. 2. At high and low temperatures these approach the value L_0, but in the case of a normal metal such as copper, there is a

Fig. 1

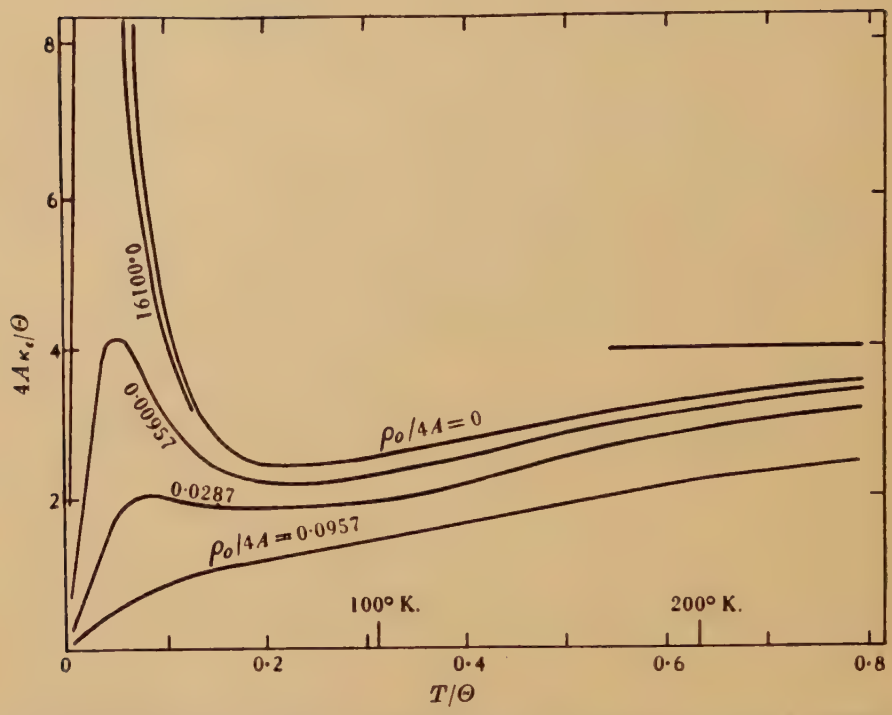

Theoretical electronic thermal conductivity for a monovalent metal showing the effect of impurity. The temperatures marked correspond to copper (θ=315° K). (Makinson 1938.)

Fig. 2

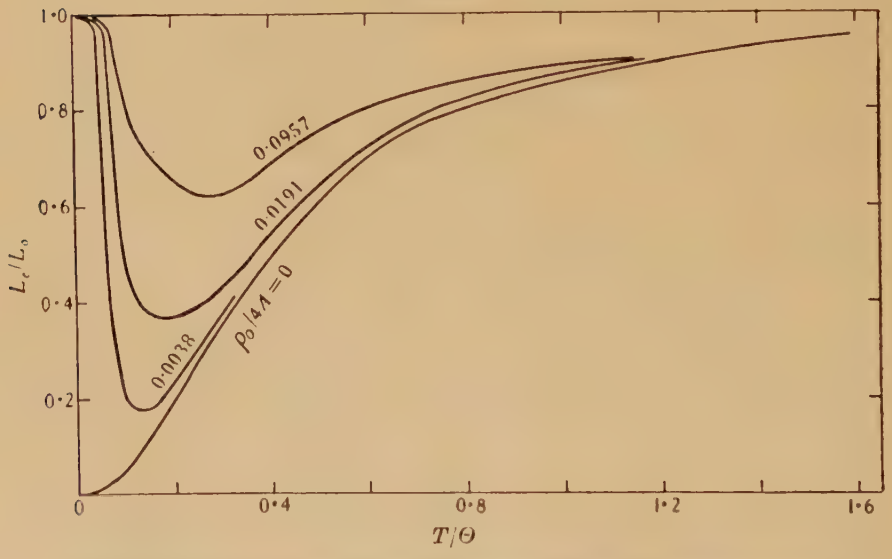

The ratio L_e/L_0 for monovalent metals showing its dependence on impurity and temperature. (Makinson 1938.)

decrease at intermediate temperatures, this decrease being more the greater the purity. For an ideally pure metal L_e tends to zero as T tends to 0° K. For the bismuth model, with small N_a, there is a marked difference. As the temperature is lowered, L_e first increases to a maximum above L_0 and then goes to a minimum below L_0 as the temperature is lowered further, the variations from L_0 being again greater for higher purity.

2.4. *Sondheimer's Treatment*

A more accurate treatment of the problem valid for all temperatures has been given by Sondheimer (1950) who uses a method which is a synthesis of methods due to Kroll (1938) and Kohler (1949 d).

Sondheimer's result may be expressed in the form

$$K = K_M + F \quad . \quad . \quad . \quad . \quad . \quad . \quad . \quad . \quad . \quad (16)$$

where K_M is the conductivity as obtained from Makinson's treatment and F is a correction term which is always positive. F can be expressed in terms of infinite determinants and may be calculated to any degree of accuracy by terminating the determinants at the appropriate row and column. For a monovalent metal, however, only two or three rows and columns are necessary.

The minimum in K at about $\theta/5$ is also obtained by this method, but in general Makinson's results are found to be only qualitatively correct and his K is about 25% too small at low temperatures for an ideal metal.

A discrepancy which is more serious in principle arises from the fact that F depends upon both K_0 and K_i, and thus Matthiesen's rule breaks down. The departure from Matthiesen's rule is however only of the order of 1%.

The existence of the minimum has also been confirmed by Umeda and Yamamoto (1949) by an examination of Kroll's work (1933 a, b, 1938). There is thus no doubt that the minimum is inherent in the model used and is not a result of an inadequate degree of approximation in the solution of the equations.

2.5. *The Lattice Conductivity*

The lattice conductivity may, as will be seen in § 4.2, be taken to be very small in most metals due to the strong scattering of the lattice waves by the electrons. There is also some experimental evidence (§ 5) to support this theoretical conclusion, and in the discussion of the electronic thermal conductivity which follows we shall assume that K_g is either negligible or is known in some way.

2.6. *Comparison of the Theory with Experimental Results*

At first sight the agreement between theory and experiment is quite good. The general shape of the conductivity curve is close to that shown in fig. 1. The conductivity increases linearly with temperature at the lowest temperatures, and as the temperature is raised a quadratic term appears in the resistance, so that the conductivity rises to a maximum and then falls above approximately $\theta/10$. At intermediate temperatures,

however, no sign of a minimum in K_e is observed and the conductivity always decreases monotonically with increasing temperature once the maximum has been passed.

A less obvious, but much more serious objection to the theory is the fact that when N_a is calculated from the experimental value of α using expression (12), then N_a is seen to be of the order of 2×10^{-2} (Hulm 1950) for a large number of metals where the number of free electrons is generally thought to be of the order of one per atom. If this low value of N_a had any real significance we would also expect an appreciable lattice conductivity in monovalent metals and there is no evidence of this.

It should of course be remembered that the model used is only a very rough first approximation to the situation in a real metal. A rather simpler objection to the above calculation may be made on the grounds that the calculation of N_a has been made using the Debye θ rather than a θ, θ_L, specially associated with the longitudinal vibrations only, as would be expected from the Bloch theory (Blackman 1951). Blackman has calculated values of θ_L for a number of metals, and if these are used in the calculation of N_a much larger and more plausible values of N_a are obtained. If, however, θ_L were in fact the appropriate θ to use then it would be implied that only the longitudinal waves interacted with the electrons. In that case we should expect an appreciable lattice conductivity since to a first order the transverse waves would not be scattered by the electrons. This has not been observed experimentally.

2.7. *Modification of the Theory when N_a is small*

Very recently Sondheimer* (1952 a) has pointed out that the Wilson–Makinson theory is in any case invalid for metals in which N_a is small.

Allowance has to be made for the fact that electrons can only interact with lattice vibrations of wave number q such that

$$|q|\leqslant 2|\mathbf{k}|$$

where $\mathbf{k}$ is the wave vector of the electron. This does not affect the results when $2k_0\geqslant q_0$ (where k_0 and q_0 are the wave numbers corresponding to the top of the Fermi zone and to the cut off frequency of the Debye spectrum respectively).

When, however, $2k_0<q_0$ the usual expressions have to be modified. Since

$$D/\zeta=q_0^2/2k_0^2=2^{\frac{1}{3}}N_a^{-2/3}$$

this condition is equivalent to $D/\zeta>2$ or $N_a<\frac{1}{4}$. Thus when $N_a<\frac{1}{4}$ eqn. (5) has to be modified to

$$\frac{1}{K_i}=\frac{27h}{8\pi^3k^2\zeta^2\Lambda\theta}\left(\frac{T}{\theta}\right)^2\left\{\mathcal{J}_5\left(\frac{\theta'}{T}\right)+\frac{D}{\zeta}\left(\frac{\theta}{T}\right)^2\left(\frac{2\pi^2}{3}\mathcal{J}_5\left(\frac{\theta'}{T}\right)-\tfrac{1}{3}\mathcal{J}_7\left(\frac{\theta'}{T}\right)\right)\right\}, \quad (17)$$

where $\theta'=\sqrt{(2\zeta/D)}\,\theta$.

* We are very grateful to Dr. Sondheimer, who has shown us the manuscripts of his papers before publication.

With this modified form for eqn. (5) Sondheimer (1952 b) finds for α in eqn. (12)

$$\alpha = 6\zeta\, \mathcal{J}_5(\infty)/\pi^2\, D\, K_\infty\, \theta^2 \qquad \text{for } D/\zeta \leqslant 2,$$
$$\alpha = 3D\, \mathcal{J}_5(\infty)/2\pi^2\, \zeta\, K_\infty\, \theta^2 \qquad \text{for } D/\zeta > 2 \quad . \quad . \quad . \quad . \quad . \quad . \quad (18)$$

and this has a minimum value for $D/\zeta = 2$, and it is found that *no* values of $N_{\prime\prime}$ will yield the experimentally observed α if the usual Grüneisen or Debye θ's are used in the formulae. As in § 2.6, however, an adjustment of θ allows a more acceptable value to be obtained.

It is always difficult to decide how much parameters of this sort may justifiably be adjusted. Sondheimer considers that the simplifying assumptions made in the model are so sweeping that it would even be reasonable to treat both θ and D/ζ as arbitrary parameters.

The suggestion that the value of D/ζ might not be exactly equal to that given by the simple theory, indicates that it is not surprising that the theoretical minimum in the conductivity, which should occur only if $D/\zeta < 1{\cdot}7$ is not found in practice.

2.8. *Klemens' Work on the Form of the Distribution Function*

Klemens* (1952) has recently suggested that the disagreement between the theoretical and experimental values for α is due to a mathematical assumption in Sondheimer's and previous theories which may not be justified. Sondheimer assumes that the distribution function f of the electrons is of the usual form

$$f = f_0 - k_1 c(\eta) \frac{\partial f_0}{\partial E} \quad . \quad . \quad . \quad . \quad . \quad . \quad . \quad . \quad (19)$$

where $\eta = (E-\zeta)/kT$, f_0 is the Fermi function $1/(e^\eta+1)$, k_1, k_2, k_3 are components of the wave vector and $c(\eta)$ is an unknown function of η. He then assumes that $c(\eta)$ can be written as a series of positive powers of η. Klemens, however shows that in order to satisfy eqn. (5), $c(\eta)$ should vary between a function of the form $B\eta$, B being a constant and one proportional to η^{-2} and hence that Sondheimer's assumption as to the form of $c(\eta)$ is not justified.

Klemens has solved eqn. (5) very approximately using $c(\eta)$ in the form he suggests, and he then obtains a value of 16·1 for the numerical coefficient of α in (12) instead of 95·3 given by Wilson and by the zero approximation of Sondheimer. This new value of α does agree much better with the experimental results and lends weight to Klemens' suggestions although it must be stressed that these are at present determined in a very approximate manner. However, he hopes to give a more rigorous and exact derivation in the near future.

---

* We are very grateful to Dr. Klemens for letting us see the manuscript of his paper before publication.

§3. Experimental Work on the Thermal Conductivity in the Normal State

3.1. *General Form of the Results*

Experimental data for the thermal conductivity of pure non-superconducting metals and of superconductors above the superconducting transition temperature has been very meagre up till recently. For this reason it is only lately that it has been possible to compare theory and experiment in any detail. Qualitatively the results obtained agree with the curves of Makinson and therefore also with the later work of Sondheimer. For a fairly pure metal the conductivity does increase linearly from 0° K to a maximum at $T \sim \theta/10$° K, and then it decreases (sharply for pure metals with low θ). At higher temperatures this decrease is less steep. The value of the conductivity at the maximum is usually of the order of a few watt units except in the case of extremely pure metals or some single crystals when it may be 60 watt units or over.

Berman and MacDonald (1951, 1952) have measured the thermal and electrical conductivities of the monovalent metals sodium and copper in the range 4° K to 90° K and 2° K to 90° K respectively. Their curves for two samples of sodium are shown in fig. 3. Curve II is for the purer specimen and it can be seen that the maximum is much higher and occurs at a lower temperature than that for the less pure specimen shown by curve I. At the higher temperatures where the lattice scattering is dominant the two curves coincide. These workers made a careful search for the presence of the minimum in the thermal conductivity which should occur at 40–50° K for sodium and at about 80° K for copper, but there was no indication of any minimum at all. Work on copper has also been done by Allen and Mendoza (1948). Their determinations were in the range 1·8–4° K and hence they have only obtained part of the linear section of the curve.

For less pure metals, particularly those with a high Debye θ, the graph of thermal conductivity against temperature in the liquid hydrogen and helium region is approximately a straight line which sometimes curves slightly towards the temperature axis at higher temperatures. Such a curve is given by de Nobel (1951) for a 99·4% pure nickel in a report of some prewar work. Mendelssohn and Rosenberg (1952 b) have given similar results on an annealed nickel specimen of higher purity (99·997%). De Nobel also gives curves in the liquid hydrogen and liquid air region for a very pure iron (99·93%) and aluminium which each exhibit a broad maximum at about 50° K.

De Haas and de Nobel (1938) give measurements on a tungsten single crystal which exhibits a very high conductivity of about 75 watt units at its maximum in the region of about 15° K.

3.2. *Hulm's Work*

As can be seen from the above general outline, very little systematic research has been published on the thermal conductivity of metals in the normal state. Most workers have contented themselves with more or less isolated determinations for one or two specimens.

The first systematic set of experiments to be done and compared with theory is that of Hulm (1950). While his paper deals with superconducting metals, the part relating to their behaviour in the normal state is relevant to this section, and the superconducting aspect will be dealt with later.

Fig. 3

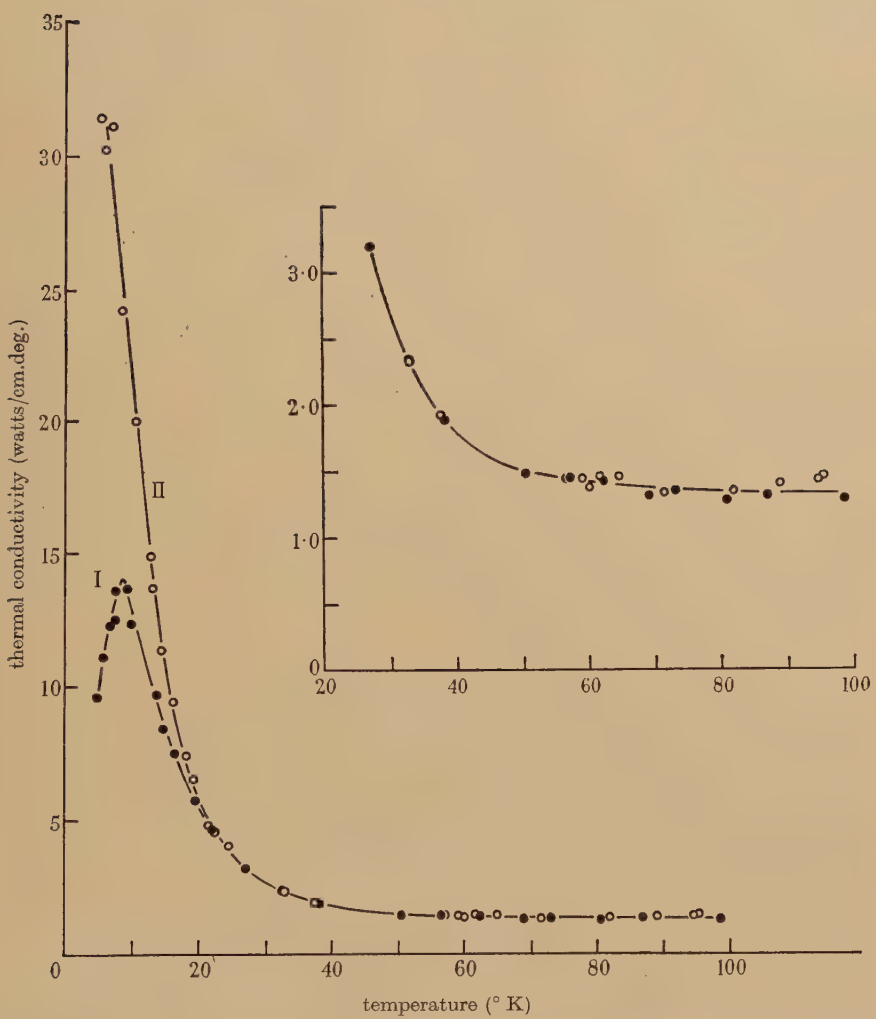

The thermal conductivity of two samples of sodium. Inset, the region between 30° and 100° K enlarged five times. (Berman and MacDonald 1951.)

Hulm has measured the thermal conductivity of pure tin, indium, mercury and tantalum, and of tin and mercury with known small amounts of impurity. The measurements were made from 1·7–4·3° K.

The results have been compared with Makinson's theory and they agree qualitatively. Spectroscopically pure tin had a maximum at about 4° K, whilst a small amount of impurity decreased the conductivity and shifted

the maximum to a higher temperature. Graphs of WT against T^3 are given for his specimens, where W is the thermal resistance, and as is to be expected from eqn. (11), these are in general straight lines for the samples of higher purity, indicating that the conductivity is nearly all electronic, the lattice conductivity being negligible. Different samples of the same metal gave $WT \sim T^3$ curves that were approximately parallel to each other, showing that the lattice scattering term in $1/T^2$ is the same for each, as the theory requires. The coefficient of T due to impurity scattering is shown to be roughly equal to ρ_0/L_0 where ρ_0 is the residual electrical resistance. This also follows from the theory.

Detailed examination of the $WT \sim T^3$ curves however, shows that they are not exactly linear (fig. 4), and this is dealt with in § 3.6.

Specimens which had an appreciable impurity did not give $WT \sim T^3$ curves which were at all consistent with the theory and Hulm assumes that in these cases there is an appreciable thermal conduction by the lattice as well as that by the electrons. In these cases he has examined the electronic conduction from the residual electrical resistance and has subtracted this from the measured conductivity hence giving the lattice conductivity K_g. In the case of impure tin K_g is approximately proportional to T^3, whilst for tantalum it varies as T^2. However, Hulm shows that in the case of tin which had large crystallites, the main resistance to lattice conduction is likely to be due to electron scattering, which should give a T^2 term as is shown in § 4.2, whereas for tantalum which had a very small grain size, the scattering at grain boundaries might also be important in determining the lattice conduction. This should be proportional to T^3 (§ 4.1).

3.3. *Hulm's Calculation of N_a*

An interesting feature of Hulm's paper is the section in which he has calculated, on the basis of Makinson's theory, the number of electrons per atom, N_a, both for his specimens and for some of earlier workers. He shows that the value of N_a comes out to be of the order of 0·03 whereas it is generally assumed that N_a is of the order of unity for the monovalent metals and should certainly be more than 0·03 even for those of higher valency.

3.4. *More Recent Work*

An investigation of the conductivity of several samples of one metal, aluminium, has been done by Andrews, Webber and Spohr (1951). They have measured the electrical and thermal conductivities of two single crystals and one polycrystalline specimen of high purity aluminium (99·995%) between 2 and 20° K. All the specimens had a very high conductivity, of the order of 50 watt units at their maxima, which occurred in the range 14–17° K. As is to be expected, the single crystals which were purer, and had fewer lattice defects had a higher conductivity than the polycrystalline specimen. They find that within the limits of experimental error, the lattice scattering term, α, is the same for each, confirming

Hulm's results mentioned above. The curves are shown to agree with those to be expected from Makinson's and Sondheimer's theories, although in order to make them fit quantitatively N_a has to be assumed to be of the order of 0·05. They suggest that this small value of N_a might be resolved

Fig. 4

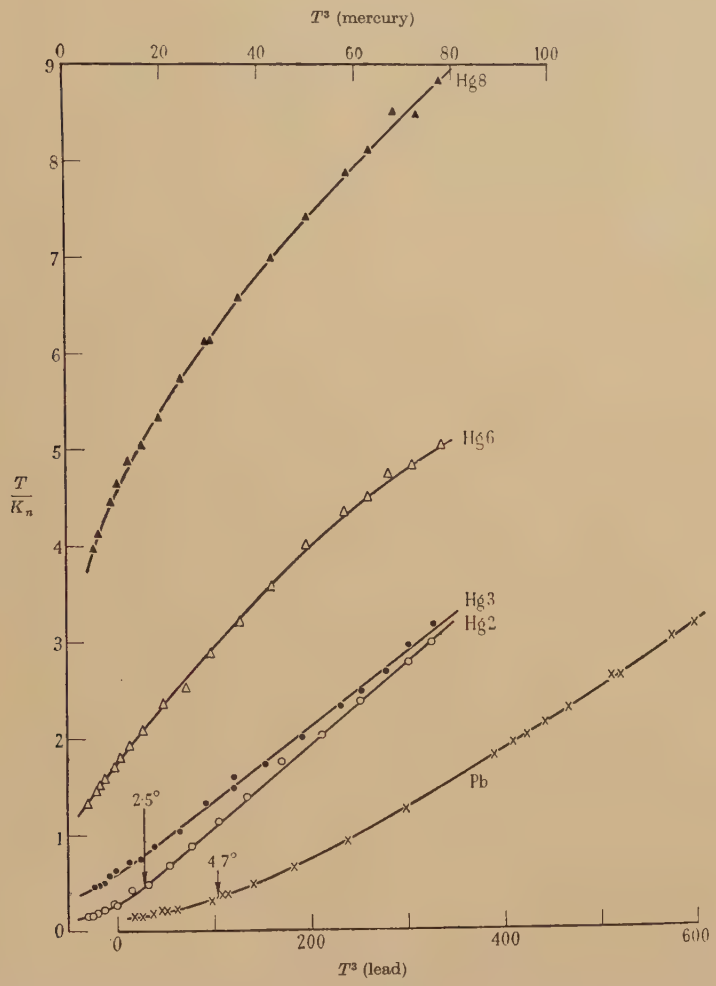

Variation of T/K_n with T^3 for mercury specimens and for the pure lead specimen of de Haas and Rademakers (1940). Hg 2, 3, 6, 8 have as impurity 0·002% Cd, 0·007% Cd, 0·10% In and 0·39% In respectively. (Hulm 1950.)

by modifying the transport theory of electrons to take into account the presence of filled and nearly filled zones in multivalent metals. Since however monovalent metals, which do not have nearly filled zones also give a small value of N_a by these theories it seems unlikely that this approach will solve the problem.

Johnston, Powers and Ziegler (1951) have measured the conductivities of pure iron, copper and aluminium and some aluminium alloys in the range 20° K to room temperature. One aluminium alloy did show a minimum in the conductivity but it is doubtful whether this really is strong evidence in favour of Makinson's theory since most alloys have an appreciable lattice conductivity and it is always possible to have suitable lattice and electronic components superimposed so that a minimum is obtained in the resultant conductivity.

A detailed series of experiments has been carried out by Mendelssohn and Rosenberg (1952 a, b) in which they have measured the thermal conductivities of as many metals as could be obtained in a very pure state. Over thirty elements have so far been investigated and the results give a general idea of thermal conductivity values and variation with temperature. All the metals of groups 1, 2, and 3 which were investigated had a fairly high conductivity of the order of 10 watt units or more in the neighbourhood of the maximum. In the 3d, 4d and 5d transition groups, the metals at the end of each group, i.e. the group 8 elements, have a much higher conductivity than the elements at the beginning of the group. Thus the conductivity of the iron specimen at 20° K was ~2 watt units, whereas the conductivity of manganese, the element before it in the 3d group, was about 0·02 watt units at the same temperature. It has been suggested by Mendelssohn and Rosenberg that this general effect is probably closely allied with the more complex crystal structure of these earlier elements and also to the fact that their general physical properties, e.g. hardness, ductility, etc. are very dependent on gaseous impurities which are very hard to remove.

3.5. *The Conductivity of Anisotropic Crystals*

One interesting set of curves that is presented is for two zinc single crystals from the same batch—one with the hexagonal axis at 80° to the rod axis and the other at 13° to the axis. The curves are identical at the high and low temperature ends but in the neighbourhood of the maximum the 13° crystal has a conductivity 10% greater than the 80° crystal. This is connected with the fact that the atomic spacing in zinc is different parallel and perpendicular to the hexagonal planes.

Later work of this type has been done on cadmium and gallium single crystals grown along different axes and this work may give an insight into the lattice–electron interaction.

3.6. *The Linearity of the $WT \sim T^3$ Curves*

Experimental results are frequently expressed in the form of curves of WT against T^3. They are seldom perfectly straight lines (fig. 4) and it seems of interest to calculate what deviation from linearity is to be expected from the theory.

At very low temperatures the function $\mathcal{J}_5$ in eqn. (5) is approximately constant and hence curves of WT against T^3 in this range will be linear.

As the temperature is increased however, $\mathcal{J}_5$ starts to decrease fairly rapidly and so the curve in this region will bend over towards the T^3 axis. The second term in T^4 involving both $\mathcal{J}_5$ and $\mathcal{J}_7$ is very small in comparison and can be neglected. It is of interest to estimate up to what temperature the $WT \sim T^3$ curve can be expected to be linear.

This we have done using the more accurate computations in Sondheimer's (1950) paper. These show (fig. 5) that for an ideally pure metal ($\rho_0/4A=0$) the curve deviates from linearity by 10% (i.e. the slope is changed by 10%) at a temperature of approximately $0{\cdot}125\,\theta$, and by 15% at $0{\cdot}144\,\theta$. With increasing impurity this deviation starts at progressively lower temperatures. With $\rho_0/4A=0{\cdot}03$ there is a 25%

Fig. 5

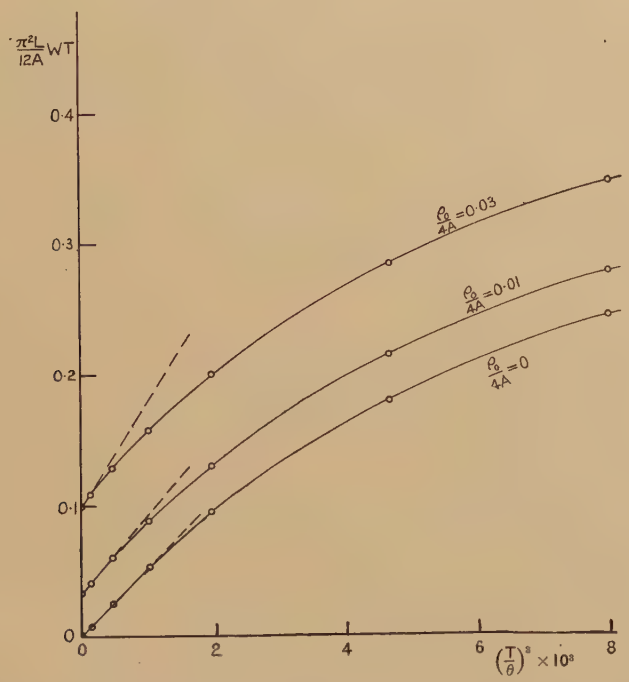

Graphs of WT against $(T/\theta)^3$ as calculated from Sondheimer (1950), showing how the departure from linearity depends on impurity.

deviation at $0{\cdot}1\,\theta$ and a 33% deviation at $0{\cdot}125\,\theta$. Incidentally this result that the impurity affects the deviation is an example of how Sondheimer's treatment shows that the ideal and impurity resistances cannot really be separated and that Matthiessen's rule is only a first approximation.

We should thus expect $WT \sim T^3$ curves to be linear up to about $0{\cdot}1\,\theta$ and above this temperature the curve should turn towards the T^3 axis. For most metals this does occur, confirming the theory, but in some cases the WT curve rises above the linear part. This is shown by Hulm (1950) for two mercury specimens Hg2 and Hg3 and also for a lead specimen of

de Haas and Rademakers (fig. 4). It also occurs in Mendelssohn's and Rosenberg's results for platinum and iridium and in later work on gallium. It seems exceedingly unlikely that in these specimens this could be due to lattice conduction, particularly since any increasing lattice conduction would tend to decrease the resistance.

It should not be expected, however, that the theory, which is only for monovalent metals, although it gives a qualitative picture for polyvalent metals as well, should hold to the extent of the higher approximations of the $W \sim T$ relationship.

§ 4. The Lattice Conductivity

4.1. *General Remarks*

The lattice conductivity in a metal is influenced by all the factors which determine it in a non-conductor, and in addition the presence of free electrons play an important role in reducing its magnitude. The lattice conductivity of non-metals is described in another article in this volume, but it will be convenient also to give a brief summary of the theoretical results for non-metals here.

In such substances the lattice conductivity is limited by a number of scattering processes to which correspond resistances which may be treated as additive. One may consequently write

$$1/K_g = W = W_D + W_B + W_U. \quad . \quad . \quad . \quad . \quad . \quad (20)$$

The terms are : W_D due to scattering of the lattice waves by defects in the crystal, these may be impurity atoms, unoccupied lattice points, or other dislocations ; W_B the term due to scattering of the lattice vibrations at the boundary of the specimen or at internal grain boundaries. W_U is the resistance due to interaction of the lattice vibrations amongst themselves. This is in the main due to umklapp processes.

The temperature dependence of these terms is given by

$$W_D \propto T,$$

$$W_B \propto T^{-3},$$

$$W_U \propto T^{v} \exp(-\theta/2T).$$

While eqn. (20) seems to be a satisfactory approximation, it is not completely reliable and in temperature regions where two of the terms are of the same order of magnitude, the total W becomes considerably larger than is to be expected from (20) (Klemens 1951). The total lattice conductivity in a pure specimen will have a maximum at about $\theta/20$ which may be of the order 20 watt units.

4.2. *The Effect of Electronic Scattering*

In the case of a metal the situation is complicated by the presence of electrons which scatter the lattice vibrations strongly. A further term has therefore to be added to the expression for W and we shall call this

resistance due to the electrons W_E. Sommerfeld and Bethe (1934) and Wilson (1936) find that this term is given by

$$1/W_E = G\left(\frac{T}{\theta}\right)^2 \mathcal{J}_3 \quad \ldots\ldots\ldots \quad (21)$$

where

$$G = \frac{k^3 h\theta^2 M}{2\pi^2 m^2 a^3 C_j^2} \quad \text{(Makinson 1938)} \quad \ldots\ldots \quad (22)$$

and the remaining symbols have the meanings used in the description of the theory of the electronic thermal conductivity in § 2.2.

Makinson assumes

$$C_j^2 = \tfrac{1}{3} C^2$$

where C is the interaction constant used in eqn. (7). This implies that the longitudinal and transverse waves interact equally with the electrons—which of course is contrary to the simple Bloch theory.

G may then be deduced from the electronic conductivity at high temperatures and it is found that

$$G = \frac{27}{4\pi^2 N_a^2} K_e \, (T > \theta) \quad \ldots\ldots\ldots \quad (23)$$

or $L_0 \sigma T$ may be substituted for K_e to give G in terms of the electrical conductivity at high temperature.

Then

$$G = \frac{27 L_0 \sigma T}{4\pi^2 N_a^2} \, (T > \theta). \quad \ldots\ldots\ldots \quad (24)$$

4.3. *The Lattice Conductivity in a Metal*

In fig. 6 we show a general picture of the variation of a typical lattice conductivity with temperature. At very low temperatures scattering by the crystal boundaries will be important and the conductivity will vary as T^3. At slightly higher temperatures scattering by the electrons will become predominant and the conductivity will vary as T^2. Still higher temperatures will make the impurities and finally the umklapp processes of importance.

It is of interest to calculate the absolute value of the lattice thermal conductivity which may be expected in a metal in the region where the scattering is mainly due to the electrons. At 10° K this yields a conductivity of 2×10^{-2} watt units for lead, and 4×10^{-3} watt units for tantalum, while a metal like bismuth with very small effective number of electrons will be expected to have a conductivity of the order of 15 watt units. It is therefore obvious that the lattice conductivity of a metal can only be measured if some steps can be taken so to reduce the electronic thermal conductivity that K_g becomes a very much more important contribution to the total conductivity than the fractional percent to be expected in a

pure metal with a large number of free electrons. This can be done in some cases in a high magnetic field, or by the addition of impurities. Descriptions of these methods are given in §§ 6 and 5 respectively.

§ 5. The Thermal Conductivity of Alloys

5.1. *The Effect of Impurities in a Metal*

As has been mentioned previously, the electronic thermal conductivity K_e is considerably reduced when a small amount of impurity is present. The impurity scattering becomes the dominant cause of thermal resistance over quite a wide temperature range, instead of being effective only at the lowest temperatures. It overshadows the resistive effect of the lattice vibrations and the curve of K_e against T shows no maximum but is linear up to quite a high temperature.

Fig. 6

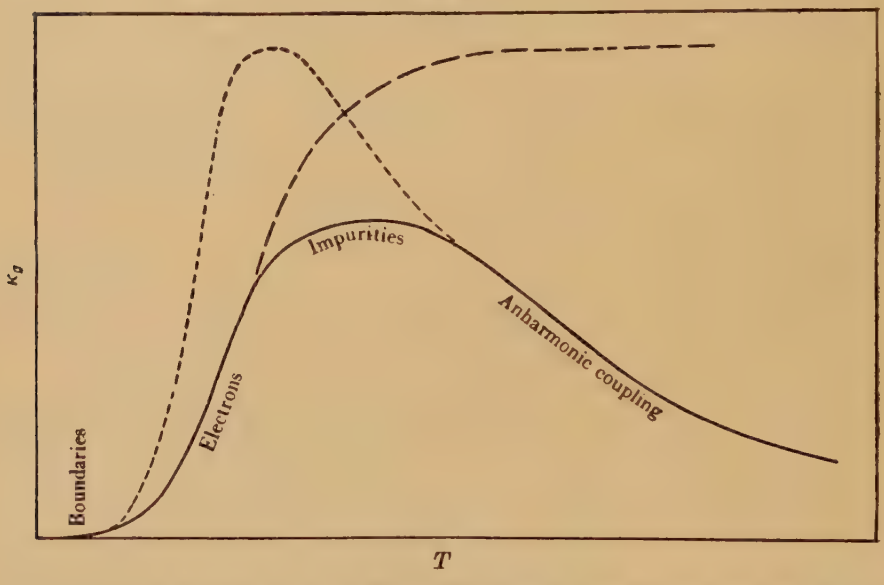

The theoretical general form of K_g. The dotted line shows the form for an insulator and the dashed line the form for a metal if only electrons scattered the lattice waves. (Makinson 1938.)

In an alloy (which will usually contain several percent of effective impurity atoms) the electronic thermal resistance is very much increased and K_e is very often reduced until it is of the same order of magnitude as K_g, the lattice conductivity, which is not affected so much. Hence the curves of total K against T for an alloy differ from those to be expected from a pure metal, not only by the orders of magnitude involved, but also by the fact that whereas in a pure metal K_g is negligible, in an alloy its contribution is a considerable proportion of K.

5.2. *Experimental Results*

Where the thermal resistance is dictated by impurity scattering the Wiedemann–Franz law holds and the value of K_e can be found from electrical measurements of the residual resistance ρ_0. Then we have

$$K_g = K - L_0 T/\rho_0 \quad . \quad . \quad . \quad . \quad . \quad . \quad . \quad . \quad (25)$$

This type of calculation has been made by Hulm (1951) and Berman (1951 b). Hulm's results on a Cu80 Ni20 specimen show that the lattice conductivity is proportional to T^2 between 2 and 20° K. This indicates that in this range the lattice waves are scattered by electrons.

This is borne out by the work of Berman (1951 b) on German silver, stainless steel and constantan in the range 2–90° K. He also finds the lattice conductivity is of the same order as the electronic conductivity and is proportional to T^2 up to 20° K. Above this temperature, however, the increase is more gradual and in all cases K_g reaches a maximum in the range 50–90° K. Berman has further analysed the lattice conductivity of his German silver specimen and has estimated the effects of the various scattering mechanisms (fig. 7). He suggests that whilst the low temperature scattering is due to the electrons, scattering due to small scale lattice defects and impurities becomes increasingly important at higher temperatures. This resistance W_D begins by being proportional to T but at higher temperatures becomes less temperature dependent. He also shows that the resistive effect due to scattering at grain boundaries W_B is only about $\frac{1}{2}\%$ of the total resistance at 2° K and it decreases rapidly at higher temperatures, hence it can be ignored.

Earlier work by Karweil and Schaeffer (1939) on German silver, silver bronze, contracid and steel also shows an abnormally high Lorenz number and hence an appreciable lattice conductivity.

5.3. *Alloys for Cryogenic Apparatus*

Cold working, which introduces dislocations into the lattice, usually decreases the conductivity (e.g. Cu90 Ni10 Estermann and Zimmerman 1951, 1952). It is difficult, however, to judge the effects of these treatments since no really systematic work on these lines has been done.

In general the conductivity of the various iron and copper alloys in the range 2–20° K is of the order of 10^{-2} or 10^{-3} watt unit. German silver and stainless steel are particularly bad conductors and for this reason are very much used in the construction of low temperature apparatus where the heat input must be cut down as much as possible. For the same reason constantan is particularly useful for the electrical leads into a cryostat or liquefier.

Berman (1951 b) has given a useful table which shows the heat flow down stainless steel, constantan and German silver when the ends of the specimen are at temperatures in the range 0–80° K. This is particularly useful when cryogenic apparatus is being designed.

5.4. *List of Alloys that have been Measured*

There would be no point in giving a full description of all the alloys that have been measured and the values obtained since this would add little to a general description of the subject. For reference, however, we give as complete a list as possible of papers which describe such experiments and the alloys that they deal with.

Fig. 7

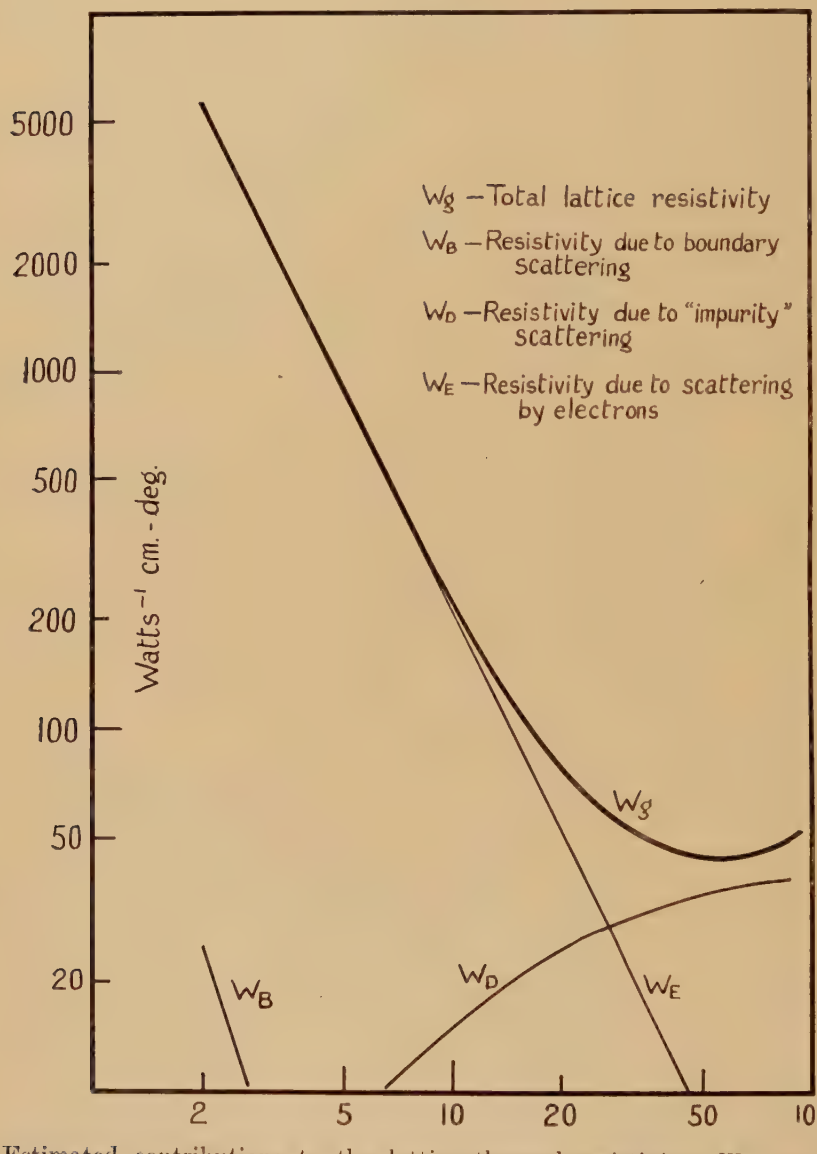

Estimated contributions to the lattice thermal resistivity, W_g, in German silver from scattering of the lattice waves by electrons, grain boundaries and ' impurities ' (i.e. lattice defects etc.). (Berman 1951 b.)

Karweil and Schaeffer (1939) German silver, silver bronze (Cu46 Zn41 Ni13), contracid B7M (Ni60 Cr15 Fe16 Mo7), steel.
Allen and Mendoza (1948) German silver.
Wilkinson and Wilks (1949) Nickel silver (Cu63 Zn17 Ni20), stainless steel, Cupro-nickel (Cu70 Ni30).
De Nobel (1951) monel, dural and various steels.
Estermann and Zimmerman (1951, 1952) monel, inconel, Cu90 Ni10, stainless steel.
Schmeissner and Meissner (1950) Croman B2Mo.
Hulm (1951) Cu80 Ni20.
Berman (1951 b) German silver, stainless steel, constantan.
Superconducting alloys.
de Haas and Bremmer (1936 a).
Mendelssohr and Pontius (1937) Pb90 Bi10.
de Haas and Rademakers (1940).
Hulm (1950) Tin/mercury, mercury/cadmium, mercury/indium.
Mendelssohn and Olsen (1950 a, b, c) and Olsen (1952). Lead/bismuth.

§ 6. Effect of a Magnetic Field on the Thermal Conductivity

6.1. *Early Work on Bismuth*

Just as the application of a magnetic field on a metal usually increases the electrical resistance, so in many cases it also increases the thermal resistance, although the thermal effect is not always so great as the corresponding electrical effect.

Some of the earliest work was done by de Haas, Gerritsen and Capel (1936) on bismuth single crystals. They found that whilst the thermal resistance increased with increasing field it tended to a saturation value in a field of 5·3 kgauss at liquid nitrogen temperatures and in a field of only 400 gauss at liquid hydrogen temperatures. This effect was interpreted by assuming that the lattice heat conductivity K_g was unaffected by the magnetic field and that the saturation value obtained by extrapolating to infinite field was in fact the value of the lattice conductivity. In this way they calculated K_g and K_e.

Experiments on bismuth at liquid air temperatures have also been carried out by Grüneisen, Rausch and Weiss (1950) who show that the effects of saturation in their specimens become evident in a transverse field of 10 kgauss. They calculate that $K_g = 0{\cdot}145$ watt units and $K_e = 0{\cdot}0493$ watt units at 85·7° K. These values are of the same order as those given by de Haas and his co-workers.

This is in agreement with theory which suggests that due to its small number of free electrons, bismuth should have an appreciable lattice conductivity. As the temperature is decreased the electronic contribution is reduced until nearly all the conductivity is due to the lattice.

Measurements by Shalyt (1944) at lower temperatures bear this out. In the range 2–4° K the conductivity curve seems to be due to the lattice, K varying as $T^{2\cdot5}$ approximately and the magnetic field of 4·2 kgauss has no effect. At 20° K this field increases the thermal resistance by 4% and at 65–80° K by 15 to 20%. This shows that the electronic contribution has reached a negligible amount in the lowest temperature region.

6.2. *Work on Antimony*

Similar work on antimony single crystals of various orientations has been done by Rausch (1947) in the liquid air region. In this case no saturation was found in a field of 10 kgauss and K_g and K_e were separated by a method (indicated below) involving the measurement of the electrical resistance in the magnetic field. Depending on the orientation of the crystal axis to the axis of the specimen the lattice conductivity varied between one-third and two-thirds of the total conductivity.

Measurements of conductivity were also taken in a constant transverse field which was rotated about the axis of the specimen. A periodicity was observed, the conductivity decreasing to a minimum and then increasing to a maximum in a rotation of 180°.

6.3. *Experiments on Tungsten*

Whilst these experiments are of interest, they do not give a good idea of the general results to be expected because neither bismuth nor antimony are good representative metals—both have a small number of free electrons and an appreciable lattice conductivity whereas in most metals the lattice conductivity is very small.

Early experiments on more normal metals were made by Grüneisen and Adenstedt (1938) who measured the effect of a field up to 12 kgauss on the thermal and electrical resistances of copper, tungsten and beryllium single crystals and of platinum and silver polycrystals at the temperature of liquid hydrogen. They found that only in the case of the single crystals was there an appreciable change in the thermal conductivity. The largest effect that they measured was for a beryllium sample whose thermal resistance increased about 60 times in a 12 kgauss field.

Experiments have also been made on a tungsten single crystal by de Haas and de Nobel (1938). Their work was in the range 14–20° K and in fields up to 26·3 kgauss. Later experiments by de Nobel (1949) extended the range of measurements up to a field of 36·4 kgauss. Both thermal and electrical conductivities were measured as a function of temperature and of field. At 15° K they found that the thermal resistance was increased 222 times in a field of 36·4 kgauss, several orders of magnitude greater than the bismuth results quoted above. Another difference they found was that the effect of the magnetic field increased at lower temperatures, whereas for antimony and bismuth the opposite occurred.

6.4. *Calculation of the Lattice Conductivity from Magnetic Effects*

The value of the lattice conductivity can be found as follows :— Since $K=K_e+K_g$ and K_e is related to the electrical conductivity, σ, by $K_e=L_e\sigma T$ where L_e is the Lorenz number, then

$$K=L_e\sigma T+K_g. \qquad \ldots\ldots\ldots (26)$$

Hence assuming that L_e does not alter in a magnetic field, a plot of K against σT as H is varied should be linear and the intercept on the K axis (i.e. at $H=\infty$) should give K_g.

This is the basis of the method for deriving K_g for antimony used by Rausch. For tungsten, however, de Nobel found that although at lower fields K was proportional to σ at constant temperature, at higher fields the slope of the curve was increased and he found it impossible to separate out the lattice and electronic components.

6.5. *Experiments on Beryllium*

Experiments on beryllium single crystals at 20° K have been done by Grüneisen and Adenstedt (1938) and Grüneisen and Erfling (1940). They measured the conductivity as a transverse field was rotated about the specimens and they found strong anisotropy, the conductivity being dependent on the angle between the field direction and the direction of the z axis of the crystal. By taking electrical measurements as well they were able to estimate the value of the lattice conductivity and confirm that at 20° K it is very small, while at 90° K it is a considerable proportion of the total conductivity. They also give rotation diagrams for copper and tungsten single crystals.

6.6. *Experiments in the Liquid Helium Region*

Up till recently very little work has been done in the liquid helium region. Hulm (1950) has determined the change in thermal resistance for pure tin at 4·29° K in a longitudinal field. He finds that the resistance is nearly doubled in a field of 1 500 gauss and that up to 400 gauss the relative change in conductivity $(K_0-K_H)/K_H$ is of the form $\lambda H/(1+\mu H^2)$ where K_0 and K_H are the conductivities in zero field and field H respectively and λ and μ are adjustable parameters. For small impurities in the tin no magnetic effect was observed.

Mendelssohn and Rosenberg (1951) have published measurements on a polycrystalline specimen of cadmium whose thermal resistance increases in a transverse field of 3·8 kgauss by a factor five at 4·4° K and by over seven times at 2·2° K (fig. 8). In a longitudinal field the effect was very much smaller. They have continued this work with other elements (1952 c) and in general they find that a field of 3·8 kgauss produces a measureable effect only in metals that have a relatively low melting point and are mechanically rather soft. So far measurements have been taken on polycrystalline indium and thallium and on single crystals of zinc,

cadmium, tin, lead and gallium. In general the graphs of thermal resistance against field are linear except for small fields up to 300 gauss. A given field usually has an appreciably larger effect at lower temperatures and the effect of a transverse field is usually much greater than that of a longitudinal field. They also find that the effect is greatly reduced in polycrystalline specimens and also by the presence of impurities.

6.7. *The Theory of Sondheimer and Wilson*

The simple quasi-free electron model of a metal is of no use for giving us an insight into the magnetic effects as it gives us zero change of resistance in a magnetic field. A more complicated model must be used which, however, must still be simple enough for us to be able to derive a result that

Fig. 8

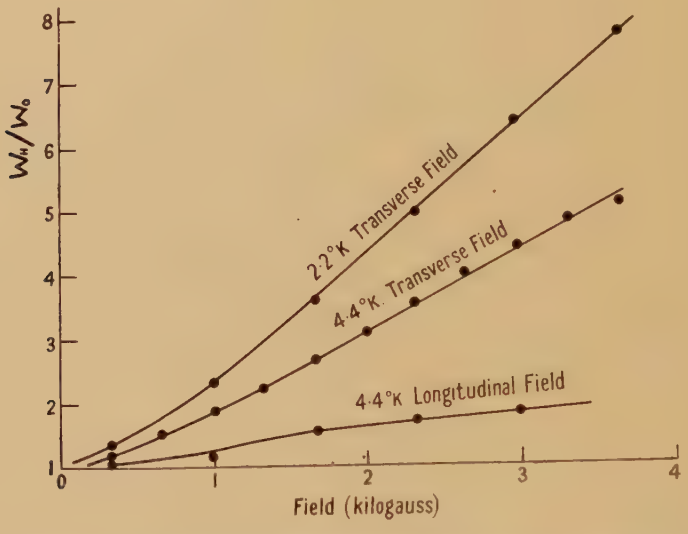

The increase in the thermal resistance of cadmium in a magnetic field. (Mendelssohn and Rosenberg 1951.)

is capable of being evaluated. The simplest model assumes that the conduction electrons occupy two overlapping bands, the s and d bands and there is no interaction between the electrons in one band and those in the other. The heat flow is calculated separately for each band and the total flow is obtained by simple addition.

This is the model used by Sondheimer and Wilson (1947) who calculate the conductivity due to each band under the influence of a transverse magnetic field using as a basis the theory given by Wilson (1936) and developed by Makinson (1938). This model is not sufficiently general to give a non-zero result for longitudinal fields. They find simplified formulae for high and low temperatures and for a large magnetic field and a general formula is given which reduces to these in the three limiting cases,

If n_s is the number of electrons in the s band, n_d is the number of holes in the d band then

$$\frac{K_0-K}{K}=\frac{CH^2}{1+FH^2}, \text{ for } n_s\neq n_d, \quad . \quad . \quad . \quad . \quad . \quad (27)$$

$$\frac{K_0-K}{K}=EH^2, \quad \text{for } n_s=n_d \quad . \quad . \quad . \quad . \quad . \quad (28)$$

where C, E and F are functions of K_0, T, n_s and n_d. Hence for $n_s\neq n_d$ we get saturation at large fields and for $n_s=n_d$ we get infinite resistance in infinite field. They also show that the application of a magnetic field does not affect the lattice thermal conductivity. The corresponding electrical effects have also been calculated and the dependence of the Lorenz number, L, on the field is given.

6.8. *The Theory of Kohler*

Similar results have been derived by Kohler (1949 a, b, c). His first paper (1949 a) gives the general equation

$$\frac{\Delta W}{W_0}=G\left(\frac{H}{W_0TL}\right) \quad . \quad . \quad . \quad . \quad . \quad . \quad . \quad (29)$$

where ΔW is the change in the thermal resistance in a field H, W_0 is the thermal resistance in zero field and L is the theoretical value of the Lorenz number. This is the type of relation we should expect on the basis of Kohler's rule for the change of electrical resistance in a magnetic field, if we assume L to be independent of T. This he applies to the results of de Haas and de Nobel for their tungsten single crystal.

He shows that a plot of $\Delta W/W_0$ against H/W_0TL gives a single curve for all the experimental points and G is a monotonically increasing function. The second paper (1949 b) deals with the special case of a metal with $n_s=n_d$ in a strong magnetic field and he derives the relation, which can be obtained from (28), that at constant temperature K_e is proportional to $1/H^2$. This he uses to give the following method for separating K_e from K_g without necessitating any electrical measurements. We have $K_H=K_g+K_e=K_g+E/H^2$. Thus a plot of K_H against $1/H^2$ should give a straight line with an intercept of K_g. This he applies to the measurements on beryllium crystals of Grüneisen and his co-workers.

The third paper (1949 c) gives the theoretical derivation of the formulae in which he obtains the same results as Sondheimer and Wilson. This he generalizes to the equation containing the function G quoted above.

6.9. *Comparison of Theory with Experiment*

Recent work seems to confirm eqn. (29) given by Kohler although the function G does not appear to be in the actual form that he or Sondheimer suggests. This is not surprising since the models used are really too simple to enable quantitative results to be obtained although they do give a qualitative picture. From the results of Mendelssohn and

Rosenberg (1952 c) in the range 2–5° K, graphs of $\Delta W/W_0$ against H/W_0T show that all the experimental points for one metal at different temperatures do lie on a single curve. Since these results cover a change in temperature of 100% this is a much more stringent test than that applied by Kohler himself from the results of de Haas and de Nobel on tungsten, since this work was in the liquid hydrogen region and the maximum temperature change was only 25%. Graphs for the effect

Fig. 9

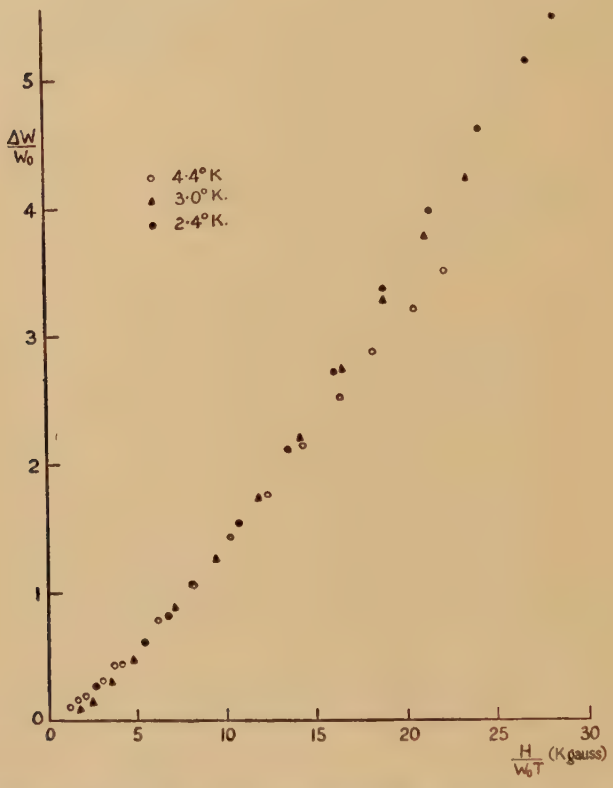

$\Delta W/W_0$ against (H/W_0T) for tin in a transverse magnetic field, showing how the points for three different temperatures fall approximately on one curve. (Mendelssohn and Rosenberg 1952 c.)

of a magnetic field on the thermal conductivity of tin are shown in fig. 9. It can be seen that whilst $\Delta W/W_0$ varies as approximately $(H/W_0T)^2$ for small values of H/W_0T, for larger values the ratio tends to become proportional to H/W_0T.

The points corresponding to high fields at the lowest temperatures, however, do tend to fall above the main line of the curve, but it should be noted that the maximum field of 4 kgauss at 2° K corresponds to 40 kgauss

at 20° K. It is possible that the variation of L with field may be appreciable in this region and this has not been taken into account. In general no sign of saturation has been observed in the normal metals.

Similar graphs for the effects due to a longitudinal field show that Kohler's equation holds in this case as well, although the curves are not linear and tend to bend over slightly towards the H/LW_0T axis.

We should note that the assumption of two bands having additive conductivities each limited by resistances obeying Matthiessen's rule cuts out any possibility of the total conductivity obeying this rule.

§ 7. The Thermal Conductivity of Superconductors

7.1. *Theory*

The theory of the thermal conductivity of a metal in the superconducting state is by no means in the advanced stage which the theory of the normal state has reached. However, a fairly simple consideration of the factors involved allows one to draw conclusions of some interest.

A superconductor below the transition point which has had its superconductivity destroyed by the application of a magnetic field will presumably (except for the effects of magneto resistance) behave in the way we have described in the preceding paragraphs for normal metals. We may then write eqn. (1) in the form

$$K_n = K_{en} + K_{gn}. \quad . \quad . \quad . \quad . \quad . \quad . \quad . \quad (30)$$

Here we have added the suffix n to indicate that it is the behaviour in the normal state that we are discussing. The values for K_{en} and K_{gn} will be governed by the same factors that were found to govern the values of K_e and K_g.

In the absence of a magnetic field, however, when the substance is superconducting, the distribution of the electrons in phase space will be altered, and it may be expected that the electronic thermal conductivity in the superconducting state K_{es}, will be different from K_{en}. Since K_{gn}, the lattice conductivity in the superconducting state, is also to a large extent dependent upon the amount of scattering by the electrons, we may expect that the new electronic distribution will also cause a change in the lattice thermal conductivity from its normal value.

It was pointed out be de Haas and Rademakers (1940) that the 'superelectrons' which carry the resistanceless current in a superconductor cannot be expected to take part in carrying the thermal current and that therefore K_{es} would be expected to be smaller than K_{en}. Hulm (1950) has pointed out that since the 'superelectrons' move without friction against the lattice, they presumably do not contribute to the scattering of the lattice waves and that therefore K_{gs} might be expected to be greater than K_{gn}.

We thus have for the superconducting state

$$K_s = K_{es} + K_{gs}, \quad . \quad . \quad . \quad . \quad . \quad . \quad . \quad . \quad (31)$$

where $K_{es}<K_{en}$, and where $K_{gs}>K_{gn}$. Since in pure substances K_{en} is much greater than K_{gn} we may expect that, unless the change in K_g is very large, the total K_s will be smaller than the total K_n.

Whilst the above general remarks give a qualitative idea of the behaviour, some more detailed prediction of the actual values of the ratios K_{es}/K_{en} and K_{gs}/K_{gn} is of course desirable. Such a calculation has been made by Heisenberg (1948) on the basis of his theory of superconductivity and the calculations of Koppe (1947).

Heisenberg considers the general formula for the thermal conductivity

$$K=\tfrac{1}{3}lvC, \quad . \quad . \quad . \quad . \quad . \quad . \quad . \quad . \quad . \quad (32)$$

where l is the mean free path, v the velocity of the particles carrying the thermal current and C their specific heat.

As a rough approximation he assumes that the mean free path of the ' normal ' heat transporting electrons in the superconducting state is longer than that of the electrons in the normal metal by a factor $1/(1-w/2)$ where w is the fraction of superelectrons. v is of course very nearly the same in the two states and

$$C_s=C_n k(w), \quad . \quad . \quad . \quad . \quad . \quad . \quad . \quad . \quad (33)$$

where $k(w)$ is a function which at the highest temperatures is very nearly equal to the value to be expected on the Casimir-Gorter (1934) theory of superconductivity. For $T/T_c>0{\cdot}3$ this gives to a fair approximation

$$K_{es}/K_{en}=2t^2/(1+t^4), \quad . \quad . \quad . \quad . \quad . \quad . \quad . \quad (34)$$

where $t=T/T_c$. At lower temperatures this is no longer correct and the ratio of the two conductivities falls exponentially with temperature (Goodman 1951). It is pointed out by Heisenberg that the approximation chosen for the mean free path of the ' normal ' electrons can only be relied upon for the case where the main scattering of the electrons is by impurities and that this calculation also contains other approximations which may be expected to break down in the vicinity of the transition temperature.

The success of the theory of Fröhlich (1950) in explaining the isotope effect on the critical field and transition temperatures of superconductors seems to indicate that the Heisenberg theory and calculations of the type described above should not be taken too literally. On the other hand it would appear that the Heisenberg theory has been so adjusted that one may expect it to give a reasonably correct estimate of the behaviour of the superconducting thermal conductivity.

7.2. *The Circulation Hypothesis*

Before continuing to a description of the experimental side of the subject it is appropriate to mention an interesting idea first suggested by Mendelssohn (1946) and later used by Mendelssohn and Olsen (1950 a, b, c) in an attempt to explain certain of their results. It was suggested that there might exist in superconductors an analogue of the fountain effect in liquid helium II. This would consist of a stream of ' superconducting '

electrons flowing from the cold to the hot end of a specimen, being converted to ' normal ' electrons there and flowing back as ' normal ' electrons with a finite heat content, which is given up at the cold end of the specimen again. Thus a circulation process is set up. This circulation might be expected to vanish at the transition temperature and at the absolute zero and to have a maximum at some intermediate temperature. Its absolute magnitude would be difficult to calculate a priori.

7.3. *Experimental Work*

While experiments were made as early as 1914 by Kammerlingh-Onnes and Holst to investigate whether the thermal conductivity showed as startling a discontinuity as the electrical conductivity, no further research was carried out in this field until the thirties (de Haas and Bremmer 1931, 1936 b, Mendelssohn and Pontius 1937, and de Haas and Rademakers 1940). The results of these investigations were that for pure substances K_n was greater than K_s, while for alloys this was not always so. The ratio K_s/K_n even for the pure metals showed two distinct types of behaviour. In the case of tin this was very like that to be expected as the result of Heisenberg's calculation, but in lead K_s/K_n did not approach unity asymptotically as predicted by eqn. (34) but the superconducting curve approached the normal one at a finite angle (fig. 10). A similar effect was also observed in mercury by Hulm (1950). He carefully investigated the behaviour of the ratio K_s/K_n in a series of tin and mercury specimens containing small known amounts of impurity. He showed that for the ideal case of a metal where the main mechanism limiting the mean free path of the electron is scattering by impurities, the ratio K_s/K_n is given by a characteristic function $f(t)$ very closely resembling that suggested by Heisenberg. For the ideal case of lattice scattering alone (pure lead and pure mercury) the ratio K_s/K_n is given by some other function which he denotes by $g(t)$. Hulm suggests that $g(t)$ is very well represented by t^5. At low temperatures even in the purest samples the impurity scattering will become predominant, and there K_s/K_n will tend to the impurity scattering type of function, $f(t)$.

In fig. 11 we show values of K_s/K_n for lead, tin and mercury specimens of various purities. This information has been drawn from papers by de Haas and Rademakers (1940), Rademakers (1949), Hulm (1950) and Olsen (1952). It seems reasonable to suppose that the shape of the K_s/K_n curve might be a function of the proportion of the impurity scattering present and we have therefore marked all the curves with a parameter X which gives this relationship. We have defined

$$X=\alpha T^3/\beta, \qquad \ldots\ldots\ldots \quad (35)$$

where α and β are the constants occurring in eqn. (11). Thus the larger the value of X the smaller the relative amount of impurity scattering. It will be seen that although K_s/K_n may to a moderate accuracy be described as a function of T/T_c and X only, this can at best be a first approximation.

Interpolation formulae have been given by Hulm (1950) and by Olsen (1952) to describe the behaviour of the thermal conductivity for specimens with finite values of X.

Neither of these formulae can be considered to be very satisfactory. That given by Hulm is based upon a method of calculation which would appear to imply that the reduced value of the thermal conductivity in the superconducting state is a consequence of a decreased mean free path of the electrons when the substance becomes superconducting, rather

Fig. 10

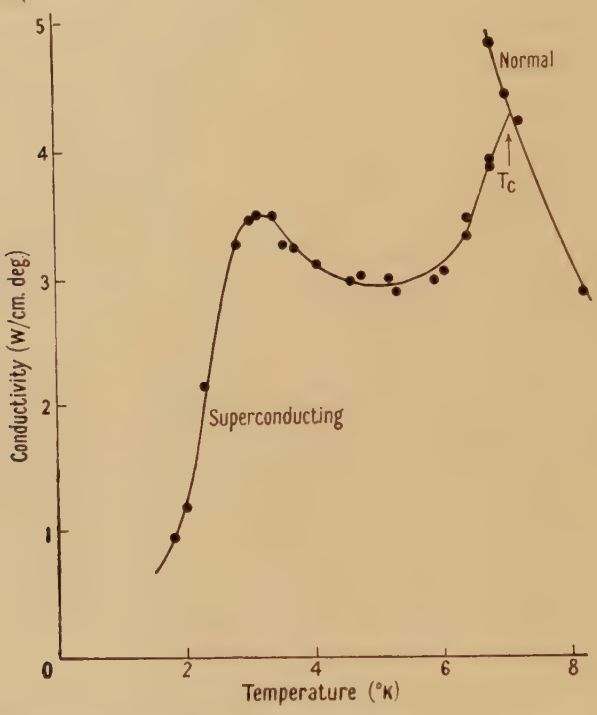

The thermal conductivity of lead in the superconducting state, showing the sharp breakaway from the normal curve at the transition temperature. (Mendelssohn and Rosenberg 1952 b.)

than being due to a fall in the effective number of electrons. The formula given by Olsen although empirical would also appear to imply a rather unrealistic solution to the problem of combining the mean free paths.

7.4. *The Lattice Conductivity in the Superconducting State.*

In some cases the thermal conductivity lies considerably above the value to be expected from the Heisenberg theory. We have seen in fig. 11 that the K_s/K_n ratio became larger in the tin and mercury alloys as

the impurity increased and the absolute value of the thermal conductivity decreased. Abnormally high values were found in the prewar results on alloys containing large percentages of indium and bismuth (de Haas and Bremmer 1936, Mendelssohn and Pontius 1937). Mendelssohn and Olsen (1950 a) were able to show that for lead–bismuth alloys the K_s/K_n function could be made to vary, as bismuth impurity was increased, from a function like that found by de Haas and Rademakers, to one where the K_s/K_n increased from unity to ten as the temperature was lowered from the critical to one third the critical temperature. They suggested that this might best be explained by some additional flow of heat such as that described in § 7.2.

Fig. 11

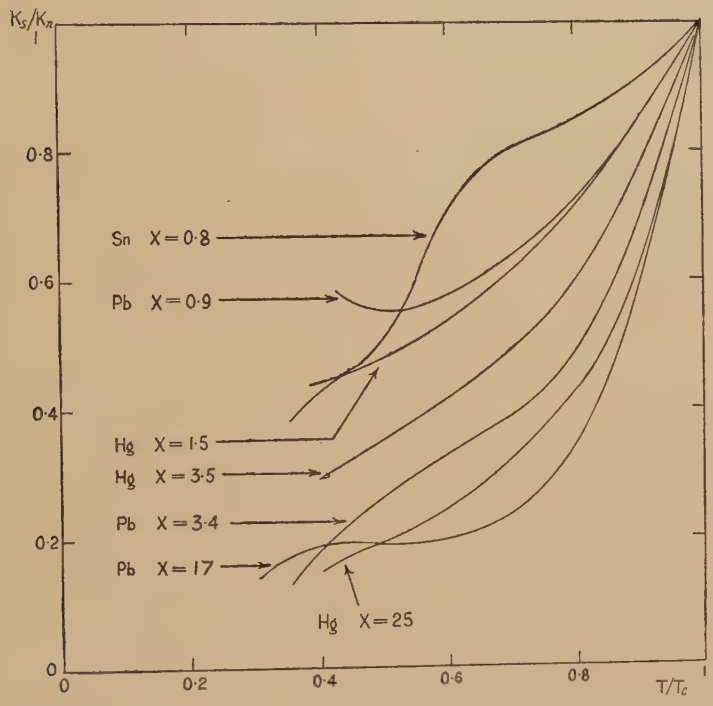

Graphs of K_s/K_n against T/T_c for tin, lead and mercury showing their dependence on X, the relative amount of impurity scattering. From various sources, see § 7.3.

An examination of the consequences of the alternative assumption (suggested by Hulm 1950), that these high values for K_s are due only to an increase in the lattice conductivity in the superconducting state, has been made by Olsen (1952). Assuming also the validity of his interpolation formula for K_{es}/K_{en} he calculated K_{gs}/K_{gn}. This could be described with very moderate accuracy by t^6. This does not seem to be far from what might be expected if one remembers that when the

electronic thermal conductivity of superconductors is limited mainly by the lattice scattering of the electrons then K_s/K_n varies as t^5. On the other hand, the only case for which Hulm has made an evaluation of the amount of the lattice conductivity indicates that the superconducting lattice conductivity increases only as the second power of the temperature. However, in the tantalum specimen for which these calculations were made the amount of impurity scattering of the lattice waves was very considerable.

In order to disentangle the problems sketched above it would appear to be extremely desirable for some more accurate work to be carried out to clarify the behaviour of the K_s/K_n ratio and hence that of the lattice conductivity. Only a series of measurements on different substances and with varying impurity contents would allow sufficiently confident estimates of K_{es}/K_{en} to be made to establish the temperature dependence of the lattice conductivity in the superconducting state.

7.5. *Thermal Conductivity in the Intermediate State*

The experiments of Mendelssohn and Pontius (1937) and of de Haas and Rademakers (1940) showed that when the superconductivity of a cylinder of pure lead was destroyed by a transverse magnetic field the heat resistance changed almost linearly from its superconducting to its normal value as the field was increased from $\frac{1}{2}H_c$ to its critical value H_c. A specimen of lead containing 10% bismuth showed a more extended transition, as might also be expected from a knowledge of the electrical behaviour of superconducting alloys. This linearity of the change of thermal resistance is in good agreement with that obtained if calculations are carried out on the assumption that the cylinder in the intermediate state is made up of a series of laminae normal to the axis, each with either the normal or the superconducting conductivity.

Measurements of the transition in a longitudinal field have been made by Hulm (1950) on tin, and Mendelssohn and Olsen on lead, and it is found that these transitions are sharp within the limits set by the demagnetization factors of the specimens. In the case of lead at 2·7° K it is even found (Olsen 1952) that the transition in the thermal conductivity is sharper than the electrical transition observed by MacDonald and Mendelssohn (1949) in very pure specimens of small demagnetizing factor.

Transverse transitions observed by Mendelssohn and Olsen (1950 c) in lead with a small (0·02%) impurity of bismuth at 5·3° K were found to be similar to those found by earlier workers. At a lower temperature (2·9° K) however, an entirely new and unexpected type of transition (fig. 12) occurred. Instead of increasing monotonically from the superconducting to the normal value as the magnetic field increased, the thermal conductivity fell very sharply when field first penetrated the metal, and then after reaching a minimum the conductivity increased to the normal value. This has since been found in pure lead by Webber and Spohr (1951), Olsen and Renton (1952) and Mendelssohn and

Rosenberg (1952 c). Detwiler and Fairbank (1952) have also observed similar transitions in very pure tin and indium at about 2·2° K. This behaviour is of course inconsistent with any combination of regions having either the normal conductivity K_n, or the superconducting conductivity K_s, and this has been pointed out by Mendelssohn and Olsen (1950 c).

A solution can however be found in terms of either of three explanations. That first suggested by Mendelssohn and Olsen was one based on the hypothesis of a heat circulation in the superconducting state. A second explanation is based on a suggestion by Landau (1943) that there might be an extra scattering of the electrons at the boundaries of the laminae

Fig. 12

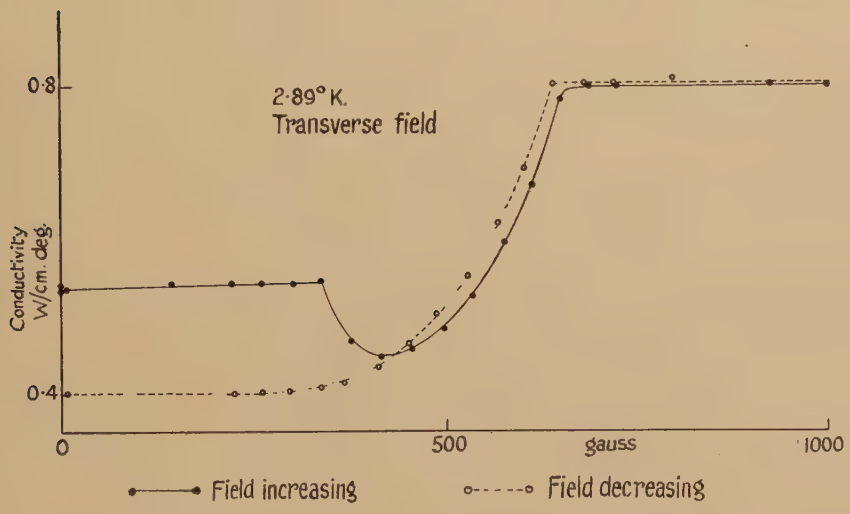

The change in the thermal conductivity of a lead–bismuth alloy during the transition from the superconducting to the normal state showing the initial decrease in the conductivity in increasing field. (Mendelssohn and Olsen 1951 c.)

constituting the intermediate state. The transitions observed may however also be explained on the basis of Hulm's suggestion of an increased superconductive lattice conductivity (Olsen 1951, Webber and Spohr 1951, Olsen 1952) if the mean free path of the electrons and/or lattice waves is comparable in length with the thickness of the regions forming the intermediate state. The appearance of a very small percentage of normal material can then remove the high lattice conductivity.

7.6. *Work below* 1° K

The first work on the thermal conductivity of superconductors below 1° K was carried out by Heer and Daunt (1949 a). They were able to measure K_s/K_n for tin and tantalum between 0·2 and 1° K and their

measurements indicated that K_s/K_n varied as $(T/T_c)^2$. For tin at 0·65° K it was found that $K_s/K_n = 1/40$, and for tantalum at 0·55° K that $K_s/K_n = 1/60$.

Goodman (1951) has measured the thermal conductivity of tin specimens of various purities down to 0·2° K. He was able to eliminate the effect of the lattice conductivity and he gives a curve for the ratio K_{es}/K_{en}. This is found to be in close agreement with the ratio obtained from Heisenberg's theory.

Olsen and Renton (1952) have made measurements on a lead single crystal down to 0·3° K. They find that the superconducting thermal conductivity follows a T^3 law below about 0·9° K. Above that temperature the conductivity rises somewhat more steeply.

Heisenberg's theory and Goodman's experimental work indicate that the electronic thermal conductivity will be very small below 1° K. It is therefore reasonable to suppose that the conductivity is entirely due to the lattice. The actual observed conductivity would correspond to the case of pure boundary scattering with free path 5 times less than the diameter of the single crystal rod. It is not clear whether this discrepancy is to be ascribed to an unreliability in the simple theory of boundary scattering or whether it is simply due to filaments of normal metal remaining frozen in after demagnetization. Such filaments might also be expected to give a $1/T^3$ term in the thermal resistance. The closeness with which the conductivity follows a T^3 law would appear to confirm that the amount of electronic scattering of the lattice waves is very small.

Olsen and Renton have also measured the variation with magnetic field of the thermal conductivity at 0·43 and 0·7° K. Their curves show the minimum observed at higher temperatures, but in a less pronounced form. The possibility of some field remaining frozen in after the demagnetization makes it difficult to draw reliable conclusions from these measurements, but the shallowness of the minimum might well be taken as evidence that K_{es} and K_{gs} are more nearly equal than is assumed above.

§8. Experimental Techniques

8.1. *General Arrangement*

The basic set-up for all the experimental work is essentially the same. The specimen is in rod form, a few centimetres long and perhaps up to five millimetres in diameter. It is usually mounted vertically by one end in an evacuated container so that no heat can be transmitted by conduction or convection to the walls. This end is in good thermal contact with a liquid helium bath for the lowest temperature measurements and with liquid hydrogen or air for readings at higher temperatures. Radiation losses are small at these temperatures, but in some cases a radiation shield is fitted to surround the specimen and the thermometers. A small electric heater is fitted to the free end of the specimen. Potential as well as current leads are fitted to the latter so that the power supplied can be measured. This is usually of the order of a few milli-watts,

8.2. *Measurement of the Temperature Difference*

The measurement of the temperature difference along the rod due to a given heat flow from the free end, was in the earlier experiments made with one thermometer (e.g. de Nobel 1951). This was attached near the heater and the fixed end of the rod was assumed to be at the temperature of the helium bath, which could be found with a knowledge of its vapour pressure. Whilst this assumption is sometimes quite justified, it requires an almost perfect thermal contact at the cold end and this is in many cases extremely difficult to make. A more satisfactory method of measuring the temperature gradient is to use two thermometers fixed a few centimetres apart along the rod. This is done in most of the recent work. The thermometers are either helium gas thermometers or electrical resistance thermometers and the measuring device either records the absolute temperature of each thermometer, or a differential arrangement is used which gives the temperature difference directly.

8.3. *Resistance Thermometers*

Electrical resistance thermometers have been used by de Nobel (1949, 1951) and by Allen and Mendoza (1948). De Nobel (1949) used lead resistance wire for measurements in the liquid hydrogen range. These were calibrated against a platinum resistance thermometer. For experiments in a magnetic field they were calibrated in that field against the vapour pressure of hydrogen. Allen and Mendoza, in the liquid helium range have used phosphor-bronze wire wound on copper formers. At each temperature where a reading was required the thermometers were calibrated at four or more points about 0·01° apart, against the helium vapour pressure. Temperature differences of 0·01 degrees were used. They state that two or three temperatures could be measured to 2% in a three to four hour run. For experiments below 1° K carbon resistance thermometers have been used (Olsen and Renton 1952).

8.4. *Gas Thermometers*

The advantage of electrical resistance thermometers is that the external equipment required is readily available—a potentiometer or a bridge—and that they are probably simpler to make and to fit than are gas thermometers. Nevertheless gas thermometers are widely used. The most important reason for this is that the calibration is unaffected by a magnetic field and hence they are particularly useful in the investigations of superconductors and magneto-resistive effects. Another advantage is that the number of calibration points required is very small because the gas can be assumed to obey the ideal gas laws so long as the pressure is not too high. Hence a calibration at the boiling point of liquid hydrogen is usually sufficient for readings between 10° and 40° K, and one at the boiling point of liquid helium for readings between 2° and 10° K, although these can be supplemented by extra calibrations against vapour pressure of the bath at various temperatures. A correction must

be applied to take into account the 'dead' or external volume of the gas thermometer system and for this reason the connecting capillary and the dead space at the top of the manometer used to measure the gas pressure should be made as small as possible. In this way the corrections can be greatly reduced. To measure temperature differences directly, it is simple to connect the two thermometers to opposite sides of a differential manometer, a U-tube containing butyl phthalate usually being used. The difference in levels then gives a direct indication of the temperature difference. Such an arrangement also cancels out certain small correction factors.

When used in this way it is important that both thermometers and their tubing have exactly the same dimensions. This is usually achieved sufficiently by careful machining and measurement although Andrews, Webber and Spohr (1951) have gone farther and have etched the copper thermometer bulbs and have then adjusted a moveable piston in a cylinder in one thermometer circuit until no difference in pressure was observed between the two thermometers when the temperature was varied from nitrogen to room temperature. It is of course important, particularly if the external volume is unavoidably large, to protect it from sudden changes of temperature. The absolute pressure in each thermometer can be measured by joining a third arm, which is kept continuously pumped, to the centre of the differential manometer. Systems on these lines are used by Hulm, Andrews, Webber and Spohr, Berman and MacDonald, Estermann and Zimmerman, Mendelssohn and Olsen, and Mendelssohn and Rosenberg. The difference in levels is measured on a scale either directly or through a telescope. Hulm (1951) illuminated the meniscuses from behind and measured the position of each on a travelling microscope and could measure temperature differences of the order of 0·01 degree to about 1%. Estermann and Zimmerman (1951) had an interesting arrangement in which a calibrated adjustable bellows in one limb of the manometer was adjusted until the difference in levels in the manometer was zero. From the amount of movement required the temperature difference could be calculated. This method had the advantage that no external volume correction was necessary. They were not able, however, to measure the absolute temperature of the thermometers and they had to estimate the temperature of the specimen from the temperature of the helium bath. This necessitates having a very good thermal contact between the bath and the specimen.

8.5. *Thermal Contact with the Specimen*

The attachment of the specimen to the thermometers occasionally causes difficulty, especially if the metal will not take hard or soft solder. In this case it is sometimes possible to copper plate the specimen and to soft solder on to this plating. This has been done for the aluminium specimens of Webber, Andrews and Spohr (1951). Another technique is to spot weld a small platinum ring to the specimen and to solder a copper contact to this ring. The copper is then soldered with Wood's

metal to the thermometer. Mendelssohn and Olsen have used this method for tantalum and niobium. Small clamps can be used if soldering techniques are not possible and in this case thermal contact can be improved by coating the clamp and specimen with glycerol or celluloid cement before tightening it up.

8.6. *Method of Mounting for Magnetic Measurements*

Most workers have mounted their specimens vertically in the apparatus. If magnetic measurements are being taken, however, it is often convenient to mount it horizontally, because readings can then be taken in both a transverse and in a longitudinal field with the same type of magnet. If the specimen is vertical two different magnets will be required—a solenoid for the longitudinal field and an ordinary magnet for the transverse field.

8.7. *Attainment of Steady Temperatures in the Full Range up to* 90° K

In order to obtain results over the full temperature range it is necessary to obtain steady temperatures not only in the helium, hydrogen and oxygen regions, but also in the ranges 4–10° K and 20–60° K. Temperatures in the 4–10° K region are obtained fairly easily if a Simon expansion liquefier is used. The gas is not expanded fully to atmospheric pressure but is allowed to expand slowly. By controlling this expansion with a needle valve any temperature between 4 and 10° K can be maintained (MacDonald and Mendelssohn 1950). For temperatures above 20° K a small heater is fitted either to the fixed end of the specimen or around the high pressure pot of the liquefier and this is used to raise the temperature of the specimen by any desired amount above 20° K. This method may also be used for temperatures between 4° and 10° K.

Further details covering the experimental technique of gas thermometry are given by Hulm (1950) and Berman (1951 a).

8.8. *Method of Wilkinson and Wilks*

A useful method of determining the mean conductivity of a specimen has been given by Wilkinson and Wilks (1948). One end of the specimen is in contact with liquid helium but the other one is kept at the temperature of liquid hydrogen. The heat input is found by measuring the amount of liquid helium which is evaporated. No heater or thermometers are required. This is a particularly useful technique when information is needed regarding materials to be used in the construction of low temperature apparatus.

8.9. *Technique below* 1° K

Measurements in the adiabatic demagnetization region present new problems both because of the limited range of thermometers available, and because of the need for very small heat input.

Heer and Daunt (1949 a) used the specimen as a connecting link between a large and a small pill of paramagnetic salt. These were demagnetized to slightly different temperatures, and the heating up rate

of the smaller pill was observed with the specimen in the normal and in the superconducting state. Goodman (1951) also used a two-pill technique, but with pills of equal size. The rate at which temperature equilibrium was established between the two pills was observed. He was able to allow for the effects of contact resistance between salt and specimen by making measurements on several specimens with a wide range of conductivities.

Olsen and Renton (1952) had only a single pill and used a technique similar to that normally used at higher temperatures. Carbon thermometers painted directly on the specimen measured the temperature gradient established by a small electric heater at one end of the specimen. It was of course necessary to work with very small heat inputs to avoid heating the paramagnetic salt too rapidly. One advantage of this technique is that it allows measurement of approximately isothermal magnetic hysteresis cycles.

8.10. *Superconducting Heat Switch*

One of the problems of very low temperature work is the need for a method of making and breaking thermal connection between different parts of an apparatus. The normal method using an exchange gas ceases to work at temperatures below about 0·7° K when even helium has too low a vapour pressure to conduct heat effectively. The use as a heat switch of a superconductor where K_n and K_s are widely different has been suggested independently by Gorter (1948), Heer and Daunt (1949 a, b) and by Mendelssohn and Olsen (1950 a).

Darby, Hatton, Rollin, Seymour and Silsbee (1951) have successfully used this type of heat connection in experiments on two stage demagnetization. The aim in designing a heat switch will be to have as high an on/off ratio of conductances as possible. This ratio will be very nearly equal to the ratio at the temperature, T, of the hot end. K_s/K_n will vary at least as $(T/T_c)^2$ at the lower temperatures, and it is thus clearly desirable to have as low a value of T as possible.

Darby *et al.* used lead as the connecting link between a pill of paramagnetic salt at 0·25° K and the pill it was desired to demagnetize to a low temperature. They were able to obtain a temperature of approximately 3×10^{-3}° K by demagnetizing from a magnetic field of only 4300 gauss, and 10^{-3}° K from a field of 9000 gauss. A heating up rate of only 1 erg/min was obtained and it was possible to keep the temperature below 10^{-2} ° K for 40 minutes. It is of interest to note, as the original paper shows, that this heating up rate may be considered a confirmation that K_{es}/K_{en} drops more rapidly that T^2 at the lowest temperatures.

§9. Conclusion

In concluding this paper we should like to list some of the programmes of experimental work on thermal conductivity which we regard as the most immediately desirable,

(*a*) An extension of the work on the thermal conductivity of the elements in the highest state of purity, preferably in the form of single crystals. This is particularly important for elements with simple atomic and crystalline structures where the theoretical predictions can be more easily evaluated.

(*b*) An investigation of the effect of known amounts of impurity and an examination of how this alters the lattice and electronic conductivities.

(*c*) An investigation into the effects of mechanical and heat treatments and the correlation between the change in the thermal conductivity and the mechanical properties of the metal. This is of course connected with the need for similar research on the electrical conductivity.

(*d*) Further measurements on anisotropic single crystals.

(*e*) Further data concerning the change of thermal and electrical conductivities, and of the Lorenz number, in a magnetic field.

(*f*) Further experiments on superconductors and superconducting alloys which will give more data on the K_s/K_n relationships.

Experiments on these lines will yield valuable information on electron and phonon scattering mechanisms.

Acknowledgments

We are very grateful to Dr. K. Mendelssohn, F.R.S., for his valuable advice during the preparation of this paper. We should like to thank the editors of the *Philosophical Magazine*, and of the *Proceedings* of the Cambridge Philosophical Society, The Physical Society and The Royal Society for permission to reproduce figures from their respective journals.

References

Allen, J. F., and Mendoza, E., 1948, *Proc. Camb. Phil. Soc.*, **44,** 280.
Andrews, F. A., Webber, R. T., and Spohr, D. A., 1951, *Phys. Rev.*, **84,** 994.
Berman, R., 1951 a, *Proc. Roy. Soc.* A, **208,** 90 ; 1951 b, *Phil. Mag.*, **42,** 642.
Berman, R., and MacDonald, D. K. C., 1951, *Proc. Roy. Soc.* A, **209,** 368 ; 1952, *Ibid.*, **211,** 122.
Blackman, M., 1951, *Proc. Phys. Soc.* A, **64,** 681.
Casimir, H. B. G., and Gorter, C. J., 1934, *Physica*, **1,** 305.
Darby, J., Hatton, J., Rollin, B. V., Seymour, E. F. W., and Silsbee, H. B., 1951, *Proc. Phys. Soc.* A, **65,** 861.
De Haas, W. J., and Bremmer, H., 1931, *Proc. Kon. Akad. Wet. Amst.*, **34,** 325 ; 1936 a, *Physica*, **3,** 672 ; 1936 b, *Ibid.*, 687.
De Haas, W. J., and de Nobel, J., 1938, *Physica*, **5,** 449.
De Haas, W. J., Gerritsen, A. N., and Capel, W. H., 1936, *Physica*, **3,** 1143.
De Haas, W. J., and Rademakers, A., 1940, *Physica*, **7,** 992.
De Nobel, J., 1949, *Physica*, **15,** 532 ; 1951, *Ibid.*, **17,** 551.
Detwiler, D. P., and Fairbank, H. A., 1952, *Phys. Rev.*, **86,** 574.
Estermann, I., and Zimmerman, J. E., 1951, *Carnegie Inst. of Technology*, O.N.R. Tech. Report No. 6 ; 1952, *J. Appl. Phys.*, **23,** 578.
Fröhlich, H., 1950, *Phys. Rev.*, **79,** 845.
Goodman, B., 1951, *Proc. Int. Conf. Low. Temp. Phys.* (Oxford), p. 129.

Gorter, C. J., 1948, *Les phénomènes cryomagnétiques* (Paris : Langevin-Perrin), p. 76.
Grüneisen, E., and Adenstedt, H., 1938, *Ann. Phys. Lpz.*, **31,** 714.
Grüneisen, E., and Erfling, H. D., 1940, *Ann. Phys. Lpz.*, **38,** 399.
Grüneisen, E., Rausch, K., and Weiss, K., 1950, *Ann. Phys. Lpz.*, **7,** 1.
Heer, C. V., and Daunt, J. G., 1949 a, *Phys. Rev.*, **76,** 854 ; 1949 b, *Ibid.*, 985.
Heisenberg, W., 1948, *Z. Naturforsch.*, **3** a, 65.
Hulm, J. K., 1950, *Proc. Roy. Soc.* A, **204,** 98 ; 1951, *Proc. Phys Soc.* B, **64,** 207 ; 1952, *Ibid.* A, **65,** 227.
Johnston, H. L., Powers, R. W., and Ziegler, J., 1951, *Proc. Int. Conf. Low Temp. Phys.* (Oxford), p. 35.
Karweil, J., and Schaeffer, K., 1939, *Ann. Phys. Lpz.*, **36,** 567.
Klemens, P. G., 1951, *Proc. Roy. Soc.* A, **208,** 108 ; 1952, to be published.
Kohler, M., 1949 a, *Naturwissenschaften*, **36,** 186 ; 1949 b, *Ann. Phys. Lpz.* (6), **5,** 181 ; 1949 c, *Ibid.*, **6,** 18 ; 1949 d, *Z. Phys.*, **125,** 679.
Koppe, H., 1947, *Ann. Phys. Lpz.* (6), **1,** 405.
Kroll, W., 1933 a, *Z. Phys.*, **80,** 50 ; 1933 b, *Ibid.*, **81,** 425 ; 1938, *Sci. Papers Inst. Phys. Chem. Res. Tokyo*, **34,** 194.
Landau, L., 1943, *J. Phys. USSR*, **7,** 99.
MacDonald, D. K. C., and Mendelssohn, K., 1950, *Proc. Roy. Soc.* A, **202,** 103.
Makinson, R. E. B., 1938, *Proc. Camb. Phil. Soc.*, **34,** 474.
Mendelssohn, K., 1946, *Roy. Coll. Sci. Journ.*, **16,** 105.
Mendelssohn, K., and Olsen, J. L., 1950 a, *Proc. Phys. Soc.* A, **63,** 2 ; 1950 b, *Ibid.*, 1182 ; 1950 c, *Phys. Rev.*, **80,** 859.
Mendelssohn, K., and Pontius, R. B., 1937, *Phil. Mag.*, **24,** 777.
Mendelssohn, K., and Rosenberg, H. M., 1951, *Proc. Phys. Soc.* A, **64,** 1067 ; 1952 a, *Ibid.*, **65,** 385 ; 1952 b, *Ibid.*, **65,** 388 ; 1952 c, to be published.
Olsen, J. L., 1951, *Proc. Int. Conf. Low Temp. Phys.* (Oxford), p. 127 ; 1952, *Proc. Phys. Soc.* A, **65,** 518.
Olsen, J. L., and Renton, C. A., 1952, *Phil. Mag.*, **43,** 946.
Onnes, H. K., and Holst, G., 1914, *Leiden Comm.*, 142c.
Rademakers, A., 1949, *Physica*, **15,** 849.
Rausch, K., 1947, *Ann. Phys. Lpz.* (6), **1,** 190.
Schmeissner, F., and Meissner, H., 1950, *Z. Angew. Phys.*, **2,** 423.
Shalyt, S., 1944, *J. Phys. USSR*, **8,** 315.
Sommerfeld, A., and Bethe, H., 1934, *Handbuch der Physik*, **24,** 2nd ed., pt. 2.
Sondheimer, E. H., 1950, *Proc. Roy. Soc.* A, **203,** 75 ; 1952 a, *Proc. Phys. Soc.* A, **65,** 561 ; 1952 b, *Ibid.*, **65,** 562.
Sondheimer, E. H., and Wilson, A. H., 1947, *Proc. Roy. Soc.* A, **190,** 435.
Umeda, K., and Yamamoto, T., 1949, *J. Fac. Sci. Hokkaido Univ.* (Series 2), **3,** 249.
Webber, R. T., and Spohr, D. A., 1951, *Phys. Rev.*, **84,** 384.
Wilkinson, K. R., and Wilks, J., 1949, *J. Sci. Instrum.*, **26,** 19.
Wilson, A. H., 1936, *Theory of Metals* (Cambridge : University Press) ; 1937, *Proc. Camb. Phil. Soc.*, **33,** 371.

*The Diffraction of Radio Waves by the Curvature of the Earth**

By M. H. L. Pryce, F.R.S.
Clarendon Laboratory, Oxford

Abstract

This paper gives a simplified approximate derivation of the field at moderate heights and distances due to an oscillating electric dipole at moderate height above the earth, taking into account the curvature and electrical constants of the earth. The method applies to both vertically and horizontally polarized waves. It is closely connected with treating the earth as flat, the propagation of the waves being curved upwards. In this way the expansions in Legendre functions can be replaced by Fourier integrals, which are simpler to handle. The results of previous workers are reproduced, but are obtained more directly in a form suitable for easy computation.

§ 1. Introduction

The diffraction of radio waves around the earth's surface has been of interest since the earliest days of radio communication. When it was first discovered that wireless signals could be transmitted over very long paths (such as across the Atlantic Ocean), in contradiction to the expectations of the time, diffraction was discussed as a possible explanation. The discovery of the Heaviside layer gave the true explanation, but not before Poincaré (1910) had developed a mathematical theory applicable to the problem and had shown that diffraction alone could not account for the phenomenon. A more complete solution has been given by Watson (1918), van der Pol and Bremmer (1937) and others, but there are so many parameters in the problem (wavelength, height of source and receiver above ground, conductivity and dielectric constant of the earth, direction of polarization) that the general solution is very cumbersome, even after making the obvious approximations, and appears in a form quite unsuited to rapid and easy computation. Also, these solutions are concerned either with the field at the surface of the earth, or with approximations for the field at great heights, which are often not very reliable at small heights ; and with the exception of Gray (1939), all workers have confined their attention to vertically polarized waves.

In nearly all practical applications, on the other hand, the heights of the transmitter and receiver above the surface are only a very small fraction of the radius of the earth, and under these conditions the solution can be put into a much more manageable form, which lends itself to relatively easy computation. This result can naturally be obtained by

* The bulk of this paper is based on work done by the author in 1941 at the Admiralty Signal Establishment, and was circulated in manuscript form to various institutions interested in radio propagation.

making the appropriate approximations and generalizations in the solutions already mentioned, but it can be derived more directly by a different method of attack on the problem. The main purpose of the present paper is to describe this new method, which was worked out originally in connection with radar coverage.

An important characteristic of the radar problem is the smallness of the range in which detectable signals are obtained as compared with the semi-circumference of the earth (a few hundred kilometres at most under normal atmospheric conditions, compared with 20 000 kilometres), and the nearly horizontal nature of the propagation (i.e., heights small compared with the range). Propagation all the way around the earth is therefore completely negligible, and the fact that the earth's curvature continues to be the same to the antipodes is quite unimportant to the structure of the field. All that is important is that the earth is uniformly curved in the region where propagation is observed. This, together with the fact that stratification of the atmosphere, by bending radio waves downwards, makes the earth's effective curvature for diffraction less than its true curvature, suggests that it is useful to treat the earth's surface as curved but extending to infinity in all directions, and so not closed. Such a treatment, as will be shown, is approximately equivalent to treating the earth's surface as ' flat ', with the geometry of space non-Euclidean (i.e. curved). It is an approximation, but one which retains the essential feature of the problem, namely the relative curvature of the earth's surface and the paths along which waves are propagated, and is in many respects no further from the true state of affairs than to treat the earth as a perfect sphere.

From the mathematical standpoint this approach is easier to handle because the slowly convergent series in Legendre polynomials of the classical papers are replaced by Fourier integrals. Indeed, the major content of the papers of Poincaré (1910), Watson (1918), van der Pol and Bremmer (1937), and others is a technique for transforming the series, by contour integration and suitably chosen approximations, into a form which the present method yields more directly. The essential simplification is that, instead of approximating by elaborate techniques to a solution of the exact differential equations of the problem, one first solves an approximate differential equation, the subsequent approximations being more straightforward. The gain in simplicity, however, is offset by a loss in rigour, in that it is more difficult to estimate the error made in using the approximate differential equation.* No attempt is made in this paper to justify the method rigorously.

The end result is that the field at height z and plan distance r, of an oscillating dipole of strength $p \exp(i\kappa ct)$, situated at height h above the earth, is given by the infinite series

$$\frac{\kappa^2 p}{h_0}\left(\frac{2\pi}{\kappa r}\right)^{1/2} e^{i(3\pi/4-\kappa r)} \sum_s \frac{f(a_s+h/h_0)\,f(a_s+z/h_0)}{(1+\tau^2 a_s)\,f'^2(a_s)} e^{ia_s r/d_0} \quad . \quad . \quad . \quad (1.1)$$

* A partial investigation of this has been made by Pekeris (1946).

Here h_0 and d_0 are certain constants which appear in the theory as natural units of height and distance respectively (they are defined in (9.6), (9.7)). $f(\nu)$ is a function satisfying the differential equation

$$f''(\nu)+\nu f(\nu)=0, \quad . \quad . \quad . \quad . \quad . \quad . \quad . \quad . \quad (1.2)$$

and having a specified behaviour as $\nu \to \infty$. It is expressible in terms of the Airy integral* (c.f. 9.19), namely

$$f(\nu)=2\, e^{-\pi i/6}\, \mathrm{Ai}\,(e^{\pi i/3}\nu). \quad . \quad . \quad . \quad . \quad . \quad . \quad . \quad (1.3)$$

The complex numbers a_s are the roots of the transcendental equation

$$f(a_s)=\tau f'(a_s), \quad . \quad . \quad . \quad . \quad . \quad . \quad . \quad . \quad . \quad (1.4)$$

and τ is a complex number (generally very small) depending on the conductivity and dielectric constant of the earth, on the wavelength, and also on whether the polarization is vertical or horizontal.

The series (1.1) converges rapidly in the shadow region, and satisfactorily enough for computational purposes near the edge of the illuminated zone. Its practical use demands the computations of the height gain functions $f(a_s+z/h_0)$, a_s being a sequence of complex numbers and z/h_0 an arbitrary positive real variable. Generally this will require computation for different values of τ, but for many practical applications τ is so small as to be negligible, and the a_s can be taken as the zeros of the function f, which are exp $(-\pi i/3)$ times the zeros of the Airy integral, which are tabulated. This is true for horizontally polarized waves of all wavelengths, and for vertically polarized waves shorter than about a metre over sea water, or ten metres over land. This considerably simplifies the computational problem. The computation of $f(a_s+z/h_0)$ for small values of z/h_0 is made easy by the differential equation that it satisfies, and for large values by the asymptotic formulae for the Airy integral.

Inside the illuminated region the series is useless for computation, but geometrical optics then furnishes a satisfactory approximation (§ 13). The practical calculation of the field along these lines has been discussed by Domb and Pryce (1947).

§ 2. History of the Problem

In a sense the earliest work on the problem is that of Rayleigh (1871, 1881, 1899) who solved the problem of the scattering of waves by spheres, in terms of an infinite series of spherical harmonics. This solution, however, is useless for practical purposes when the radius of the sphere is much greater than the wavelength, for the series is an alternating one whose most important terms are in the range $\kappa a-(\kappa a)^{1/3}<n<\kappa a+(\kappa a)^{1/3}$.

The first attempt to circumvent this difficulty was made by Poincaré (1910), specifically for the problem of radio propagation, with a vertical dipole near the surface of the earth as source. Poincaré treated the earth as a perfect conductor ($\tau=\infty$ in our notation, for vertical polarization) and obtained for the surface density of electric charge a series of the form

* The classical papers (except Poincaré's) on this subject express f in terms of the Hankel or Bessel functions of order 1/3.

(1.1) (eqn. 9 of p. 257, *loc. cit.*), specialized for $z=0$. The numbers a_s are given by him as $\exp(-\pi i/3)$ times the roots of the derivative of the Airy integral, but are not given numerically. Although Poincaré obtained the correct result in essence, his reasoning was not rigorous and was criticized by later workers. His treatment is also very elaborate, and the results themselves difficult to find.

Subsequent attempts by Nicholson (1910), March (1912), Rybczynski (1913) and Macdonald (1914), following essentially similar lines, have been subjected to the same criticism. The analysis was finally put on a sound footing by Watson (1918). Watson confined his attention to vertical polarization, and to the field on the surface ($z=0$ in our notation). His results, though complete, are not in a form which is readily applicable to practical calculation.

A paper by van der Pol (1919) reviews the results of Nicholson and Macdonald in the light of Watson's paper, and gives applications of Watson's results in rather more practical form. Laporte (1923) gives an excellent summary of previous work (though he states that Poincaré obtained no definite result for the attenuation constant at great distances —perhaps because Poincaré did not evaluate the a_s numerically), and fulfils a purpose similar to van der Pol's.

The practical difficulties of applying the results of these papers, given as they are in terms of Legendre or Hankel functions of large complex orders, led Eckersley (1932) to consider the problem from the standpoint of the radio engineer. He noted that Watson's solution is an expansion in terms of eigenfunctions of a definite type, of which only the first eigenfunction is important for large distances. He formulated the eigenfunction problem and applied the phase integral method to obtain approximate values for the eigenvalues and eigenfunctions, and thereby obtained a rough but readily usable solution. This approach was subsequently extended and made more precise by Eckersley and Millington (1938).

In a series of papers, van der Pol and Bremmer (1937 a, b, 1938, 1939) have given a rederivation of the classical results (generalized to elevated receiver as well as transmitter) in a more readily applicable form, with special emphasis on approximations of practical value. They also show (1937 b) that the methods of geometrical optics are justified well inside the illuminated zone, and use their results to treat the theory of the rainbow. A series of papers by Vvedensky (1935, 1936, 1937) has a similar purpose. All these papers deal with the field of a vertical electric dipole. More recently, Gray (1939) has applied the method of Watson to calculate the field of a vertical magnetic dipole, which gives horizontally polarized waves, and whose diffraction must in its essentials be the same as for the field of a horizontal electric dipole. Fock (1945, 1946, 1949), starting from Watson's transformation, obtains practically applicable results in terms (essentially) of the Airy Integral, for both horizontal and vertical polarization. Leontovich and Fock (1946) use an interesting method to solve

the problem for a vertical dipole on the surface, which, in its choice of coordinates, bears a relation to the method of the present paper. The final formulation of the result in Fock's 1949 paper, also, is identical, apart from notation, with that given here.

A coherent account of the work of van der Pol and Bremmer is given in Bremmer's book 'Terrestrial Radio Waves' (1949). The practical aspects of the problem are well discussed in the volume on 'Propagation of Short Radio Waves' of the M.I.T. Radiation Laboratory Series (Kerr 1951).

§ 3. Co-ordinates and Metric

The co-ordinates to be used in treating the problem will be denoted by x, y, z. In the neighbourhood of the source of radiation they approximate to rectangular Cartesian co-ordinates, and are defined in terms of spherical polar co-ordinates R, Θ, ϕ, whose origin is at the centre of the sphere and whose axis passes through the source, by

$$\left.\begin{aligned} x&=a\Theta\cos\phi,\\ y&=a\Theta\sin\phi,\\ z&=a\log(R/a). \end{aligned}\right\} \quad . \quad . \quad . \quad . \quad . \quad . \quad . \quad . \quad . \quad (3.1)$$

The surface of the sphere is thus characterized by $z=0$.

In terms of these co-ordinates the metric

$$ds^2=dR^2+R^2d\Theta^2+R^2\sin^2\Theta\,d\phi^2$$

is

$$ds^2=e^{2z/a}\left[dx^2+dy^2+dz^2-\left(1-\frac{\sin^2\Theta}{\Theta^2}\right)\frac{(xdy-ydx)^2}{(x^2+y^2)}\right]. \quad . \quad (3.2)$$

As we shall be concerned with regions where Θ is very small compared with unity, we may expand the last term in powers of Θ, giving

$$ds^2=e^{2z/a}[dx^2+dy^2+dz^2-(x\,dy-y\,dx)^2/3a^2+O(a^{-4})]. \quad . \quad . \quad (3.3)$$

When we come to work out the expressions for the divergence and curl of the electromagnetic vectors in terms of our co-ordinates we shall find terms in $1/a^2$ and higher powers of $1/a$ corresponding to these terms in the metric. The essence of our method is to neglect all terms in $1/a^2$ and higher powers of $1/a$ occurring in Maxwell's equations, while retaining terms in $1/a$. This is equivalent to ignoring such terms in the metric, and we therefore write, after first introducing the abbreviation

$$\eta=e^{z/a}, \quad . \quad . \quad . \quad . \quad . \quad . \quad . \quad . \quad . \quad (3.4)$$

$$ds^2=\eta^2(dx^2+dy^2+dz^2). \quad . \quad . \quad . \quad . \quad . \quad . \quad (3.5)$$

No proof will be attempted that this procedure gives a rigorous approximation to the solution, but it will be clear that the consequences of the neglected terms will be no greater than, say, the consequences of the departure of the earth's shape from that of a smooth sphere, when the theory is applied to microwave propagation over the earth. The method must naturally be used with caution, but no special justification will be given for each step in the following argument.

The advantage of the approximation is that, since x and y do not occur explicitly in the metric (3.5), the equations of the problem are invariant under translations of x and y, and can be handled by Fourier transforms, which are simpler to use than the corresponding spherical harmonics which form the basis of the exact treatment.

Before proceeding to a direct attack on the problem it is instructive to consider the geodesics in a non-Euclidean space whose metric is given by (3.5), for in the limit of very short wavelengths the electromagnetic field can be derived from considerations of geometrical optics, the rays (in our approximation) being these geodesics (§ 13). We confine our attention to geodesics passing through the source, supposed to be at the point $x=y=0$, $z=h$; from symmetry it is clear that they lie wholly in a plane through the z-axis, and we may without any loss of generality confine ourselves to geodesics in the xz-plane. The metric (3.5) differs from the true metric (3.2) of actual space by terms which vanish for curves lying wholly in such a plane ; these geodesics therefore coincide with the straight lines through the source.* Indeed it is easy to verify directly that the geodesics are given parametrically by

$$\left.\begin{aligned} x&=a\arctan(\tan\psi+\frac{s}{a}\sec\psi\,\mathrm{e}^{-h/a})-a\psi,\\ z&=h+\tfrac{1}{2}a\log\left(1+\frac{2s}{a}\sin\psi\,\mathrm{e}^{-h/a}+\frac{s^2}{a^2}\mathrm{e}^{-2h/a}\right),\end{aligned}\right\}\quad\ldots\quad(3.6)$$

where s is the geodesic distance from the source and ψ is a constant along the geodesic, being the angle it makes with the horizontal at the source, and, in terms of the spherical polar co-ordinates R, Θ, ϕ, by substituting (3.1), this reduces to the parametric equation for a straight line,

$$\left.\begin{aligned} R\sin\Theta&=s\cos\psi,\\ R\cos\Theta&=s\sin\psi+a\,\mathrm{e}^{h/a}.\end{aligned}\right\}\quad\ldots\ldots\quad(3.7)$$

The geodesic distance between the points $(0,\ 0,\ h)$ and $(r,\ 0,\ z)$ is

$$s=a[\mathrm{e}^{2h/a}-2\mathrm{e}^{(h+z)/a}\cos(r/a)+\mathrm{e}^{2z/a}]^{1/2}\quad\ldots\ldots\quad(3.8)$$

We shall have occasion (13.7) to use an approximation to this for the case that h/a, z/a and $(h+z)/r$ are small, namely

$$s=r+\frac{(h-z)^2}{2r}+\frac{r(h+z)}{2a}-\frac{r^3}{24a^2}+\ldots\ldots\quad(3.9)$$

---

* In the original manuscript report the co-ordinates x, y, z were defined by $x=a\sin\Theta\cos\phi$, $y=a\sin\Theta\sin\phi$, $z=R-a$, instead of by (3.1) (cf. Kerr 1951). In the region of interest near the source, the two differ only by terms which are unimportant, but the present choice offers considerable formal simplification. In the original co-ordinates the geodesics did not correspond exactly to straight lines, but only approximately so. I am indebted to Professor E. T. Copson for the remark that $z=a\log(R/a)$ is preferable to $z=R-a$, and to the paper by C. L. Pekeris (1946) for the advantage of Θ over $\sin\Theta$ in x and y.

Actually, what we shall need is the geodesic distance with the metric (3.5) in which η^2 has been approximated by $1+2z/a$, but to this order of approximation this makes no difference.

In dealing with vectors we follow the practice usual in vector analysis when dealing with orthogonal co-ordinate systems, of denoting by A_x, etc., the components of the vector **A** resolved in the x-direction, etc., as distinct from the practice of tensor calculus, where we have two possible sets of components for a vector, one covariant and one contravariant, connected by the metric tensor. We then have the following expressions for the curl and divergence of a vector:

$$\left.\begin{aligned}(\mathbf{curl\ A})_x &= \frac{1}{\eta}\frac{\partial A_z}{\partial y} - \frac{1}{\eta^2}\frac{\partial}{\partial z}(\eta A_y),\\ (\mathbf{curl\ A})_y &= -\frac{1}{\eta}\frac{\partial A_z}{\partial x} + \frac{1}{\eta^2}\frac{\partial}{\partial z}(\eta A_x),\\ (\mathbf{curl\ A})_z &= \frac{1}{\eta}\left(\frac{\partial A_y}{\partial x} - \frac{\partial A_x}{\partial y}\right),\end{aligned}\right\} \quad . \quad . \quad . \quad (3.10)$$

$$\operatorname{div}\mathbf{A} = \frac{1}{\eta}\left(\frac{\partial A_x}{\partial x} + \frac{\partial A_y}{\partial y}\right) + \frac{1}{\eta^3}\frac{\partial}{\partial z}(\eta^2 A_z). \quad . \quad . \quad . \quad (3.11)$$

In these expressions terms in $1/a^2$ and higher powers have been neglected; alternatively they may be regarded as exact expressions for a non-Euclidean space whose metric is (3.5).

§ 4. General Procedure

We shall consider the field due to an oscillating Hertzian dipole at the point given by $x=y=0$, $z=h$. Its height above the sphere is $a[\exp(h/a)-1]$, which is approximately h if h/a is small. We shall consider horizontal and vertical dipoles separately. The field due to any distribution of charges and currents can naturally be obtained by a superposition of these two fundamental types of solution, since any source distribution can be obtained by superposing Hertzian dipoles. We shall confine ourselves to fields with a single frequency and assume that all field quantities contain a factor $\exp(i\omega t)$, which will be omitted systematically from the equations; the actual field is to be obtained by taking the real part.

We shall suppose that h/a is small, and that we are only interested in regions where the horizontal distance r from the source, and the height z above the sphere are small compared with a. On the other hand, r^2/ah need not be small, for we shall definitely be interested in the field beyond what may conveniently be termed the horizon. The first step will be to express the field vectors **E**, **H** in terms of their Fourier transforms with respect to x and y (but not to z), namely

$$\left.\begin{aligned}\mathbf{E}(x,y,z) &= \int\int \tilde{\mathbf{E}}(\alpha,\beta,z)\, e^{i(\alpha x+\beta y)}\, d\alpha\, d\beta,\\ \mathbf{H}(x,y,z) &= \int\int \tilde{\mathbf{H}}(\alpha,\beta,z)\, e^{i(\alpha x+\beta y)}\, d\alpha\, d\beta,\end{aligned}\right\} \quad . \quad . \quad . \quad . \quad (4.1)$$

and to write Maxwell's equations in terms of $\tilde{\mathbf{E}}$ and $\tilde{\mathbf{H}}$, with α, β and z as independent variables, omitting terms in $1/a^2$. The charge and current densities, defined for a dipole in terms of delta-functions, will similarly be expressed by Fourier transforms.

The various components of $\tilde{\mathbf{E}}$ and $\tilde{\mathbf{H}}$ can now be written in terms of the z-components alone,* and Maxwell's equations expressed as a second-order differential equation in z for these.

At this stage it will be supposed that outside the sphere the dielectric constant ϵ and magnetic permeability μ depend in any manner on the height z, but not on x and y. It will then be shown that if they vary approximately linearly with z the equations are, to the degree of approximation being considered, identical with the equations for constant ϵ and μ, and a different value of a. This will be called the effective radius of the sphere. From this point on it will be assumed that ϵ and μ have the constant value unity; the modification needed for constant values different from unity is elementary and will not be discussed.

Inside the sphere it will be assumed that the medium is conducting and that the waves are so rapidly attenuated going in from the surface that the effect of curvature may be neglected. As is well known, the effect of conductivity can be represented by a 'complex dielectric constant'

$$\epsilon' = \epsilon_0 - 4\pi i\sigma/\omega, \quad . \quad . \quad . \quad . \quad . \quad . \quad . \quad . \quad (4.2)$$

where ϵ_0 is the actual dielectric constant and σ the conductivity measured in e.s.u. The magnetic permeability will be assumed to be unity; again, the modification for a different value is elementary.

The next step is to consider the boundary conditions at the surface of the sphere and to investigate more closely the behaviour on the sphere $z=h$, where the Fourier components of the charge and current density have singularities. This will lead to a complete solution for $\tilde{\mathbf{E}}$ and $\tilde{\mathbf{H}}$ in terms of solutions of the differential equation

$$\frac{d^2u}{dz^2} + \left(\kappa^2 - \alpha^2 - \beta^2 + \frac{2\kappa^2}{a}z\right)u = 0, \quad . \quad . \quad . \quad . \quad . \quad (4.3)$$

where $\kappa = \omega/c$.

This is essentially identical with the differential equation satisfied by the Airy integral,

$$\frac{d^2}{d\xi^2}\mathrm{Ai}(\xi) = \xi\,\mathrm{Ai}\,(\xi),$$

and the results will be expressed in terms of the Airy integral. It can be expressed in terms of the more familiar Hankel functions of order 1/3,

---

* The classical treatments express the field components in terms of Hertzian potentials and solve the differential equation for the potentials. Deciding whether to work directly with field components or with potentials is largely a matter of taste, and no claim is made that the present method is superior to the other.

but its properties are considerably simpler than those of the Hankel function and it is probable that it will become better known in the future, since it occurs in many problems of theoretical physics and mathematics, and has now been extensively tabulated for real arguments.*

The Fourier transforms being completely determined, it is then possible to express the field at any point as a definite integral. This can then be transformed by complex integration to a sum of residues, yielding an infinite series ; beyond the horizon this series converges rapidly. Alternatively the definite integral may be approximated by steepest descents, giving the field as the sum of a direct field and a reflected field, as would be calculated by an elementary combination of geometrical optics and physical optics ; this ' ray theory approximation ' is useful within the horizon.

§5. Notation

As it is impossible to avoid using a large number of different symbols during the course of the work, they will be assembled here, together with their definitions (or references to the equations in the text which define them), for the convenience of the reader who is more interested in the results than in the details of the method. They are listed as nearly as is possible in the order in which they occur.

a : radius of the earth (or effective radius, see § 6).
R, Θ, ϕ : spherical polar co-ordinates, referred to earth's centre.
x, y, z : approximately Cartesian co-ordinates, referred to an origin on the earth's surface, (3.1).
$\eta = e^{z/a}$.
$r = (x^2+y^2)^{1/2}$: plan distance.
h : height of the source (more precisely $a(e^{h/a}-1)$ is the height).
s : (geodesic) distance from source, (3.6).
ψ : angle characterizing a ray or geodesic, (3.6).
$\mathbf{A}$, A_x, etc. : arbitrary vector and its components, (3.8).
ω : angular frequency.
c : velocity of light.
$\kappa = \omega/c$.
$\lambda = 2\pi/\kappa$: wavelength.
$\mathbf{E}$, $\mathbf{H}$: electric and magnetic field.
$\tilde{\mathbf{E}}$, $\tilde{\mathbf{H}}$: Fourier transforms of $\mathbf{E}$, $\mathbf{H}$, (4.1).
α, β : variables conjugate to x, y in ' Fourier space ', (4.1).
ϵ, μ : dielectric constant and magnetic permeability of atmosphere (later set equal to 1).
ϵ_0, μ_0 : the same for the earth ($\mu_0 = 1$ later assumed).

---

* A good account of the Airy integral and its uses is to be found in Jeffreys and Jeffreys (1950). It is tabulated by Miller (1946).

σ : conductivity of earth.
$\epsilon'=\epsilon_0-4\pi i\sigma/\omega$: ' complex dielectric constant ' of earth, (4.2).
u, v : two independent solutions of eqn. (4.3), or equivalently of (9.1). Specialized in (9.15), (9.17), (9.20).
ρ, $\mathbf{j}$: charge and current density.
$\tilde{\rho}$, $\tilde{\mathbf{j}}$: their Fourier transforms.
$\mathbf{F}=\epsilon\mathbf{E}+(4\pi i/\kappa)\mathbf{j}$, (6.3).
$\mathscr{E}=\eta^{3/2}F_z$, (6.6). (Modified in 6.6*a*.)
$\mathscr{H}=\eta^{3/2}H_z$, (6.6).
S_1, S_2 : quantities formed from current density of the source according to (6.7), (6.8).
$\tilde{S}_1, \tilde{S}_2$: their Fourier transforms.
n : related to refractive index of atmosphere, (6.11).
a' : effective radius of earth when atmospheric refraction is considered (6.11).
$\gamma'=(\kappa^2\epsilon'-\alpha^2-\beta^2)^{1/2}$, (8.1).
W : Wronskian of u, v, (9.2), later specialized to $-1/\pi h_0$, (9.18).
$K=(\frac{1}{2}\kappa a)^{1/3}$, (9.5) (a large number).
$h_0=(a/2\kappa^2)^{1/3}=K\lambda/2\pi$, a natural unit of height, (9.6).
$d_0=(2a^2/\kappa)^{1/3}=K^2\lambda/\pi$, a natural unit of plan distance, (9.7).
$\zeta=h_0{}^2(\kappa^2-\alpha^2-\beta^2)$, (9.9) (later treated as a complex variable).
$\xi=-\zeta-z/h_0$, (9.10).
$\mathrm{Ai}(\xi)=\dfrac{1}{\pi}\displaystyle\int_0^\infty \cos(\tfrac{1}{3}t^3+\xi t)\,dt$: the Airy integral of ξ, (9.12).
$\mathrm{Bi}(\xi)$: the second Airy integral, (9.13).
ν : an arbitrary variable.
$f(\nu)=\mathrm{Bi}(-\nu)-i\,\mathrm{Ai}(-\nu)=2e^{-\pi i/6}\,\mathrm{Ai}(e^{\pi i/3}\nu)$, (9.19).
$g(\nu)=\mathrm{Ai}(-\nu)$, (9.19).
p : strength of dipole (amplitude of electric dipole moment).
$\delta(x)$: Dirac's delta-function.
$\Phi=\Phi(\zeta\,;\,h, z)$: defined by (10.5).
$\Psi=\Psi(\zeta\,;\,h, z)$: defined by (11.6).
$E_r, E_\varphi, H_r, H_\varphi$: polar components of $\mathbf{E}$, $\mathbf{H}$ in a horizontal plane.
I_1, I_2, I_3, I_4 : defined by (11.8).
w, δ : modulus and phase of a complex variable, (12.3).
$\tau_1=-i\epsilon'K^{-1}(\epsilon'-1)^{-\frac{1}{2}}$, (12.9).
$\tau_2=-iK^{-1}(\epsilon'-1)^{-1/2}$, (12.10).
$a_1, a_2, \ldots a_s, \ldots$: the roots of $f(a_s)=\tau_1 f'(a_s)$, (12.11).
$b_1, b_2, \ldots b_s, \ldots$: the roots of $f(b_s)=\tau_2 f'(b_s)$, (12.12).
ζ_1 : point of stationary phase in the ζ-integration, (13.5).
$\tau=-i\epsilon'/\gamma' h_0$, (13.11).
D : divergence factor, (13.15).
$-\alpha_1, -\alpha_2, \ldots -\alpha_s, \ldots$: the roots of the Airy integral.
$-\beta_1, -\beta_2, \ldots, -\beta_s, \ldots$: the roots of the derivative of the Airy integral,
G_s : height gain function, (14.4).

§6. Maxwell's Equations

Maxwell's equations for a field with time dependence $\exp(i\omega t)$, in a medium of constant dielectric constant ϵ and permeability μ, are

$$\left.\begin{aligned}
\frac{1}{\eta}\frac{\partial E_z}{\partial y}-\frac{1}{\eta^2}\frac{\partial}{\partial z}(\eta E_y)+i\kappa\mu H_x=0, &\quad \ldots \quad (6.1.1)\\
-\frac{1}{\eta}\frac{\partial E_z}{\partial x}+\frac{1}{\eta^2}\frac{\partial}{\partial z}(\eta E_x)+i\kappa\mu H_y=0, &\quad \ldots \quad (6.1.2)\\
\frac{1}{\eta}\left(\frac{\partial E_y}{\partial x}-\frac{\partial E_x}{\partial y}\right)+i\kappa\mu H_z=0, &\quad \ldots \quad (6.1.3)\\
\frac{1}{\eta}\left(\frac{\partial H_x}{\partial x}+\frac{\partial H_y}{\partial y}\right)+\frac{1}{\eta^3}\frac{\partial}{\partial z}(\eta^2 H_z)=0\,; &\quad \ldots \quad (6.1.4)
\end{aligned}\right\}$$

$$\left.\begin{aligned}
\frac{1}{\eta}\frac{\partial H_z}{\partial y}-\frac{1}{\eta^2}\frac{\partial}{\partial z}(\eta H_y)-i\kappa\epsilon E_x=4\pi j_x, &\quad \ldots \quad (6.2.1)\\
-\frac{1}{\eta}\frac{\partial H_z}{\partial x}+\frac{1}{\eta^2}\frac{\partial}{\partial z}(\eta H_x)-i\kappa\epsilon E_y=4\pi j_y, &\quad \ldots \quad (6.2.2)\\
\frac{1}{\eta}\left(\frac{\partial H_y}{\partial x}-\frac{\partial H_x}{\partial y}\right)-i\kappa\epsilon E_z=4\pi j_z, &\quad \ldots \quad (6.2.3)\\
\frac{\epsilon}{\eta}\left(\frac{\partial E_x}{\partial x}+\frac{\partial E_y}{\partial y}\right)+\frac{\epsilon}{\eta^3}\frac{\partial}{\partial z}(\eta^2 E_z)=4\pi\rho. &\quad \ldots \quad (6.2.4)
\end{aligned}\right\}$$

We shall be concerned with the field arising from a Hertzian dipole; for any oscillatory distribution of current can be made up by a superposition of Hertzian dipoles, so that the solution for a single dipole of arbitrary orientation is sufficient to yield a complete solution. The arbitrary orientation can be regarded as arising from a superposition of a vertical and a horizontal dipole, and our problem will therefore reduce to the study of these two special cases.

The representation of an arbitrary current distribution as a superposition of Hertzian dipoles, though convenient, has some disadvantages, connected with the strong singularity in the electric field of a dipole, which gives rise to spurious convergence difficulties. These give rise to no ambiguity when one is only interested, as here, in the field outside the source distribution, but as a matter of practical convenience in carrying out the calculations it turns out to be easier to work with the vector

$$\mathbf{F}=\epsilon\mathbf{E}+\frac{4\pi}{i\kappa}\mathbf{j}. \quad \ldots \quad (6.3)$$

In a flat space, the Cartesian components of $\mathbf{E}$ (or $\mathbf{F}$) and $\mathbf{H}$ each satisfy a differential equation of the second order, obtained by eliminating all but one of the components. With the present choice of coordinates this is true only for the z-components, F_z and H_z. Indeed, multiplying (6.2.4) by η^2/ϵ and differentiating with respect to z, differentiating (6.1.1)

with respect to y, and (6.1.2) with respect to x, and taking appropriate linear combinations of these results and (6.2.3), leads to the result

$$\left[\frac{\partial^2}{\partial x^2}+\frac{\partial^2}{\partial y^2}+\frac{1}{\eta}\frac{\partial}{\partial z}\frac{1}{\eta}\frac{\partial}{\partial z}\eta^2+\kappa^2\epsilon\mu\eta^2\right]F_z$$
$$=\frac{4\pi}{i\kappa}\left[\left(\frac{\partial^2}{\partial x^2}+\frac{\partial^2}{\partial y^2}\right)j_z-\frac{1}{\eta}\frac{\partial}{\partial z}\eta\left(\frac{\partial j_x}{\partial x}+\frac{\partial j_y}{\partial y}\right)\right]. \quad . \quad . \quad . \quad (6.4)$$

A similar elimination for H_z gives

$$\left[\frac{\partial^2}{\partial x^2}+\frac{\partial^2}{\partial y^2}+\frac{1}{\eta}\frac{\partial}{\partial z}\frac{1}{\eta}\frac{\partial}{\partial z}\eta^2+\kappa^2\epsilon\mu\eta^2\right]H_z=4\pi\eta\left(\frac{\partial j_x}{\partial y}-\frac{\partial j_y}{\partial x}\right). \quad . \quad (6.5)$$

These equations can be put into a more useful form by introducing

$$\left.\begin{aligned}\mathscr{E}&=\eta^{3/2}F_z,\\ \mathscr{H}&=\eta^{3/2}H_z,\end{aligned}\right\} \quad . \quad . \quad . \quad . \quad . \quad . \quad . \quad (6.6)$$

in terms of which, on neglecting terms of order $1/a^2$, they become

$$\left[\frac{\partial^2}{\partial x^2}+\frac{\partial^2}{\partial y^2}+\frac{\partial^2}{\partial z^2}+\kappa^2\epsilon\mu\left(1+\frac{2z}{a}\right)\right]\mathscr{E}=\frac{4\pi}{i\kappa}\left[\eta^{3/2}\left(\frac{\partial^2}{\partial x^2}+\frac{\partial^2}{\partial y^2}\right)j_z-\eta^{1/2}\frac{\partial}{\partial z}\eta\left(\frac{\partial j_x}{\partial x}+\frac{\partial j_y}{\partial y}\right)\right]$$
$$\equiv S_1, \text{ say}; \quad . \quad . \quad . \quad . \quad . \quad . \quad . \quad (6.7)$$

$$\left[\frac{\partial^2}{\partial x^2}+\frac{\partial^2}{\partial y^2}+\frac{\partial^2}{\partial z^2}+\kappa^2\epsilon\mu\left(1+\frac{2z}{a}\right)\right]\mathscr{H}=4\pi\eta^{5/2}\left(\frac{\partial j_x}{\partial y}-\frac{\partial j_y}{\partial x}\right)$$
$$\equiv S_2, \text{ say}; \quad . \quad . \quad . \quad . \quad . \quad . \quad . \quad (6.8)$$

where η^2 has been replaced by $1+2z/a$ in the differential operator.

The solution of eqns. (6.7) and (6.8) is sufficient to give a solution to the whole problem, for the x- and y-components of **F** and **H** are given in terms of $\mathscr{E}$ and $\mathscr{H}$ by

$$\left.\begin{aligned}\left(\frac{\partial^2}{\partial x^2}+\frac{\partial^2}{\partial y^2}\right)F_x&=-\frac{1}{\eta^2}\frac{\partial^2}{\partial x\partial z}\eta^{1/2}\mathscr{E}+i\kappa\epsilon\mu\eta^{-1/2}\frac{\partial\mathscr{H}}{\partial y}-\frac{4\pi}{i\kappa}\frac{\partial}{\partial y}\left(\frac{\partial j_y}{\partial x}-\frac{\partial j_x}{\partial y}\right),\\ \left(\frac{\partial^2}{\partial x^2}+\frac{\partial^2}{\partial y^2}\right)F_y&=-\frac{1}{\eta^2}\frac{\partial^2}{\partial y\partial z}\eta^{1/2}\mathscr{E}-i\kappa\epsilon\mu\eta^{-1/2}\frac{\partial\mathscr{H}}{\partial x}+\frac{4\pi}{i\kappa}\frac{\partial}{\partial x}\left(\frac{\partial j_y}{\partial x}-\frac{\partial j_x}{\partial y}\right),\end{aligned}\right\}$$
and
$$. \quad . \quad . \quad (6.9)$$

$$\left.\begin{aligned}\left(\frac{\partial^2}{\partial x^2}+\frac{\partial^2}{\partial y^2}\right)H_x&=-\frac{1}{\eta^2}\frac{\partial^2}{\partial x\partial z}\eta^{1/2}\mathscr{H}-i\kappa\eta^{-1/2}\frac{\partial\mathscr{E}}{\partial y},\\ \left(\frac{\partial^2}{\partial x^2}+\frac{\partial^2}{\partial y^2}\right)H_y&=-\frac{1}{\eta^2}\frac{\partial^2}{\partial y\partial z}\eta^{1/2}\mathscr{H}+i\kappa\eta^{-1/2}\frac{\partial\mathscr{E}}{\partial x}.\end{aligned}\right\} \quad . \quad . \quad . \quad . \quad . \quad (6.10)$$

These differential equations may be regarded as completely determining F_x, F_y, H_x, H_y. Their actual solution is yielded quite simply by the Fourier integral method to be described in § 7.

The above analysis has been given for the sake of simplicity for a medium in which ϵ and μ are constants. It may readily be extended, however, to the important practical case where ϵ and μ vary with z (height above the earth) in an approximately linear fashion in the relevant range of z. In this context, the relevant range of z means roughly that range through which the direct, reflected and diffracted rays pass. If we write

$$\epsilon\mu \approx n^2 \exp\left[2z\left(\frac{1}{a'}-\frac{1}{a}\right)\right], \quad . \quad . \quad . \quad . \quad . \quad (6.11)$$

(n and a' constants), and modify the definition (6.6) of $\mathscr{E}$ and $\mathscr{H}$ to

$$\left.\begin{aligned}\mathscr{E} &= \epsilon^{-1/2}\eta^{3/2}F_z,\\ \mathscr{H} &= \mu^{1/2}\eta^{3/2}H_z,\end{aligned}\right\} \quad . \quad . \quad . \quad . \quad . \quad . \quad (6.6a)$$

then the differential operator on the left of eqns. (6.7) and (6.8) is modified to

$$\frac{\partial^2}{\partial x^2}+\frac{\partial^2}{\partial y^2}+\frac{\partial^2}{\partial z^2}+n^2\kappa^2\left(1+\frac{2z}{a'}\right). \quad . \quad . \quad . \quad . \quad (6.12)$$

The right hand sides are slightly modified also, but in a manner which is of no importance to the general results. The significance of this is that the problem of propagation in a stratified medium of the kind described by (6.11) is equivalent to the problem of propagation in free space above a sphere of modified radius a', with κ replaced by κn (i.e., wavelength decreased in the ratio n). This is of considerable importance in the propagation of radio waves over the earth, and more particularly over the sea, where there is often a steady decrease of ϵ with height because of the decrease of water vapour content. In temperate climates the effective radius a' of the earth is usually about 8 000 km as compared with the true radius a 6 400 km.

It may also happen, particularly in tropical climates, that the rate of decrease of ϵ with height is so rapid that $1/a'$ is negative. In this case the analysis of the present paper breaks down. We are then dealing with a particular case of ' anomalous propagation ', which is more properly handled by the theory of propagation ducts, though the general method is the same.

In view of the foregoing equivalence, we shall henceforth assume $\epsilon=\mu=1$ outside the sphere. Inside the sphere we shall take the dielectric constant to have the complex value ϵ' given by (4.2), and $\mu_0=1$, there being no driven sources.

§7. The Fourier Transforms

We now introduce the Fourier transforms $\tilde{\mathscr{E}}$, $\tilde{\mathscr{H}}$, $\tilde{\mathbf{j}}$, $\tilde{\rho}$ of the corresponding quantities $\mathscr{E}$ etc., with respect to x and y defined as in (4.1), namely

$$\mathscr{E}(x, y, z)=\iint \tilde{\mathscr{E}}(\alpha, \beta, z)\, e^{i(\alpha x+\beta y)}\, d\alpha\, d\beta, \quad . \quad . \quad . \quad . \quad (7.1)$$

etc. They depend on the variables α, β and z.

The fundamental eqns. (6.7) and (6.8) now become

$$\left.\begin{aligned}\left[\frac{d^2}{dz^2}+\kappa^2-\alpha^2-\beta^2+\frac{2\kappa^2}{a}z\right]\tilde{\mathscr{E}}&=-\frac{4\pi}{i\kappa}\left[(\alpha^2+\beta^2)\eta^{3/2}\tilde{j}_z\right.\\&\qquad\left.+i\eta^{1/2}\frac{\partial}{\partial z}\eta(\alpha\tilde{j}_x+\beta\tilde{j}_y)\right]\\&\equiv\tilde{S}_1,\end{aligned}\right\}\quad\ldots\quad(7.2)$$

$$\left.\begin{aligned}\left[\frac{d^2}{dz^2}+\kappa^2-\alpha^2-\beta^2+\frac{2\kappa^2}{a}z\right]\tilde{\mathscr{H}}&=4\pi i\eta^{5/2}(\beta\tilde{j}_x-\alpha\tilde{j}_y)\\&\equiv\tilde{S}_2,\end{aligned}\right\}\quad\ldots\quad(7.3)$$

outside the sphere ; and

$$\left.\begin{aligned}\left[\frac{d^2}{dz^2}+\epsilon'\kappa^2-\alpha^2-\beta^2+\frac{2\epsilon'\kappa^2}{a}z\right]\tilde{\mathscr{E}}_1&=0,\quad\ldots\quad(7.4)\\\left[\frac{d^2}{dz^2}+\epsilon'\kappa^2-\alpha^2-\beta^2+\frac{2\epsilon'\kappa^2}{a}z\right]\tilde{\mathscr{H}}_1&=0,\quad\ldots\quad(7.5)\end{aligned}\right\}$$

inside the sphere. (The suffix 1 is used to refer to the inside.) These are now ordinary differential equations of the second order, directly related to the differential equation satisfied by the Airy integral.

It may at first sight seem illogical to use the approximation

$$\eta^2\equiv e^{2z/a}=1+\frac{2z}{a},$$

which is the origin of the term in z in the differential operator, in view of the fact that the unapproximated equation is soluble in terms of Bessel functions of argument $\kappa a\eta$. But their use would entail asymptotic forms of the Bessel functions of arbitrary order for large values of the argument, which in turn rest on the theory of the Airy integral, and which is a fundamentally simpler function than a Bessel function of arbitrary order. The present approach is therefore more direct.

The eqns. (6.9) and (6.10) for the x and y components of the field strengths, when expressed in Fourier transforms, become algebraic equations, and are immediately soluble.

§8. Equations inside the Sphere : Boundary Conditions at the Surface

We assume that the medium inside the sphere is conducting (conductivity σ referred to e.s.u.), has dielectric constant ϵ_0 and unit magnetic permeability, and that there are no driven sources of current inside. The current density is then proportional to $\mathbf{E}$ and as is well known the equations are identical with those for zero charge- and current-densities if the dielectric constant ϵ_0 is replaced by the complex quantity ϵ' given by (4.2),

$$\epsilon'=\epsilon_0-4\pi i\sigma/\omega.$$

$\tilde{\mathscr{E}}_1$ and $\tilde{\mathscr{H}}_1$ inside the sphere both satisfy the same equation (7.4), (7.5).

The solution of this equation represents a damped wave proceeding inwards from the surface, and we shall assume that the damping is so rapid that η does not vary appreciably in the region where $\tilde{\mathscr{E}}_1$ is appreciable.* We can then apply the Jeffreys–Wentzel–Kramers–Brillouin method to obtain the required solution to the desired approximation.

It is convenient, however, to make a further approximation. We are dealing with a wave problem, and the solution can be regarded as a product of an amplitude and a unimodular phase factor, and it is clear that while a small fractional error in a large phase angle (argument of the exponent) may lead to an appreciable error, this is not so for the amplitude. We are therefore justified in neglecting terms in $1/a$ when they occur in the amplitude, though it would lead to serious error to ignore them in the phase. Such terms as $1/\kappa a$, z/a, when occurring in the amplitude part of the solution will therefore be omitted, and η will be replaced by 1.

With this further simplification, then, $\tilde{\mathscr{E}}_1$ and $\tilde{\mathscr{H}}_1$ will depend on z only through the factor $\exp(i\gamma' z)$, where the complex quantity γ' is given by

$$\gamma'^2=\epsilon'\kappa^2-\alpha^2-\beta^2, \quad . \quad . \quad . \quad . \quad . \quad . \quad . \quad . \quad (8.1)$$

and the sign is determined by the condition that the wave attenuates inwards, i.e. the imaginary part of γ' is negative.

We now turn to the boundary conditions for $\tilde{\mathscr{E}}$ and $\tilde{\mathscr{H}}$ at $z=0$, which is a surface of discontinuity of dielectric constant. They are given by the continuity of the tangential components of **E** and **H**, which substituted in the Fourier transforms of eqns. (6.9) and (6.10), and neglecting terms in $1/a$, give

$$\left.\begin{aligned} \tilde{\mathscr{E}}&=\epsilon'^{1/2}\tilde{\mathscr{E}}_1, & \frac{d\tilde{\mathscr{E}}}{dz}&=\epsilon'^{-1/2}\frac{d\tilde{\mathscr{E}}_1}{dz}, \\ \tilde{\mathscr{H}}&=\tilde{\mathscr{H}}_1, & \frac{d\tilde{\mathscr{H}}}{dz}&=\frac{d\tilde{\mathscr{H}}_1}{dz}, \end{aligned}\right\} \quad z=0, \quad . \quad . \quad . \quad (8.2)$$

where $\tilde{\mathscr{E}}$, $\tilde{\mathscr{H}}$ refer to the solutions outside, and $\tilde{\mathscr{E}}_1$, $\tilde{\mathscr{H}}_1$ the solution inside. In deriving this, use has been made of the fact that in the outside region **j** and ρ are zero in the immediate neighbourhood of $z=0$, and in the inside region $\rho=0$ and $\mathbf{j}=\sigma\mathbf{E}$. The continuity conditions for the normal components of electric displacement and magnetic induction are not independent conditions, and are contained in this result.

The quantities $\tilde{\mathscr{E}}_1$ and $\tilde{\mathscr{H}}_1$, referring to the field inside the sphere, can be eliminated from these equations if use is made of the fact that

$$\left.\begin{aligned} \frac{d\tilde{\mathscr{E}}_1}{dz}&=i\gamma'\tilde{\mathscr{E}}_1, \\ \frac{d\tilde{\mathscr{H}}_1}{dz}&=i\gamma'\tilde{\mathscr{H}}_1, \end{aligned}\right\} \quad z\leqslant 0, \quad . \quad . \quad . \quad . \quad . \quad (8.3)$$

* This is certainly true for radio waves inside the earth or in sea water.

leading to the result

$$\left.\begin{aligned} \frac{d\tilde{\mathscr{E}}}{dz} &= \frac{i\gamma'}{\epsilon'}\tilde{\mathscr{E}}, \\ \frac{d\tilde{\mathscr{H}}}{dz} &= i\gamma'\tilde{\mathscr{H}}, \end{aligned}\right\} \quad z=0. \qquad \ldots\ldots \quad (8.4)$$

The problem is therefore reduced to solving the second-order differential eqn. (7.2) and (7.3) with the boundary conditions (8.4) at $z=0$, and the condition that as $z\to\infty$ the solution corresponds to an outgoing wave.

§9. Formal Solution in Terms of Solutions of the Homogeneous Equation

The solution is given in terms of the solutions of the corresponding homogeneous equation in the standard manner. Let $u(\alpha, \beta, z)$, $v(\alpha, \beta, z)$ be two independent solutions of the equation

$$\frac{d^2u}{dz^2} + \left(\kappa^2-\alpha^2-\beta^2+\frac{2\kappa^2}{a}z\right)u=0, \qquad \ldots\ldots \quad (9.1)$$

z being regarded as the independent variable, with α and β as parameters. Then the Wronskian W,

$$W=v\frac{du}{dz}-u\frac{dv}{dz}, \qquad \ldots\ldots \quad (9.2)$$

is independent of z. The solution u will be chosen to represent an outgoing wave at infinity, it being observed that for any α, β the solution becomes oscillatory for sufficiently large positive z. The choice of v will be left open for the moment.

The required solution is then

$$\tilde{\mathscr{E}}(z)=\frac{1}{W}\left[u(z)\int_0^z v(z')\tilde{S}_1(z')\,dz'+v(z)\int_z^\infty u(z')\tilde{S}_1(z')\,dz' - \left(\frac{i\gamma'v(0)-\epsilon'v'(0)}{i\gamma'u(0)-\epsilon'u'(0)}\right)u(z)\int_0^\infty u(z')\tilde{S}_1(z')\,dz'\right], \qquad \ldots \quad (9.3)$$

$$\tilde{\mathscr{H}}(z)=\frac{1}{W}\left[u(z)\int_0^z v(z')\tilde{S}_2(z')\,dz'+v(z)\int_z^\infty u(z')\tilde{S}_2(z')\,dz' - \left(\frac{i\gamma'v(0)-v'(0)}{i\gamma'u(0)-u'(0)}\right)u(z)\int_0^\infty u(z')\tilde{S}_2(z')\,dz'\right], \qquad \ldots\ldots \quad (9.4)$$

where z' is a variable of integration, $u(0)$ means the value of u at $z=0$, etc., explicit reference to the dependence on α and β being omitted.

To study the solutions of (9.1) it is convenient to introduce a non-dimensional quantity K, and two lengths h_0 and d_0 which will be natural units for height and plan distance respectively, as follows

$$K=(\tfrac{1}{2}\kappa a)^{1\,3}, \qquad \ldots\ldots \quad (9.5)$$

$$h_0=(a/2\kappa^2)^{1,3}, \qquad \ldots\ldots \quad (9.6)$$

$$d_0=(2a^2/\kappa)^{1\,3}. \qquad \ldots\ldots \quad (9.7)$$

K is a large number* and the four lengths λ, h_0, d_0, a bear the following ratios

$$\frac{\lambda}{2\pi}=\frac{h_0}{K}=\frac{d_0}{2K^2}=\frac{a}{2K^3}. \quad . \quad . \quad . \quad . \quad . \quad . \quad . \quad (9.8)$$

We also define ζ (depending on α, β) and ξ (depending on α, β and z) by

$$\zeta=h_0^2(\kappa^2-\alpha^2-\beta^2)=K^2\left(1-\frac{\alpha^2+\beta^2}{\kappa^2}\right), \quad . \quad . \quad . \quad . \quad (9.9)$$

$$-\xi=h_0^2\left(\kappa^2-\alpha^2-\beta^2+\frac{2\kappa^2}{a}z\right)=\zeta+z/h_0. \quad . \quad . \quad . \quad . \quad (9.10)$$

If we re-write eqn. (9.1) with ξ instead of z as independent variable, we obtain the equation for the Airy integral,

$$\frac{d^2u}{d\xi^2}=\xi u, \quad . \quad . \quad . \quad . \quad . \quad . \quad . \quad . \quad . \quad (9.11)$$

of which the functions $\mathrm{Ai}(\xi)$, $\mathrm{Bi}(\xi)$ defined by

$$\mathrm{Ai}(\xi)=\frac{1}{\pi}\int_0^\infty \cos\left(\tfrac{1}{3}t^3+\xi t\right)dt, \quad . \quad . \quad . \quad . \quad . \quad (9.12)$$

$$\mathrm{Bi}(\xi)=\frac{1}{\pi}\int_0^\infty \left[\exp\left(\xi t-\tfrac{1}{3}t^3\right)+\sin\left(\tfrac{1}{3}t^3+\xi t\right)\right]dt, \quad . \quad . \quad (9.13)$$

are two independent solutions (Jeffreys and Jeffreys 1950, p. 508). We are interested in the asymptotic behaviour as $z\to\infty$, with α, β fixed; i.e. as $\xi\to-\infty$. For large negative real values,

$$\left.\begin{aligned}\mathrm{Ai}(\xi)&\sim\pi^{-1/2}(-\xi)^{-1/4}\sin\left[\tfrac{2}{3}(-\xi)^{3/2}+\pi/4\right],\\ \mathrm{Bi}(\xi)&\sim\pi^{-1/2}(-\xi)^{-1/4}\cos\left[\tfrac{2}{3}(-\xi)^{3/2}+\pi/4\right].\end{aligned}\right\} \quad . \quad . \quad (9.14)$$

The combination

$$u(\alpha,\beta,z)=\mathrm{Bi}(-\zeta-z/h_0)-i\mathrm{Ai}(-\zeta-z/h_0) \quad . \quad . \quad . \quad (9.15)$$

has the asymptotic behaviour, as $z\to\infty$,

$$u(\alpha,\beta,z)\sim\pi^{-1/2}(\zeta+z/h_0)^{-1/4}\exp\left\{-i\left[\tfrac{2}{3}(\zeta+z/h_0)^{3/2}+\pi/4\right]\right\} \quad . \quad (9.16)$$

which, in conjunction with the time factor $\exp(i\omega t)$, represents an outward travelling wave at infinity; we therefore take this to be our solution u.

Before choosing v it should be remarked that the first two terms of eqns. (9.3) and (9.4) are independent of the nature of the medium inside the sphere and it would be convenient to interpret them as the field due to a source in the absence of the sphere, the third term then representing the reflected or secondary wave due to currents induced in the sphere.

---

* As a practical example consider $a=8\,000$ km (effective radius of the earth under normal atmospheric conditions) and $\lambda=10$ cm. Then $K=631$, $h_0=10{\cdot}0$ m, $d_0=12{\cdot}7$ km.

This interpretation will be correct if v has the correct asymptotic form as $z\to-\infty$. This is $v\to 0$. That this is the correct condition, rather than that v should behave like an outgoing wave is perhaps easiest seen by considering the geometrical optics limit, for a ray starting downwards at any angle reaches a certain maximum value of $-z$ and then comes up again. We shall therefore choose

$$v=\mathrm{Ai}(-\zeta-z/h_0). \qquad (9.17)$$

With this choice the Wronskian has the value

$$W=v\frac{du}{dz}-u\frac{dv}{dz}=-\frac{1}{\pi h_0}. \qquad (9.18)$$

For the sake of brevity we introduce the functions f and g, which for an arbitrary variable ν are defined by

$$\left.\begin{aligned} f(\nu)&=\mathrm{Bi}(-\nu)-i\,\mathrm{Ai}(-\nu)=2e^{-\pi i/6}\,\mathrm{Ai}(e^{\pi i/3}\nu),\\ g(\nu)&=\mathrm{Ai}(-\nu),\end{aligned}\right\} \qquad (9.19)$$

so that

$$\left.\begin{aligned} u(\alpha,\beta,z)&=f(\zeta+z/h_0),\\ v(\alpha,\beta,z)&=g(\zeta+z/h_0).\end{aligned}\right\} \qquad (9.20)$$

§10. Field of a Vertical Dipole

We now apply our results to the field produced by a vertical dipole of strength p^* situated at $x=y=0$, $z=h$. The current and charge-densities are

$$\left.\begin{aligned} j_x&=j_y=0,\\ j_z&=\frac{i\kappa p}{\eta^2}\delta(x)\,\delta(y)\,\delta(z-h),\\ \rho&=-\frac{p}{\eta^3}\delta(x)\,\delta(y)\,\delta'(z-h),\end{aligned}\right\} \qquad (10.1)$$

with the Fourier transforms

$$\left.\begin{aligned} \tilde{j}_z&=\frac{i\kappa p}{4\pi^2\eta^2}\delta(z-h),\\ \tilde{\rho}&=\frac{-p}{4\pi^2\eta^3}\delta'(z-h).\end{aligned}\right\} \qquad (10.2)$$

The terms occurring on the right of eqns. (7.2) and (7.3) are therefore

$$\left.\begin{aligned} \tilde{S}_1&=-\frac{p}{\pi}e^{-h/2a}(\alpha^2+\beta^2)\,\delta(z-h),\\ \tilde{S}_2&=0.\end{aligned}\right\} \qquad (10.3)$$

* More exactly, of strength $p\,e^{Wa}$.

The solution, given by eqns. (9.3), (9.4), and using (9.18), (9.20), is therefore

$$\left.\begin{aligned} \mathscr{E} &= h_0 p \iint \Phi(\zeta\,;\ h,\, z)(\alpha^2+\beta^2)\, e^{i(\alpha x+\beta y)}\, d\alpha\, d\beta, \\ \mathscr{H} &= 0, \end{aligned}\right\} \quad . \ . \ . \quad (10.4)$$

where for $z \leqslant h$, $\Phi(\zeta\,;\ h,\, z)$ is defined by

$$\Phi(\zeta\,;\ h,\, z) = \left[g(\zeta+z/h_0) - \frac{i\gamma' h_0\, g(\zeta) - \epsilon'\, g'(\zeta)}{i\gamma' h_0 f(\zeta) - \epsilon' f'(\zeta)} f(\zeta+z/h_0) \right] f(\zeta+h/h_0), \quad . \ . \ . \quad (10.5)$$

and for $z \geqslant h$, h and z are to be interchanged. In (10.4) we have replaced $\exp(-h/2a)$ by 1, as it occurs in the amplitude only. The field therefore depends in a symmetrical way on h and z, as is to be expected from general reciprocity relations.

The double integral can be reduced to a single integral by introducing polar coordinates in the $\alpha\beta$-plane, and carrying out the angular integration. It is convenient to use the variable ζ to characterize the radius vector, giving

$$\mathscr{E} = \frac{\pi\kappa^2 p}{h_0} \int_{-\infty}^{K^2} (1-\zeta/K^2) J_0(\kappa r(1-\zeta/K^2)^{1/2}) \Phi(\zeta\,;\ h,\, z)\, d\zeta, \quad (10.6)$$

where

$$r = \sqrt{(x^2+y^2)}. \quad . \ . \ . \ . \ . \ . \ . \ . \ . \quad (10.7)$$

Equation (10.6) gives E_z directly, since from eqns. (6.3), (6.6), and dropping the factor $\eta^{-3/2}$ in the amplitude,

$$E_z = \mathscr{E} - 4\pi p \delta(x)\delta(y)\delta(z-h). \quad . \ . \ . \ . \ . \quad (10.8)$$

The other field components are easily derived from eqns. (6.9), (6.10) and are

$$\left.\begin{aligned} E_r &= -\frac{\pi\kappa p}{h_0} \int_{-\infty}^{K^2} (1-\zeta/K^2)^{1/2} J_1(\kappa r(1-\zeta/K^2)^{1/2}) \frac{\partial}{\partial z} \Phi(\zeta\,;\ h,\, z)\, d\zeta, \\ H_\varphi &= -\frac{\pi i\kappa^2 p}{h_0} \int_{-\infty}^{K^2} (1-\zeta/K^2)^{1/2} J_1(\kappa r(1-\zeta/K^2)^{1/2}) \Phi(\zeta\,;\ h,\, z)\, d\zeta, \\ E_\varphi &= H_z = H_r = 0, \end{aligned}\right\} \quad . \ . \ . \quad (10.9)$$

where the subscripts r and ϕ refer to ' radial ' and azimuthal components in the xy-plane.

§11. Field of a Horizontal Dipole

For a horizontal dipole we take

$$\left.\begin{aligned} j_x &= \frac{i\kappa p}{\eta^2} \delta(x)\, \delta(y)\, \delta(z-h), \\ j_y &= j_z = 0, \\ \rho &= -\frac{p}{\eta^3} \delta'(x)\, \delta(y)\, \delta(z-h), \end{aligned}\right\} \quad . \ . \ . \ . \quad (11.1)$$

and therefore

$$\left.\begin{aligned} \tilde{j}_x &= \frac{i\kappa p}{4\pi^2\eta^z}\delta(z-h), \\ \tilde{\rho} &= -\frac{i\alpha p}{4\pi^2\eta^3}\delta(z-h)\,; \end{aligned}\right\} \quad . \quad . \quad . \quad . \quad . \quad . \quad (11.2)$$

$$\left.\begin{aligned} \tilde{S}_1 &= -\frac{i\alpha p}{\pi}\,\mathrm{e}^{-h/2a}\,\delta'(z-h), \\ \tilde{S}_2 &= -\frac{\beta\kappa p}{\pi}\,\mathrm{e}^{h\,2a}\,\delta(z-h). \end{aligned}\right\} \quad . \quad . \quad . \quad . \quad (11.3)$$

Following the same procedure as for the vertical dipole one finds

$$E_z = \frac{\pi\kappa p}{h_0}\cos\phi\int_{-\infty}^{K^2}(1-\zeta/K^2)^{1/2}J_1(\kappa r(1-\zeta/K^2)^{1/2})\,\frac{\partial}{\partial h}\Phi(\zeta\,;\ h,\,z)\,d\zeta, \quad . \quad . \quad . \quad (11.4)$$

$$H_z = \frac{\pi i\kappa^2 p}{h_0}\sin\phi\int_{-\infty}^{K^2}(1-\zeta/K^2)^{1/2}J_1(\kappa r(1-\zeta/K^2)^{1/2})\Psi(\zeta\,;\ h,\,z)\,d\zeta \quad . \quad . \quad . \quad (11.5)$$

where Ψ is a function similar to Φ, also symmetrical in h and z, defined for $z\leqslant h$ by

$$\Psi(\zeta\,;\ h,z)=\Psi(\zeta\,;\ z,h)$$
$$=\left[g(\zeta+z/h_0)-\frac{i\gamma' g(\zeta)-g'(\zeta)}{i\gamma' f(\zeta)-f'(\zeta)}\,f(\zeta+z/h_0)\right]f(\zeta+h/h_0). \quad (11.6)$$

For the other components, one finds, after some calculation,

$$\left.\begin{aligned} E_r &= \frac{\pi p}{2h_0}\cos\phi\,\{\kappa^2(I_1-I_2)+\partial^2(I_3+I_4)/\partial h\,\partial z\}, \\ E_\varphi &= \frac{\pi p}{2h_0}\sin\phi\,\{\kappa^2(I_1+I_2)+\partial^2(I_3-I_4)/\partial h\,\partial z\}, \\ H_r &= \frac{\pi i\kappa p}{2h_0}\sin\phi\,\{\partial(I_1+I_2)/\partial z+\partial(I_4-I_3)/\partial h\}, \\ H_\varphi &= \frac{\pi i\kappa p}{2h_0}\cos\phi\,\{\partial(I_1-I_2)/\partial z-\partial(I_3+I_4)/\partial h\}, \end{aligned}\right\} \quad . \quad (11.7)$$

where

$$\left.\begin{aligned} I_1 &= \int J_0\Psi\,d\zeta, \\ I_2 &= -\int J_2\Psi\,d\zeta, \\ I_3 &= \int J_0\Phi\,d\zeta, \\ I_4 &= -\int J_2\Phi\,d\zeta, \end{aligned}\right\} \quad . \quad . \quad . \quad . \quad . \quad (11.8)$$

the range of integration in each case being $(-\infty,\ K^2)$ and the argument of the Bessel function $\kappa r(1-\zeta/K^2)^{1/2}$.*

* A term proportional to $\delta(z-h)$ has been suppressed for brevity in the expressions for E_r, E_φ, which arises because $\partial^2\Phi/\partial h\,\partial z$ has a delta function singularity. In using these results it is of no importance, for the field is continuous (for $r,\ h,\ z>0$), and so can be obtained by continuity from the expression for $z\neq h$.

It will be shown that in the wave zone $(\kappa r \gg 1) I_1 \sim I_2$ and $I_3 \sim I_4$, so that half of the terms in (11.7) disappear. For nearly horizontal propagation it will be seen in §12, that E_φ and H_r are the dominant components, the others being smaller by factors of K^{-1} or $(h+z)/r$, as was to be expected.

It may also be noted that E_z and H_z can be expressed in terms of $\partial^2 I_3/\partial h\, \partial x$ and $\partial I_1/\partial y$ respectively. $I_1 (\sim I_2)$ and $\partial I_3/\partial h (\sim \partial I_4/\partial h)$ therefore play a role analogous to that of potentials.

§12. Evaluation of the Integrals as Sums of Residues

The expressions we have obtained for the electro-magnetic field in terms of definite integrals are of little practical value as they stand. In order to proceed further it is necessary to make a few more approximations. For this we need to have some notion of the behaviour of the integrand, particularly its asymptotic behaviour for large positive and negative values of ζ. It will be noticed that the range of integration is from $-\infty$ to K^2, which is a large number (4×10^5 in the example already quoted), and we shall show that the only important contributions to the integral come from the region in which ζ is not very large (the important range is determined by h/h_0, z/h_0 and r/d_0, which in the practical applications are numbers which are neither very large nor very small). After a suitable approximation, therefore, it will be permissible to extend the range of integration to ∞, and then to reduce the integral to a contour integral around a suitable loop, which can then be evaluated by the method of residues.

The integrals are all of the same type, and it will be sufficient to consider (10.6). The function Φ occurring in the integrand falls off to zero exponentially for large negative ζ, and oscillates with decreasing amplitude for large positive ζ, as will be shown in a moment. The Bessel function $J_0(\kappa r(1-\zeta/K^2)^{1/2})$ oscillates rapidly in the region of moderate ζ, if as will be assumed, κr is large. The integrand therefore oscillates rapidly, its amplitude rising exponentially from zero as ζ increases from $-\infty$, reaches a maximum amplitude and perhaps a point of stationary phase, and then keeps on oscillating rapidly, with decreasing amplitude, as ζ goes to K^2. A more careful study of the behaviour of the Bessel function at $\zeta = K^2$ shows that the cutting off of the oscillation at the end-point contributes a negligible amount to the integral. We are therefore justified in saying that the important contributions only come from moderate ζ ; and therefore in replacing the argument of the Bessel function by

$$\kappa r(1-\zeta/2K^2) = \kappa r - \zeta r/d_0 \; ; \qquad . \; . \; . \; . \; . \; . \qquad (12.1)$$

in using the asymptotic expansion of the Bessel function

$$J_0(\kappa r - \zeta r/d_0) \sim (2/\pi\kappa r)^{1/2} \cos(\kappa r - \zeta r/d_0 - \pi/4) \; ; \qquad (12.2)$$

and in extending the upper limit to infinity. Also γ' may be replaced by $\kappa(\epsilon'-1)^{1/2}$.

The asymptotic behaviour for large complex ζ of the function Φ, on which this reasoning depends, is easily derived from the asymptotic behaviour of the Airy integral (c.f. H. and B. Jeffreys, "Mathematical Physics", Cambridge, 1950, p. 511), namely (for real w and δ, $w>0$),

$$\left.\begin{aligned} &\mathrm{Ai}\,(w\,e^{i\delta})\sim\tfrac{1}{2}\pi^{-1/2}\,w^{-1/4}\,e^{-i\delta/4}\exp\left(-\tfrac{2}{3}\,w^{3/2}\,e^{3i\delta/2}\right), \qquad (-\pi<\delta<\pi),\\ &\mathrm{Ai}\,(-w)\sim\pi^{-1/2}\,w^{-1/4}\sin\left(\tfrac{2}{3}w^{3/2}+\frac{\pi}{4}\right),^{*}\end{aligned}\right\} \quad . \quad . \quad . \quad (12.3)$$

supplemented with the closely related result

$$g(\zeta+z/h_0)\,f(\zeta)-f(\zeta+z/h_0)\,g(\zeta)\sim\frac{\sin\left(\zeta^{1/2}z/h_0\right)}{\pi\zeta^{1/2}}, \quad . \quad . \quad (12.4)$$

for large ζ and constant z/h_0. It is

$$\Phi(\zeta\,;\,h,\,z)\sim\frac{-i}{2\pi\zeta^{1/2}}$$

$$\times\left\{\exp\left(-i|\,h-z\,|\zeta^{1/2}/h_0\right)+\frac{\epsilon'\zeta^{1/2}-\gamma' h_0}{\epsilon'\zeta^{1/2}+\gamma' h_0}\exp\left(-i|\,h+z\,|\zeta^{1/2}/h_0\right)\right\}, \quad (12.5)$$

where the sign of $\zeta^{1/2}$ is chosen such that

$$\zeta^{1/2}\equiv(|\,\zeta\,|\,e^{i\delta})^{1/2}=|\,\zeta\,|^{1/2}\,e^{i\delta/2}$$

when

$$-4\pi/3<\delta<2\pi/3. \quad . \quad . \quad . \quad . \quad . \quad . \quad . \quad (12.6)$$

For $\delta=2\pi/3$ (12.5) fails and Φ has an infinite number of poles which cluster close to the line $\zeta=|\zeta\,|\exp(2\pi i/3)$.

For real ζ (12.5) gives the asymptotic behaviour already quoted (with the almost trivial exception of when $h=z$, in which case Φ decreases with $|\zeta\,|$, but not exponentially).

We shall therefore replace (10.6) by

$$\mathscr{E}=\frac{\kappa^2 p}{h_0}\left(\frac{2\pi}{\kappa r}\right)^{1/2}\int_{-\infty}^{\infty}\Phi(\zeta\,;\,h,\,z)\cos\left(\kappa r-\zeta r/d_0-\pi/4\right)d\zeta, \quad (12.7)$$

and in the definition of Φ we shall replace γ' by $\kappa(\epsilon'-1)^{1/2}$ i.e.

$$\Phi(\zeta\,;\,h,\,z)=\Phi(\zeta\,;\,z,\,h)$$

$$=\left[g(\zeta+z/h_0)-\frac{g(\zeta)-\tau_1 g'(\zeta)}{f(\zeta)-\tau_1 f'(\zeta)}f(\zeta+z/h_0)\right]f(\zeta+h/h_0), \quad z\leqslant h, \quad (12.8)$$

where

$$\tau_1=-i\epsilon'/K(\epsilon'-1)^{1/2}. \quad . \quad . \quad . \quad . \quad . \quad . \quad . \quad (12.9)$$

The corresponding function Ψ, which occurs in the horizontal dipole problem, is defined by the same equation as (12.8), but with τ_1 replaced by τ_2,

$$\tau_2=-i/K(\epsilon'-1)^{1/2}. \quad . \quad . \quad . \quad . \quad . \quad . \quad (12.10)$$

It is to be noted that with these approximations Φ and Ψ are single-valued functions of ζ.

---

* This asymptotic form involving the sine is actually valid for $\mathrm{Ai}(-we^{i\delta})$ in the more extended region $-\pi/3<\delta<\pi/3$. For large w and fixed δ, however, it coincides with the first expression because one of the exponential parts of the sine is negligible compared with the other.

In applications to radio propagation over the earth or sea τ_2 is always very small, and can usually be replaced by zero ; while τ_1 is small for microwaves, but may be appreciable for longer waves.

The integrand in (12.7) is a regular function of ζ, except for poles at the zeros of $f(\zeta)-\tau_1 f'(\zeta)$, which occur near the line $\zeta=|\zeta|\exp(2\pi i/3)$. We shall call these zeros $a_1, a_2, \ldots$, i.e.

$$f(a_s)=\tau_1 f'(a_s),$$

or
$$\mathrm{Ai}\,(a_s e^{\pi i/3})=\tau_1 e^{\pi i/3}\,\mathrm{Ai}'(a_s e^{\pi i/3}) ; \quad . \quad . \quad . \quad . \quad (12.11)$$

and b_s the corresponding zeros of $f(\zeta)-\tau_2 f'(\zeta)$ where Ψ has poles,

$$\mathrm{Ai}\,(b_s e^{\pi i/3})=\tau_2 e^{\pi i/3}\,\mathrm{Ai}'(b_s e^{\pi i/3}). \quad . \quad . \quad . \quad . \quad (12.12)$$

It can be shown that, provided the imaginary parts of τ_1 and τ_2 are positive, as they are from the condition that the imaginary part of γ' is negative, since the solution inside the sphere attenuates downwards, then all the poles are in the second quadrant of the ζ-plane, $\frac{1}{2}\pi<\arg a_s$, $\arg b_s<\pi$.

Fig. 1

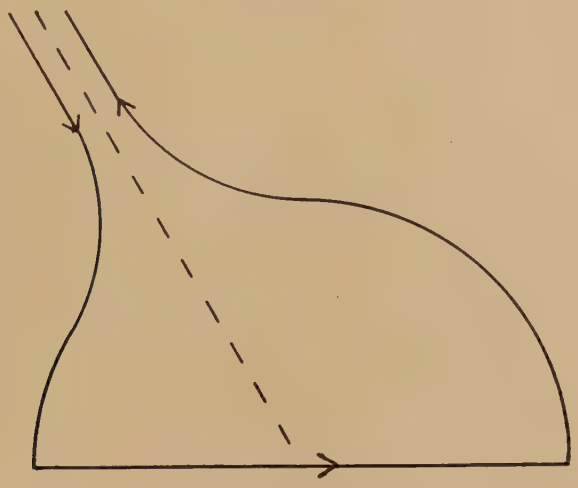

We now decompose the cosine in (12.7) into two exponentials. Far away from the real axis the factors $\exp(\pm i\zeta r/d_0)$ dominate the weaker exponential behaviour of Φ, which contains $\zeta^{1/2}$ in the exponent. The path of the integral containing $\exp(-i\zeta r/d_0)$ can therefore be closed by an infinite semicircle in the lower half-plane, and since the resulting contour contains no poles, this integral vanishes. Similarly the path of the integral with $\exp(i\zeta r/d_0)$ can be extended and deformed to the contour shown in fig. 1, leaving

$$\mathscr{E}=\frac{\kappa^2 p}{h_0}\left(\frac{\pi}{2\kappa r}\right)^{1/2} e^{i(\pi/4-\kappa r)}\int_C \Phi(\zeta\,;\,h,\,z)\,e^{i\zeta r/d_0}\,d\zeta, \quad . \quad (12.13)$$

and this integral can be expressed as $2\pi i$ times the sum of the residues at the poles $\zeta=a_s$. The residue of Φ at a_s is

$$-\frac{g(a_s)-\tau_1 g'(a_s)}{f'(a_s)-\tau_1 f''(a_s)} f(a_s+h/h_0) f(a_s+z/h_0),$$

which, on using the Wronskian condition and the differential equation satisfied by $f(\zeta)$ can be written

$$\frac{f(a_s+h/h_0) f(a_s+z/h_0)}{\pi(1+\tau_1{}^2 a_s) f'^2(a_s)}. \quad . \quad . \quad . \quad . \quad . \quad (12.14)$$

We therefore finally obtain for the vertical dipole

$$E_z=\frac{\kappa^2 p}{h_0}\left(\frac{2\pi}{\kappa r}\right)^{1/2} e^{i(3\pi/4-\kappa r)} \sum_s \frac{f(a_s+h/h_0) f(a_s+z/h_0)}{(1+\tau_1{}^2 a_s) f'^2(a_s)} e^{ia_s r/d_0}, \quad (12.15)$$

and similar results for the other components.

This (apart from differences of notation) is the solution of Watson, of Van der Pol and Bremmer, and of Fock. This form of the solution is particularly useful for the field in the shadow region, for then the series is rapidly convergent. Each term decreases exponentially with r, since the real part of ia_s is positive. Ultimately, for distances sufficiently far over the horizon, the first term by itself gives a good approximation to the field. This is Eckersley's approximation. It is the product of an exponential function of r, a function of h and a function of z (height gain functions).

For the horizontal dipole the field has been seen to be given in terms of I_1, I_2, I_3 and I_4, which, to the approximation of this section, are equal to

$$I_1=I_2=\left(\frac{2}{\pi\kappa r}\right)^{1/2} e^{i(3\pi/4-\kappa r)} \sum_s \frac{f(b_s+h/h_0) f(b_s+z/h_0)}{(1+\tau_2{}^2 b_s) f'^2(b_s)} e^{ib_s r/d_0}, \quad (12.16)$$

$$I_3=I_4=\left(\frac{2}{\pi\kappa r}\right)^{1/2} e^{i(3\pi/4-\kappa r)} \sum_s \frac{f(a_s+h/h_0) f(a_s+z/h_0)}{(1+\tau_1{}^2 a_s) f'^2(a_s)} e^{ia_s r/d_0}. \quad (12.17)$$

Neglecting i/K in comparison with unity we obtain

$$H_z=E_\varphi=\frac{\kappa^2 p}{h_0}\left(\frac{2\pi}{\kappa r}\right)^{1/2} e^{-i(\pi/4+\kappa r)} \sin\phi \sum_s \frac{f(b_s+h/h_0) f(b_s+z/h_0)}{(1+\tau_2{}^2 b_s) f'^2(b_s)} e^{ib_s r/d_0}.$$

. . . (12.18)

The other components are smaller since they contain a factor $i/\kappa h_0=i/K$ (except that at extremely great distances the exponential factor in (12.16) may become so small compared with the corresponding factor in (12.17) that this compensates for the greater factor multiplying the exponential).

§ 13. Evaluation of the Integrals by Steepest Descents

When the source and receiver are well elevated and also well within each other's horizon it is possible to estimate the integrals by the method of stationary phases, equivalent to the method of steepest descents. One then obtains as first approximation the results predicted by geometrical optics. This has been studied in detail by van der Pol and Bremmer

(1937 b), and the method is already to be found, though not in great detail, in Poincaré's paper (1910). We shall therefore discuss only the broad outlines here.

We shall again confine ourselves to the radiation zone ($\kappa r \gg 1$) and in order that our general method of neglecting terms in $1/a^2$ shall be a good approximation, to heights such that $h/a \ll 1$ and $z/a \ll 1$. Furthermore, for the sake of simplicity, we shall restrict ourselves to nearly horizontal propagation, i.e. $(h+z) \ll r$.*

We now consider the typical expression (12.7), derived from (10.6) after the above approximations have been made. We find that the integrand has points of stationary phase in the region where it is oscillating (i.e. roughly in the range of positive ζ). We decompose Φ into two terms, the first

$$f(\zeta+h/h_0)\, g(\zeta+z/h_0), \qquad (z \leqslant h),$$

corresponding to the primary radiation (i.e. what would be present if there were no earth), and the second

$$-\frac{g(\zeta)+(i\epsilon'/\gamma' h_0)\, g'(\zeta)}{f(\zeta)+(i\epsilon'/\gamma' h_0)\, f'(\zeta)} f(\zeta+h/h_0)\, f(\zeta+z/h_0),$$

corresponding to the secondary radiation caused by the earth. We also decompose $\cos(\kappa r - \zeta r/d_0 - \pi/4)$ into two exponentials, and confine our attention to the term $\exp i(-\kappa r + \zeta r/d_0 + \pi/4)$ as we have already shown that the other exponential gives a zero contribution;† indeed it is easily verified that it gives rise to no point of stationary phase.

The primary field is therefore given by

$$\mathscr{E}_p = \frac{\kappa^2 p}{h_0}\left(\frac{\pi}{2\kappa r}\right)^{1/2} e^{i(\pi/4-\kappa r)} \int_{-\infty}^{\infty} f(\zeta+h/h_0)\, g(\zeta+z/h_0)\, e^{i\zeta r/d_0}\, d\zeta. \qquad (13.1)$$

We now use the asymptotic forms

$$\left.\begin{aligned} f(\zeta+h/h_0) &\sim \pi^{-1/2} e^{-\pi i/4} (\zeta+h/h_0)^{-1/4} \exp(-\tfrac{2}{3} i(\zeta+h/h_0)^{3/2}), \\ g(\zeta+z/h_0) &\sim \tfrac{1}{2}\pi^{-1/2} e^{-\pi i/4} (\zeta+z/h_0)^{-1/4} \{\exp(-\tfrac{2}{3} i(\zeta+z/h_0)^{3/2}) \\ &\qquad - i \exp(\tfrac{2}{3} i(\zeta+z/h_0)^{3/2})\}, \end{aligned}\right\} \qquad (13.2)$$

for positive real ζ. The condition for stationary phase is therefore

$$\frac{\partial}{\partial \zeta}[-\tfrac{2}{3}(\zeta+h/h_0)^{3/2} \mp \tfrac{2}{3}(\zeta+z/h_0)^{3/2} + \zeta r/d_0] = 0 \qquad (13.3)$$

or

$$(\zeta+h/h_0)^{1/2} \pm (\zeta+z/h_0)^{1/2} = r/d_0. \qquad (13.4)$$

This has only one solution,

$$\zeta_1 = \frac{1}{4}\left\{\frac{r^2}{{d_0}^2} - \frac{2(h+z)}{h_0} + \frac{(h-z)^2 {d_0}^2}{{h_0}^2 r^2}\right\}, \qquad (13.5)$$

---

* The results go through equally well without this restriction, but are slightly more cumbersome.

† Actually we have only proved this for Φ as a whole, but it is easily seen to be true for each part separately. It is not possible, however, to deform the contour of integration of (13.1) as was done in § 12 for Φ as whole.

corresponding to the positive sign of the square root in (13.4), namely

$$\left.\begin{aligned}(\zeta_1+h/h_0)^{1/2}&=\frac{1}{2}\left\{\frac{r}{d_0}+\frac{(h-z)\,d_0}{h_0 r}\right\},\\(\zeta_1+z/h_0)^{1/2}&=\frac{1}{2}\left\{\frac{r}{d_0}-\frac{(h-z)\,d_0}{h_0 r}\right\}.\end{aligned}\right\} \quad . \ . \ . \quad (13.6)$$

If we now expand the phase in the neighbourhood of ζ_1 by Taylor's theorem, keeping no terms above those of second order, we find for the integrand of (13.1), including the factors outside the integral

$$\frac{\kappa^2 p}{h_0}(2\pi\kappa r)^{-1/2}\left[\frac{r^2}{d_0^{\,2}}-\frac{(h-z)^2\,d_0^{\,2}}{h_0^{\,2}r^2}\right]^{-1/2} e^{i(\pi/4-\kappa s)}\exp\left\{\frac{-i(\zeta-\zeta_1)^2 r/d_0}{r^2/d_0^{\,2}-(h-z)^2\,d_0^{\,2}/r^2}\right\}, \quad . \ . \ . \quad (13.7)$$

where

$$s=r+\frac{(h-z)^2}{2r}+\frac{r(h+z)}{2a}-\frac{r^3}{24a^2}, \quad . \ . \ . \ . \quad (13.8)$$

which is just the geodesic distance between source and receiver, to the approximation we are using. We now say that the integral can be evaluated by using this approximate value of the integrand, the limits being $-\infty$ to ∞, and find

$$\mathscr{E}_p\sim\frac{\kappa^2 p}{r}e^{-i\kappa s}, \quad . \ . \ . \ . \ . \ . \ . \ . \quad (13.9)$$

which is the correct value of the field in the wave zone, if quantities of order z/a are neglected.

The secondary field is similarly

$$\mathscr{E}_s=-\frac{\kappa^2 p}{h_0}\left(\frac{\pi}{2\kappa r}\right)^{1/2} e^{i(\pi/4-\kappa r)}\int_{-\infty}^{\infty}\frac{g(\zeta)-\tau g'(\zeta)}{f(\zeta)-\tau f'(\zeta)}f(\zeta+h/h_0)\,f(\zeta+z/h_0)\,e^{i\zeta r/d_0}\,d\zeta, \quad . \ . \ . \quad (13.10)$$

where τ stands for the slowly varying quantity

$$\tau=-i\epsilon'/\gamma' h_0. \quad . \ . \ . \ . \ . \ . \ . \ . \quad (13.11)$$

Only the first term in the curly brackets of the asymptotic form of $g(\zeta)$, ((13.2)), gives rise to a stationary phase if the source and receiver are within each other's horizon. This can be seen from the fact that the second term gives the same condition of stationary phase (13.4) as for the primary field, and this is at a negative value of ζ ((13.5)), for which the asymptotic form of $g(\zeta)$ is different and corresponds to taking only the first term in (13.2).

The phase of the integrand is then

$$\tfrac{2}{3}(\zeta+h/h_0)^{3/2}+\tfrac{2}{3}(\zeta+z/h_0)^{3/2}-\tfrac{4}{3}\zeta^{3/2}-\zeta r/d_0, \quad . \ . \quad (13.12)$$

which is stationary when

$$(\zeta+h/h_0)^{1/2}+(\zeta+z/h_0)^{1/2}-2\zeta^{1/2}=r/d_0. \quad . \ . \ . \quad (13.13)$$

A closer inspection of this equation shows that it has a simple geometrical interpretation, namely that $\zeta^{1/2}$ is K times the angle between the horizontal

and both the incident and the reflected ray of the geometrical optics construction, and the equation itself specifies that these rays go through source and receiver respectively.

When one carries out the integration in the same manner as already done for the primary field one finds that the secondary field has the phase as predicted by geometrical optics for a ray reflected from a sphere, and that the amplitude differs from that of the primary field by the reflexion coefficient

$$\frac{\epsilon'\zeta^{1/2}-\gamma' h_0}{\epsilon'\zeta^{1/2}+\gamma' h_0}, \qquad (13.14)$$

and a ' divergence factor '

$$D=\left\{\frac{2d_0}{r}[(\zeta+h/h_0)^{1/2}(\zeta+z/h_0)^{1/2}\zeta^{-1/2}-\zeta^{1/2}]-1\right\}^{-1/2}, \qquad (13.15)$$

in which ζ stands for the root of eqn. (13.13).

The reflexion and divergence factors are what are to be expected according to geometrical optics (Van der Pol and Bremmer 1937 b, Domb and Pryce 1947), as may be verified by a short calculation.

If, however, the receiver is beyond the horizon then it is only the second term of (13.2) which gives a point of stationary phase, and the secondary field in this approximation completely cancels out the primary field, as was to be expected.

§14. Conclusion

The final result we have obtained is that, with the exception of some trivial factors, the field is a function only of the three real variables r/d_0, h/h_0, z/h_0 and of the complex parameter τ_1 or τ_2. For the earth problem, the physical constants are such that $|\tau_2|$ never exceeds 10^{-3} for any wavelength, and $|\tau_1|<0{\cdot}04$ if $\lambda<1$ metre over sea water or $\lambda<50$ metres over average land. The error committed in replacing τ_2 by 0 is therefore very small, and similarly with τ_1 for sufficiently short waves. It will be remembered that τ_2 occurs in the formula for horizontal polarization, and τ_1 for vertical. Setting $\tau_1=\tau_2=0$ means that the expressions become the same for the two polarizations and that they are universal functions of the three variables of r/d_0, h/h_0, z/h_0. This means that a calculation of the field for arbitrary r, h, z at one wavelength can, by a simple change of scale, be applied to any other wavelength.

The coefficients a_s, b_s which occur in the eqns. (12.15), etc. are now the roots of $f(\zeta)$ or in terms of the roots $-\alpha_s$ of the Airy integral

$$a_s=b_s=e^{2\pi i/3}\alpha_s, \qquad (14.1)$$

the α_s being real and positive.

For vertical polarization the contrary case of τ_1 being so large that it can be replaced by ∞ occurs if the wavelength is sufficiently long. The a_s in this case are the roots of $f'(\zeta)$ or

$$a_s=e^{2\pi i/3}\beta_s, \qquad (14.2)$$

where $-\beta_s$ are the roots of $\mathrm{Ai}'(\beta)$. The original work of Poincaré and Watson was performed primarily for application to such long waves, which were then the only ones in use for radio communication.

The numerical values of the first few α_s and β_s are (Miller 1946)

$\alpha_1=2{\cdot}33811$	$\beta_1=1{\cdot}01879$
$\alpha_2=4{\cdot}08795$	$\beta_2=3{\cdot}24820$
$\alpha_3=5{\cdot}52056$	$\beta_3=4{\cdot}82010$
$\alpha_4=6{\cdot}78671$	$\beta_4=6{\cdot}16331$
$\alpha_5=7{\cdot}94413$	$\beta_5=7{\cdot}37218$
$\alpha_6=9{\cdot}02265$	$\beta_6=8{\cdot}48849$

With the simplification of putting $\tau_1=\tau_2=0$, one can write the field of either a horizontal or a vertical dipole as

$$\frac{\kappa^2 p}{h_0}\left(\frac{\lambda}{r}\right)^{1/2} e^{i(3\pi/4-\kappa r)}\sum_s G_s(h/h_0)G_s(z/h_0)\exp\{-(\sqrt{(3)}+i)\alpha_s r/2d_0\}, \qquad (14.3)$$

where (setting h/h_0 or z/h_0 equal to x)

$$G_s(x)=e^{\pi i/3}\mathrm{Ai}(-\alpha_s+e^{\pi i/3}x)/\mathrm{Ai}'(-\alpha_s). \qquad (14.4)$$

The computation, once the α_s are known, involves computing the height gain functions G_s, the other steps being straightforward. It may be remarked that $G_s(x)$ satisfies the differential equation

$$G_s''(x)+(x+\alpha_s e^{2\pi i/3})G_s(x)=0, \qquad (14.5)$$

with the initial conditions

$$\left.\begin{aligned} G_s(0)&=0,\\ G_s'(0)&=1,\end{aligned}\right\} \qquad (14.6)$$

and this completely determines G_s.

Table 1

x	$\ln\lvert G_1(x)\rvert$	x	$\ln\lvert G_1(x)\rvert$	x	$\ln\lvert G_1(x)\rvert$
0	$-\infty$	1·6	0·736	7·0	3·551
0·1	−2·300	1·8	0·903	8·0	3·912
0·2	−1·602	2·0	1·058	9·0	4·250
0·3	−1·189	2·2	1·204	10·0	4·570
0·4	−0·890	2·4	1·343	20·0	7·145
0·5	−0·654	2·5	1·409	30·0	9·123
0·6	−0·456	2·6	1·474	40·0	10·793
0·8	−0·134	2·8	1·600	50·0	12·268
1·0	0·129	3·0	1·721	60·0	13·602
1·2	0·354	4·0	2·264	70·0	14·831
1·4	0·555	5·0	2·737	80·0	15·976
1·5	0·647	6·0	3·162	90·0	17·053
				100·0	18·074

At very great distances the amplitude of the field is given by the first term, and reduces to

$$\frac{\kappa^2 p}{h_0}\left(\frac{\lambda}{r}\right)^{1/2}\lvert G_1(h/h_0)\rvert\,\lvert G_1(z/h_0)\rvert\, e^{-2{\cdot}0249r/d_0}. \qquad (14.7)$$

The numerical values of $\ln|G_1|$ (computed by Dr. Domb) are given in table 1. Further numerical and graphical results are given by Domb and Pryce (1947). More detailed numerical results are given in the following paper by Domb.

Acknowledgements

I am grateful to the Admiralty for permission to publish this paper. I also wish to thank Dr. C. Domb for many valuable discussions.

References

Bremmer, H., 1949, *Terrestrial Radio Waves* (Elsevier Publishing Co., Inc.).
Domb, C., and Pryce, M. H. L., 1947, *J.I.E.E.*, **94,** III, 325.
Eckersley, T. L., *Proc. Roy. Soc.* A, 1932, **136,** 499.
Eckersley, T. L., and Millington, G., 1938, *Phil. Trans. Roy. Soc.*, **237,** 297.
Fock, V. A., 1945, *J. Phys. U.S.S.R.*, **9,** 255 ; 1946, *Ibid.*, **10,** 399 ; 1949, *J. Exp. Theor. Phys. U.S.S.R.*, **19,** 916.
Gray, M. C., 1939, *Phil. Mag.*, **27,** 421.
Jeffreys, H. and B., 1950, *Mathematical Physics* (Cambridge University Press, 2nd Edition).
Kerr, D. E., 1951, *Propagation of Short Radio Waves.* M.I.T. Radiation Laboratory Series, Vol. 13.
Laporte, O., 1923, *Ann. d. Phys.*, **70,** 595.
Leontovich, M., and Fock, V. A., 1946, *J. Phys. U.S.S.R.*, **10,** 13.
Macdonald, H. M., 1914, *Proc. Roy. Soc.* A, **90,** 50.
Miller, J. C. P., 1946, *B. A. Maths Tables*, Part vol. B (Cambridge University Press).
Nicholson, J. W., 1910, *Phil. Mag.*, **20,** 157 ; **21,** 62.
Pekeris, C. L., 1946, *Phys. Rev.*, **70,** 518.
Poincaré, H., 1910, *Palermo, Rendiconti*, **29,** 169.
van der Pol, B., 1919, *Phil. Mag.*, **38,** 365.
van der Pol, B., and Bremmer, H., 1937 a, *Phil. Mag.*, **24,** 141 ; 1937 b, *Ibid.*, **24,** 825 ; 1938, *Ibid.*, **25,** 817 ; 1939, *Ibid.*, **26,** 261.
Rayleigh, Lord, 1871, *Phil. Mag.*, **41,** 107, 274, 447 ; 1881, *Ibid.*, **12,** 81 ; 1899, *Ibid.*, **47,** 375.
Vvedensky, B., 1935, *Tech. Phys. U.S.S.R.*, **2,** 624; 1936, *Ibid.*, **3,** 915 ; 1937, *Ibid.*, **4,** 579.
Watson, G. N., 1918, *Proc. Roy. Soc.* A, **95,** 83.

Tables of Functions occurring in the Diffraction of Electromagnetic Waves by the Earth

By C. Domb
The Royal Society Mond Laboratory, Cambridge

§1. Introduction

The theory of the diffraction of electromagnetic waves by the earth has been discussed in the previous paper by Professor Pryce. The problem of the practical calculation of field strengths was considered in detail in a paper by Domb and Pryce (1947), and curves and formulae were provided which enable this calculation to be undertaken with fair accuracy and relative ease. In the region well beyond the optical range the approximation of the first term of the diffraction series was employed, the curves having been derived from tabulations of the Airy Integral along particular lines in the complex plane. It is the purpose of the present paper to supply details of these and related tabulations, which enable one to undertake more refined calculations and to assess the region of validity of the one-term approximation.

§2. Notation

The notation of the present appendix is designed to conform with Domb and Pryce 1947, and differs from the theoretical part of the paper. The number of symbols entering the theoretical analysis is so large that it seemed desirable to treat the practical aspects of the calculation completely separately.

§3. Horizontal Polarization

For horizontally polarized waves over the surface of the sea the conductivity can be regarded as infinite to a high degree of approximation, and the field in the diffraction region is then given (in the conventional engineering units : see Domb and Pryce 1946) by

$$\mathscr{E}=\frac{7\sqrt{PG}}{d_0}F(x, y, z) \quad . \quad . \quad . \quad . \quad . \quad . \quad . \quad (1)$$

where $$F(x, y, z)=\sqrt{\frac{4\pi}{x}}\sum_{n=1}^{\infty} f_n(y)\, f_n(z) \exp\{-\tfrac{1}{2}(\sqrt{3}+i)a_n x\} \quad . \quad . \quad (2)$$

P, G are the power of the transmitter and gain of the aerial respectively, x the plan distance in units of d_0, y and z the heights of transmitter and receiver in units of h_0. The definitions of d_0 and h_0 are given in the foregoing paper.

The numbers $-a_n$ are the zeros of the Airy Integral, and the values for $n=1$ to 5 are as follows :

n	1	2	3	4	5
a_n	2·3381	4·0879	5·5206	6·7867	7·9441.

. (3)

The functions $f_n(y)$ are given by

$$f_n(y)=\frac{Ai(-a_n+\exp(\pi i/3)y)}{\exp(\pi i/3)\,Ai'(-a_n)}, \quad \ldots\ldots\ldots \quad (4)$$

and it will be seen from (2) that a tabulation of these functions enables $F(x, y, z)$ to be calculated, the limits of applicability being determined by the number of values of n available.

The functions $f_n(y)$ for values of n from 1 to 5 were tabulated by the writer at the beginning of 1942 at Liverpool University under the guidance of Dr. J. C. P. Miller. These tables were subsequently checked, corrected, and sub-tabulated by the Mathematics Division of the National Physical Laboratory. A summary of the results is given in table 1, the functions $f_n(y)$ being written in the form $\exp(\lambda_n+i\mu_n)$. The detailed tables give the values of λ_n and μ_n at intervals of 0·1 from $y=0$ to 10, 0·2 from $y=10$ to 20, 0·5 from $y=20$ to 60, and 1·0 from $y=60$ to 100. Photostatic copies are available from the Nautical Almanack Office.

It is perhaps of interest to give a brief summary of the methods used for computation in the different regions. If we write $f_n(y)$ in the form u_n+iv_n it is easy to show that u_n, v_n satisfy the simultaneous equations

$$\left.\begin{aligned} u_n''&=-(y+\tfrac{1}{2}a_n)\,u_n-\frac{\sqrt{3}}{2}a_n\,v_n,\\ v_n''&=-(y+\tfrac{1}{2}a_n)\,v_n+\frac{\sqrt{3}}{2}a_n\,u_n. \end{aligned}\right\} \quad \ldots\ldots \quad (5)$$

The initial conditions are $u_n=0$, $v_n=0$, $u_n'=1$, $v_n'=0$ when $y=0$. These equations can readily be differentiated successively to obtain recurrence relations for higher derivatives, and the function can then be evaluated by a step-by-step procedure using a Taylor series at each point. This method was satisfactory for $y\leqslant 2$.

For sufficiently large y (>10) an asymptotic series was used, the first terms of which are as follows

$$\left.\begin{aligned} \lambda_n&=-\frac{\sqrt{3}}{2}a_n y^{1/2}-\frac{1}{4}\log_e y+\log_e\frac{1}{2\sqrt{\pi}}-\log_e|Ai'(a_n)|\\ &\quad-\frac{\sqrt{3}}{8}a_n^2\,y^{-1/2}-\frac{1}{8}a_n\,y^{-1}-\frac{1}{16}a_n^2\,y^{-2}+O(y^{-5/2}),\\ \mu_n&=-\frac{2}{3}y^{3/2}-\frac{1}{2}a_n\,y^{1/2}+\left(\frac{7}{12}-n\right)\pi+\frac{1}{8}a_n^2\,y^{-1/2}+\frac{\sqrt{3}}{8}a_n\,y^{-1}\\ &\quad-\frac{1}{24}a_n^2\,y^{-3/2}-\frac{\sqrt{3}}{16}a_n^2\,y^{-2}+O(y^{-5/2}). \end{aligned}\right\} \quad \ldots \quad (6)$$

In the intermediate range $2<y<10$, which is usually troublesome in calculations of this kind, it was found that the direct equations for λ_n and μ_n could be satisfactorily used:

$$\left.\begin{aligned} \lambda_n''+\lambda_n'^2-\mu_n'^2+(y+\tfrac{1}{2}\,a_n)&=0,\\ \mu_n''+2\lambda_n'\mu_n'-\frac{\sqrt{3}}{2}a_n&=0. \end{aligned}\right\} \quad \ldots\ldots \quad (7)$$

Table 1. λ_n and μ_n (Horizontal Polarization)

y	λ_1	μ_1	λ_2	μ_2	λ_3	μ_3	λ_4	μ_4	λ_5	μ_5
0·0	$-\infty$	0·000	$-\infty$	0·000	$-\infty$	0·000	$-\infty$	0·000	$-\infty$	0·000
0·2	−1·602	−0·013	−1·596	−0·023	−1·592	−0·031	−1·587	−0·039	−1·583	−0·045
0·4	0·890	0·053	0·866	0·092	0·846	0·124	0·828	0·151	0·812	0·176
0·6	0·456	0·119	0·400	0·203	−0·353	0·270	−0·311	0·326	−0·273	0·377
0·8	−0·134	0·209	−0·030	0·350	+0·056	0·458	+0·132	0·548	+0·201	0·626
1·0	+0·129	−0·321	+0·296	−0·527	+0·433	−0·678	+0·552	−0·801	+0·658	−0·905
1·2	0·354	0·455	0·601	0·727	0·797	0·919	0·964	1·071	1·110	−1·198
1·4	0·555	0·609	0·894	0·944	1·154	1·172	1·371	1·350	1·559	1·499
1·6	0·736	0·782	1·180	−1·173	1·507	−1·434	1·774	−1·636	2·003	−1·804
1·8	0·903	0·972	1·458	1·412	1·854	1·701	2·171	1·926	2·441	2·113
2·0	+1·058	−1·180	+1·730	−1·659	+2·194	−1·975	+2·563	−2·221	+2·874	−2·427
2·2	1·204	1·403	1·994	1·913	2·527	2·253	2·947	2·520	3·300	2·744
2·4	1·343	1·642	2·251	2·174	2·853	2·538	3·325	2·824	3·721	3·066
2·6	1·474	−1·896	2·500	2·443	3·172	2·828	3·697	3·134	4·135	3·393
2·8	1·600	−2·163	2·741	2·720	3·484	3·124	4·062	3·449	4·543	3·724
3·0	+1·721	−2·445	+2·974	−3·005	+3·789	−3·427	+4·420	−3·769	+4·945	−4·060
4·0	−2·264	−4·036	4·040	4·564	5·215	5·044	6·120	5·456	6·869	5·816
5·0	+2·737	−5·905	4·967	6·352	6·493	6·842	7·675	7·296	8·652	7·707
6·0	+3·162	−8·018	5·793	8·364	7·647	8·832	9·101	9·300	10·307	9·742
7·0	3·551	−10·352	6·543	10·588	8·701	11·013	10·414	11·474	11·845	11·929
8·0	3·912	−12·888	7·234	13·012	9·672	13·381	11·631	13·819	13·280	14·272
9·0	4·250	−15·613	7·876	15·624	10·576	15·929	12·767	16·333	14·625	16·772
10·0	+4·570	−18·513	+8·480	−18·415	+11·424	−18·650	+13·834	−19·012	+15·891	−19·429

y	λ_1	$\mu_1+\frac{2}{3}y^{3/2}$	λ_2	$\mu_2+\frac{2}{3}y^{3/2}$	λ_3	$\mu_3+\frac{2}{3}y^{3/2}$	λ_4	$\mu_4+\frac{2}{3}y^{3/2}$	λ_5	$\mu_5+\frac{2}{3}y^{3/2}$
10·0	+4·570	+2·569	+8·480	+2·667	+11·424	+2·432	+13·834	+2·070	+15·891	+1·653
20·0	7·145	4·052	13·254	5·143	18·073	5·619	22·186	5·797	25·822	5·798
30·0	9·123	5·205	16·851	7·113	23·035	8·223	28·380	8·932	33·165	9·389
40·0	10·793	6·182	19·863	8·795	27·169	10·465	33·524	11·651	39·245	12·532
50·0	12·268	7·046	22·508	10·288	30·789	12·460	38·017	14·082	44·547	15·351
60·0	13·602	7·828	24·894	11·643	34·049	14·275	42·058	16·297	49·309	17·926
70·0	14·831	8·548	27·086	12·892	37·039	15·952	45·761	18·346	53·669	20·311
80·0	15·976	9·218	29·125	14·058	39·817	17·517	49·198	20·260	57·713	22·541
90·0	17·053	9·849	31·039	15·154	42·423	18·990	52·420	22·064	61·502	24·644
100·0	+18·074	+10·445	+32·848	+16·192	+44·885	+20·386	+55·463	+23·773	+65·079	+26·637

§4. Vertical Polarization

Although the diffraction formula in the case of vertical polarization,

$$F(x, y, z)=\sqrt{\frac{4\pi}{x}}\sum_{n=1}^{\infty} F_n(y)F_n(z)\exp\{\tfrac{1}{2}(\sqrt{3}+i)b_n x\}, \quad . \quad . \quad (8)$$

is analogous to that for horizontal polarization, detailed computation of the corresponding functions is much more complicated since the ground constants play an essential part. In many cases of practical interest, however, the ground constants depend on only one real parameter t, and the calculations of the present paper are designed to apply to these cases.

The numbers b_n are the roots of the equation

$$Ai(w)=t\exp(-5\pi i/12)\,Ai'(w), \quad . \quad . \quad . \quad . \quad . \quad . \quad (9)$$

and the first task is to evaluate b_n as a function of t. As was observed by previous writers, the zeros b_n satisfy the differential equation

$$\frac{db_n}{du}=\frac{1}{b_n-u^2}\{u=\exp(5\pi i/12)/t\}, \quad . \quad . \quad . \quad . \quad . \quad (10)$$

and this can readily be integrated to give the required values. The results are presented in Table 2 where ξ_n and η_n, given by

$$\xi_n+i\eta_n=\exp(\pi i/6)\,b_n=\tfrac{1}{2}(\sqrt{3}+i)\,b_n\,, \quad . \quad . \quad . \quad . \quad . \quad (11)$$

are tabulated as functions of t from $t=0$ to 1, and of $t'(=1/t)$ from $t'=0$ to 1. The exponential factor on the right of (8) is thus equal to

$$\exp(\xi_n+i\eta_n)\,. \quad . \quad . \quad . \quad . \quad . \quad . \quad . \quad . \quad . \quad (12)$$

The height functions $F_n(y)$ are given by

$$F_n(y)=\frac{Ai\{b_n+y\exp(\pi i/3)\}}{\exp(\pi i/3)Ai'(b_n)\sqrt{\{1-t^2b_n\exp(-5\pi i/6)\}}}=\exp(\Lambda_n+i\mu_n). \quad . \quad . \quad . \quad (13)$$

The methods used for tabulating these functions were similar to those used for $f_n(y)$, although the detailed work was more involved. For example, in the region $3<y<10$ the generalization of equation (7),

$$\left.\begin{aligned}\Lambda_n''+\Lambda_n'^2-M_n'^2+(y+\eta_n)&=0,\\ M_n''+2\Lambda_n'\,M_n'-\xi_n&=0,\end{aligned}\right\} \quad . \quad . \quad . \quad . \quad . \quad (14)$$

was found to be satisfactory. The detailed tables are somewhat lengthy as they involve two parameters, y and t. They are not reproduced here, but photostatic copies are available on application to the Nautical Almanack Office.

For large values of y an asymptotic expansion similar to (6) can be used, and is given by

$$\left.\begin{aligned}\Lambda_n=&-\xi_n y^{1/2}-\tfrac{1}{4}\log_e y+\gamma_n-\tfrac{1}{2}\xi_n\eta_n y^{-1/2}-\tfrac{1}{4}\eta_n y^{-1}\\ &-\tfrac{1}{24}(\xi_n^3-3\xi_n\eta_n^2)y^{-3/2}-\tfrac{1}{8}(\xi_n^2-\eta_n^2)y^{-2}+O(y^{-5/2}),\\ M_n=&-\tfrac{2}{3}y^{3/2}-\eta_n y^{1/2}+\delta_n+\tfrac{1}{4}(\xi_n^2-\eta_n^2)y^{-1/2}+\tfrac{1}{4}\xi_n y^{-1}\\ &-\tfrac{1}{24}(2\xi_n^2\eta_n-\eta_n^3)y^{-3/2}-\tfrac{1}{4}\xi_n\eta_n y^{-2}+O(y^{-5/2}).\end{aligned}\right\} \quad . \quad (15)$$

Table 2. ξ_n and η_n (Vertical Polarization)

t	ξ_1	η_1	ξ_2	η_2	ξ_3	η_3	ξ_4	η_4	ξ_5	η_5
0·0	−2·025	−1·169	−3·540	−2·044	−4·781	−2·760	−5·877	−3·393	−6·880	−3·972
0·1	1·953	1·240	3·468	2·115	4·708	2·831	5·804	3·465	6·806	4·043
0·2	1·877	1·311	3·387	2·187	4·624	2·904	5·715	3·537	6·714	4·117
0·3	1·790	1·383	3·284	2·258	4·505	2·971	5·582	3·598	6·567	4·167
0·4	1·685	1·449	3·144	2·308	4·340	2·986	5·411	3·571	6·409	4·103
0·5	−1·559	−1·497	−2·983	−2·290	−4·204	−2·905	−5·322	−3·466	−6·355	−4·001
0·6	1·420	1·510	2·865	2·210	4·149	2·809	5·299	3·385	6·345	3·935
0·7	1·293	1·486	2·806	2·121	4·132	2·738	5·295	3·332	6·345	3·892
0·8	1·189	1·439	2·780	2·049	4·129	2·689	5·296	3·295	6·347	3·862
0·9	1·110	1·383	2·769	1·993	4·129	2·652	5·298	3·268	6·350	3·840
1·0	−1·051	−1·326	−2·765	−1·950	−4·131	−2·624	−5·301	−3·247	−6·353	−3·823
t' (=1 t)										
1·0	1·051	−1·326	2·765	−1·950	−4·131	−2·624	−5·301	−3·247	6·353	−3·823
0·9	1·002	1·267	2·765	1·913	4·134	2·600	5·304	3·229	6·355	3·808
0·8	0·958	1·201	2·766	1·877	4·137	2·577	5·307	3·211	6·358	3·794
0·7	0·921	1·128	2·769	1·842	4·141	2·555	5·310	3·194	6·361	3·780
0·6	0·891	1·050	2·773	1·808	4·145	2·533	5·313	3·178	6·364	3·766
0·5	−0·868	−0·967	−2·778	−1·776	4·149	2·512	−5·318	3·161	6·367	−3·752
0·4	0·854	0·880	2·784	1·745	4·154	2·491	5·321	3·145	6·371	3·739
0·3	0·848	0·790	2·791	1·714	4·159	2·471	5·325	3·129	6·374	3·726
0·2	0·850	0·698	2·798	1·684	4·164	2·450	5·329	3·113	6·378	3·712
0·1	0·862	0·604	2·805	1·654	4·169	2·430	5·333	3·097	6·381	3·699
0·0	−0·882	−0·509	−2·813	−1·624	−4·174	−2·410	−5·338	−3·082	−6·384	−3·686

Table 3. γ_n and δ_n (Vertical Polarization)

t	γ_1	δ_1	t	γ_2	δ_2	t	γ_3	δ_3	t	γ_4	δ_4	t	γ_5	δ_5
0·0	−0·911	−1·309	0·0	−1·047	−4·450	0·00	−1·121	−7·592	0·00	−1·172	−10·734	0·00	−1·211	−13·875
0·1	0·906	1·311	0·1	1·051	4·457	0·05	1·122	7·589	0·05	1·173	10·734	0·05	1·208	13·875
0·2	0·915	1·308	0·2	1·049	4·451	0·10	1·122	7·592	0·10	1·173	10·734	0·10	1·207	13·874
0·3	0·915	1·305	0·3	1·054	4·446	0·15	1·122	7·592	0·15	1·175	10·734	0·15	1·208	13·874
0·4	0·924	1·302	0·4	1·067	4·451	0·20	1·122	7·592	0·20	1·177	10·733	0·20	1·211	13·873
0·5	−0·943	−1·307	0·5	−1·078	−4·472	0·25	−1·122	−7·591	0·25	−1·178	−10·732	0·25	−1·215	−13·873
0·6	0·965	1·325	0·6	1·068	4·500	0·30	1·127	7·590	0·30	1·182	10·732	0·30	1·220	13·877
0·7	0·979	1·355	0·7	1·045	4·509	0·35	1·135	7·592	0·35	1·187	10·739	0·35	−1·224	−13·884
0·8	0·978	1·389	0·8	−1·029	−4·507	0·40	1·141	7·600	0·40	−1·188	−10·749			
0·9	0·965	1·420				0·45	1·141	7·614						
1·0	−0·944	−1·443				0·50	−1·134	−7·623						
$t'=$ (1/t)	γ_1	δ_1	t'	γ_2	δ_2	t'	γ_3	δ_3	t'	γ_4	δ_4	t'	γ_5	δ_5
1·0	−0·944	−1·443	1·6	−1·062	−4·503	2·0	−1·134	−7·623	2·6	−1·189	−10·745	3·2	−1·222	−13·877
0·9	0·919	1·459	1·4	1·042	4·509	1·8	1·123	7·628	2·4	1·186	10·754	2·8	1·224	13·885
0·8	0·891	1·470	1·2	1·025	4·506	1·6	1·113	7·627	2·2	1·179	10·758	2·4	1·217	13·893
0·7	0·858	1·476	1·0	1·012	4·498	1·4	1·105	7·624	2·0	1·173	10·760	2·0	1·209	13·896
0·6	0·822	1·474	0·8	1·002	4·488	1·2	1·099	7·619	1·8	1·166	10·759	1·6	1·203	13·894
0·5	−0·786	−1·464	0·6	−0·995	−4·478	1·0	−1·095	−7·614	1·6	−1·160	−10·757	1·2	−1·197	−13·888
0·4	0·750	1·447	0·4	0·991	4·469	0·8	1·092	7·609	1·2	1·154	10·750	0·8	1·194	13·881
0·3	0·718	1·422	0·2	0·988	4·460	0·6	1·090	7·605	0·8	1·151	10·744	0·4	1·193	13·878
0·2	0·690	1·391	0·0	−0·985	−4·451	0·4	1·088	7·601	0·4	1·149	10·739	0·0	−1·192	−13·876
0·1	0·667	1·353				0·2	1·087	7·596	0·0	−1·147	−10·734			
0·0	−0·651	−1·309				0·0	−1·085	−7·592						

Here γ_n and δ_n are given by

$$\exp(\gamma_n + i\delta_n) = \frac{\frac{1}{2}\pi^{-1/2}}{\exp(5\pi i/12) Ai'(b_n)\sqrt{(1 - t^2 b_n \exp(-5\pi i/6))}} \quad . \quad (16)$$

and are presented in table 3.

§5. Tabulations of the Airy Integral

The Airy Integral has been tabulated along the real axis by Dr. J. C. P. Miller (*B.A. Mathematical Tables*, Part Vol. B) and in the complex plane by Woodward and Woodward (1946). However, the range covered by the latter tabulations overlaps only to a small extent with the present tables.

Acknowledgments

The tables referred to in the text were computed at H.M. Nautical Almanac Office for Admiralty Computing Service during the years 1942–4. The work was under the direction of Mr. D. H. Sadler, and the following took a major part in the computations : Dr. R. H. Corkan, Mr. P. H. Haines, Mr. R. G. Taylor and Mr. E. M. Wilson ; Dr. L. Fox devised the technique of solving the differential equations by relaxation methods, which substantially reduced the amount of computation. This material is published here by permission of the Admiralty.

References

Domb, C., and Pryce, M. H. L., 1947, *J. Instn., Elect., Engrs.*, **94,** III, 325.
Woodward, P. M., and Woodward, A. M., 1946, *Phil. Mag.*, **37,** 236.

The Thermal Conductivity of Dielectric Solids at Low Temperatures

By R. Berman
Clarendon Laboratory, Oxford

CONTENTS

§ 1. Introduction

The measurements of thermal conductivity of dielectric solids have not, until recently, been sufficiently extensive for detailed comparison between theory and experiment to be made. In the last few years, however, a considerable amount of work has been carried out in Oxford and it now seems a suitable time to review the present state of knowledge and to describe the types of experiment which are being carried out. From the theoretical point of view the most interesting effects occur at fairly low temperatures ; the temperature range of interest is related to the specific heat and to the size of the specimen and in most cases lies below room temperature and extends down to the lowest temperatures attainable.

In this paper the experimental techniques used will not be described ; they are usually the same as those mentioned by Olsen and Rosenberg in the companion paper. Reference will only be made to some special methods.

As the work described here will not, on the whole, be discussed in chronological order, an outline will first be given of the actual development of the subject over the last forty years.

§2. Historical Development

2.1. *Dielectric Solids in General*

As a result of numerous measurements on dielectric crystals and on amorphous solids, Eucken (1911 a, b) concluded that, in general, the conductivity of single crystals increases with decreasing temperature while that of amorphous solids decreases. Most of the measurements were made at the steam point, ice point and at liquid air temperature, with a few measurements at the boiling point of liquid hydrogen. In this temperature range the conductivity was found to be roughly inversely proportional to the absolute temperature for crystals and in the case of amorphous solids to be roughly proportional to the specific heat.

These different variations with temperature were explained by Debye's theory (1914), according to which the heat is transported by travelling elastic waves which are coupled together on account of their anharmonicity. In crystals the waves are scattered by regions of differing density arising from thermal motion and Debye calculated the attenuation of the waves produced by this scattering. From the dependence of attenuation on temperature he derived a variation of conductivity which is in agreement with Eucken's experiments.

More recent theories lead to the same temperature variation at sufficiently high temperatures but show that at low temperatures the scattering of the waves falls off more rapidly.

2.2. *Crystals*

In Peierls' theory of heat conductivity of crystals (1929) the normal modes of a perfect lattice are quantized : the quanta of vibrational energy are now called phonons. Thermal resistance is due to a certain type of collision between phonons (Umklapp processes) and Peierls showed that the probability of such collisions falls off exponentially at low temperatures, leading to a corresponding exponential increase in the conductivity. De Haas and Biermasz (1935) carried out experiments designed to test the validity of Peierls' theory. Although they found that the conductivity of quartz in the liquid hydrogen range increases more rapidly than the inverse of the temperature, their most interesting result was that in the helium range the conductivity actually decreases with decreasing temperature and must, therefore, pass through a maximum at about 10° K.

Peierls suggested that this behaviour was due to scattering of the lattice waves at the boundaries of the crystal and the consequences of this suggestion were developed by Casimir (1938). He showed that such a scattering would lead to a conductivity, at sufficiently low temperatures, proportional to the diameter of the crystal and to the cube of the temperature. The later experiments of de Haas and Biermasz were almost entirely confined to the study of this effect and although exact agreement with the theory was not obtained, the results indicated that the size and temperature dependence calculated by Casimir might be accurately obeyed at temperatures considerably lower than those at which measurements had yet been made.

Mean free path treatments of thermal conductivity have been given by Pomeranchuk (1941 a, b ; 1942) and by Klemens (1951). Exact expressions are found for the variation of conductivity with temperature by picking out the processes which are chiefly responsible for limiting the phonon mean free path. It is then possible to calculate the conductivity to be expected when two or more processes combine in limiting the mean free path. (Even in an ideal crystal, there must be at least two such processes in the region of the conductivity maximum.)

Recent experiments (Berman, Simon and Wilks 1951) have shown that the exponential increase in conductivity predicted by Peierls can be observed for sufficiently pure crystals over a relatively small temperature range. There are, nevertheless, considerable discrepancies between the expected variation of conductivity and that found experimentally and experiments now in progress in Oxford are designed to investigate these discrepancies.

The present theories enable us to predict the conductivity as a function of temperature, provided that we know one value at a comparatively high temperature. Figure 1 shows the conductivity of ideal sapphire crystals of two different diameters, calculated according to Klemens' theory ; the conductivity actually found is also shown. It is evident that the greatest discrepancies occur in the region of the conductivity maximum but, even for real crystals, the conductivity reaches values comparable with those of pure metals at their maxima.

2.3. *Amorphous Solids*

Several observers have reported values for the conductivity of glasses which indicate that below liquid air temperatures the conductivity begins to fall off more slowly than the specific heat. The explanation of this was given by Kittel (1949) and the theory was developed in detail by Klemens (1951) who showed that at sufficiently low temperatures the conductivity should be proportional to the absolute temperature although the specific heat is proportional to the cube of the temperature. This temperature variation has been confirmed for several glasses and for some plastics (Bijl 1949, Berman 1951).

Figure 2 shows the measured values of the thermal conductivity of quartz glass together with the curve calculated by Klemens (for which the empirical constants have been found by comparison with experiment) ; except at the very lowest temperatures the specific heat varies as curve II in the figure, so that the difference between the present theory and an extrapolation of Debye's relationship is clearly seen.

§ 3. Theory of the Conductivity of Ideal Crystals

For an ideal crystal we assume there are only two types of process which give rise to thermal resistance : Umklapp processes and boundary scattering. The resistances due to these two causes are only comparable over a small temperature range which, for crystals of a few millimetres diameter, is in the neighbourhood of one thirtieth of the Debye characteristic

temperature. At higher temperatures the conductivity is almost entirely determined by Umklapp processes and at lower temperatures by boundary scattering. These three temperature regions will be treated separately in the following discussion.

3.1. *The Region above the Conductivity Maximum*

Although Debye's theory has been superseded, it introduced important concepts which are still valid. Debye treated a crystal as a continuum in which heat is carried by travelling elastic waves of a single frequency. He pointed out that if the waves were purely harmonic there would be no coupling between waves ; consequently attenuation of the waves by

Fig. 1

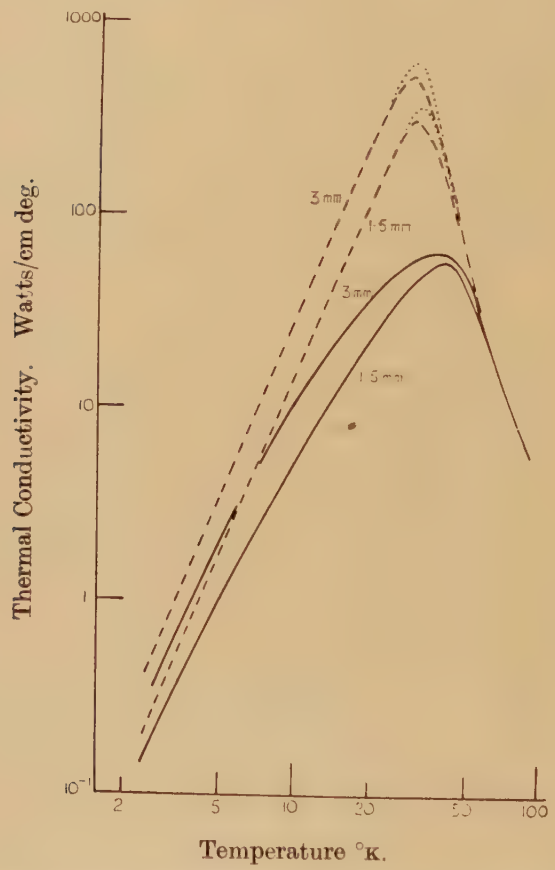

The thermal conductivity of sapphire single crystals of diameters 1·5 and 3 mm.

Theoretical curves { – – – resistances combined according to Klemens (1951).
. . . simple addition of resistances.

Experimental curves ——— .

mutual scattering could not occur. It would not, therefore, be possible to set up a temperature gradient within a crystal so that there would be no definable thermal resistance. The lattice vibrations must be assumed to be anharmonic to account for thermal expansion and Debye explained the required coupling between the waves in terms of this anharmonicity.

As a measure of the scattering, Debye defined the mean free path l of a wave as the distance which the wave travels before its intensity is reduced to $1/e$ of its initial value. The thermal conductivity, κ, is then given by the equation :

$$\kappa = \tfrac{1}{4} c v l \quad . \quad . \quad . \quad . \quad . \quad . \quad . \quad . \quad . \quad (1)$$

where c is the specific heat per unit volume and v is the wave velocity.

Fig. 2

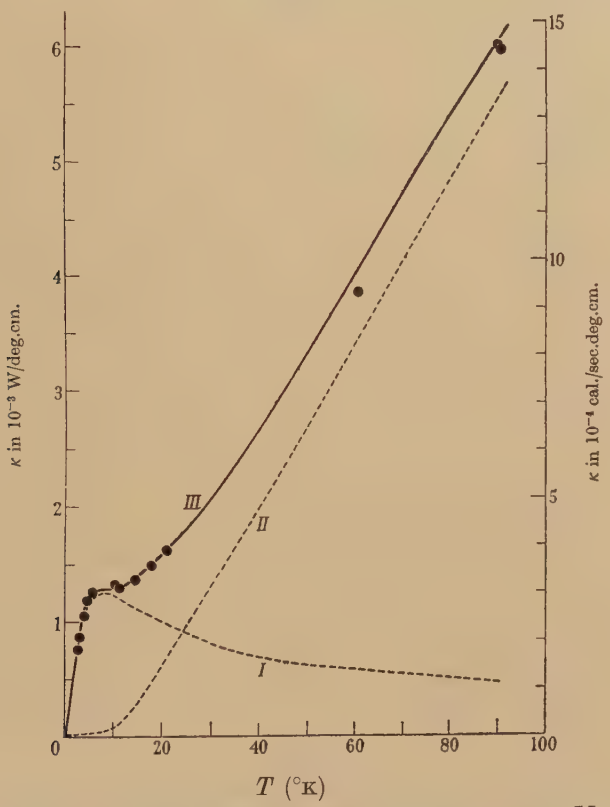

Thermal conductivity of quartz glass. Curve *I* denotes κ_{I}, curve *II* κ_{II}, curve *III* $\kappa = \kappa_{\mathrm{I}} + \kappa_{\mathrm{II}}$. Full circles denote experimental points of Berman (1951); measurements of three specimens differing slightly in their absolute value of conductivity are here brought into agreement by multiplication with an appropriate constant (Klemens 1951).

Debye supposed that a wave is scattered when it passes through regions whose density and elastic constants differ from the average value throughout the crystal. These density variations result from the anharmonicities

in the thermal motion of the lattice and, for purposes of calculation were considered to be static. This assumption is only justified at high temperatures, when the density variations are not correlated with the scattered waves. The calculation showed that the mean free path is inversely proportional to the absolute temperature and, since the wave velocity is nearly independent of temperature, the thermal conductivity must be inversely proportional to temperature for temperatures where the specific heat is constant.

In Peierls' theory (1929, 1935) a crystal is treated as a lattice of atoms rather than a continuum. The coupling between normal modes of vibration is ascribed to anharmonicities arising from third and higher order terms in the potential energy of a displaced atom. The part played by these terms is analogous to that of collisions in the theory of a perfect gas; though introducing only a small perturbation of the motion they are responsible for the coupling between the normal modes which is essential in producing thermal equilibrium. In Peierls' theory the normal modes of vibration are quantized and, by analogy with the photons of radiation theory, these quanta are now termed phonons. For a phonon associated with an angular frequency ω and wave number $\mathbf{K}$, $\hbar\omega$ gives the energy while $\hbar\mathbf{K}$ behaves rather like a momentum.

In the presence of a temperature gradient the phonon distribution differs from that corresponding to the equilibrium distribution at uniform temperature—the Planck distribution. Collisions between phonons tend to restore the equilibrium distribution and the rate of the restoring process determines the thermal conductivity. Collisions are possible if the three values of ω and $\mathbf{K}$ obey the equations:

$$\omega_1+\omega_2=\omega_3 \quad . \quad . \quad . \quad . \quad . \quad . \quad . \quad . \quad . \quad (2)$$

and

$$\mathbf{K}_1+\mathbf{K}_2=\mathbf{K}_3 \quad . \quad . \quad . \quad . \quad . \quad . \quad . \quad . \quad . \quad (3)$$

which are conditions corresponding to the conservation of energy and momentum. Equation (2) states that after a collision the resulting wave or waves still carry the same energy as before and eqn. (3) implies that this energy is still flowing in the same direction. Such collisions do not in themselves give rise to a thermal resistance. Peierls also showed that, for a discrete lattice, collisions are possible in which eqn. (3) does not hold but is replaced by

$$\mathbf{K}_1+\mathbf{K}_2=\mathbf{K}_3+\frac{2\pi\boldsymbol{\epsilon}}{a} \quad . \quad . \quad . \quad . \quad . \quad . \quad . \quad . \quad (4)$$

where a is the lattice constant and $\boldsymbol{\epsilon}$ is a unit vector, the possible directions of which depend on the crystal symmetry. Equation (4) implies that the direction of flow of the energy is changed after a collision and, as $\boldsymbol{\epsilon}$ can take up one of several directions (e.g. six directions parallel to the axes of a cubic crystal), the result of such collisions is much the same as if the waves were scattered at random. This type of collision, which Peierls called an Umklapp process (in the following discussion the abbreviation U-process will be used), gives rise to thermal resistance.

It is convenient to use the concept of mean free path, as in Debye's theory, but since the waves have been replaced by phonons, eqn. (1) is rewritten as

$$\kappa = \tfrac{1}{3} c v l \quad . \quad . \quad . \quad . \quad . \quad . \quad . \quad . \quad . \quad (5)$$

by analogy with kinetic theory. For the case being considered l is the mean free path for U-processes. It is now necessary to take into account the contributions to the right hand side of (5) from phonons corresponding to waves of all frequencies up to the Debye limit and of three possible polarizations, so that eqn. (5) should be written :

$$\kappa = \tfrac{1}{3} \sum_{Kj} c_{Kj} v_{G_{Kj}} l_{Kj}, \quad . \quad . \quad . \quad . \quad . \quad . \quad . \quad . \quad (6)$$

where j denotes the direction of polarization and v_G is the group velocity. At sufficiently high temperatures the contribution to the specific heat, c_{Kj}, is the same for all waves and is independent of temperature. The mean free path is inversely proportional to the rate of loss of energy of a wave, which Peierls showed to be proportional to its own additional energy and to the intensities of the other waves with which it can interact. The mean free path is thus inversely proportional to the intensity of the other waves taking part and at high temperatures all the intensities are proportional to T, so that $l \propto 1/T$ and the conductivity is inversely proportional to the absolute temperature, which is the relation also deduced by Debye.

For treating the low temperature conductivity Peierls did not use a mean free path method, but pointed out that eqn. (4) implies that the phonons must have a minimum energy for an Umklapp process to occur. He further showed that as a rough criterion we may take this threshold energy as $k\theta/2$, where k is Boltzmann's constant and θ is the Debye characteristic temperature. The intensity of excitation of such phonons is proportional to $1/(e^{\theta/2T} - 1)$, which at low temperatures approaches the value $e^{-\theta/2T}$. The probability of U-processes therefore contains the term $e^{-\theta/2T}$ and the thermal resistance is proportional to $f(T)\, e^{-\theta/2T}$, where at sufficiently low temperatures the function $f(T)$ behaves as a power of T.

Experiments confirm the main features of the temperature variation predicted by Peierls, but comparison is difficult when several scattering mechanisms have to be taken into account. Mean free path treatments of thermal conductivity have, however, been given by Pomeranchuk (1941 a, b ; 1942) and Klemens (1951), and these are more easily applied to discussions of experimental results.

The expressions for the conductivity found by Pomeranchuk differ considerably from those of other authors mainly because of the long mean free paths which are assumed for long waves. At high temperatures four phonon processes are considered essential for ensuring a finite conductivity and for $T \gg \theta$ the deduced conductivity is proportional to $T^{-3/2}$. At somewhat lower temperatures the effect of the long free paths of long waves is to make the conductivity weakly size-dependent at temperatures

considerably higher than those for which Casimir's relation holds. The conductivity is proportional to $L^{1\cdot4}\,T^{-3\cdot4}$ where L is the smallest dimension of the crystal.

At still lower temperatures Pomeranchuk shows that the form of the conductivity-temperature relation is very sensitive to the concentration of defects in the crystal. There is a range of temperature where there is a true conductivity, independent of size, only for crystals of sufficient purity. For these the conductivity is inversely proportional to the temperature and to the defect concentration. It is not shown whether the conductivity of an ideal crystal would vary exponentionally with the temperature, as predicted by Peierls. For crystals with a defect concentration greater than a certain minimum there should exist a temperature region in which the conductivity is independent of temperature, but is again proportional to $L^{1\cdot4}$. Finally, at sufficiently low temperatures Casimir's relation will hold for all crystals.

There does not seem to be any experimental confirmation of even the more striking of Pomeranchuk's conclusions, such as the size dependence at high temperatures and the temperature independent conductivity. It is probable that the dependence on size at relatively high temperatures has not been looked for under conditions which would enable an exact comparison to be made. Pomeranchuk remarks that a temperature independent conductivity should be observed in diamond ; for an impurity concentration of 4×10^{-4} this would extend from 54 to 380° K. The existence of such a temperature independent conductivity between 24 and 340° K was deduced from the measurements of Eucken (1911 c) and of de Haas and Biermasz (1938 a). These experiments are discussed in § 5.1 where it is pointed out that it does not seem justifiable to draw this conclusion.

Pomeranchuk considers that the chief contribution to the conductivity of crystals comes from longitudinal phonons of long wavelength. In order to obtain numerical agreement with experiment the calculated mean free path has to be divided by a factor of 100. Klemens, however, while he uses Pomeranchuk's expressions for the mean free paths for various scattering processes, considers all processes tending to restore equilibrium, including those in which momentum is conserved. He shows that a longitudinal mode of vibration tends to return to its equilibrium value mainly by means of interactions with transverse waves of about the same frequency and a low frequency transverse mode by interactions with modes of frequency kT/h. It is thus shown that 3-phonon processes are sufficient for producing a finite conductivity and the contribution to the conductivity from longitudinal modes is of similar magnitude to that from transverse modes in the case of crystals. The conductivity is not size-dependent except where Casimir's relation holds. According to Klemens the resistance due to Umklapp processes is proportional to $T^{-1}\,e^{-\theta/2T}$. As will be discussed in § 5.1, it is difficult to verify this power of temperature by experiment.

It should be realized that it is only the temperature variation of conductivity which has been calculated and not its absolute magnitude. The latter obviously depends on the strength of the coupling between the modes of vibration or on the number of collisions between phonons, which is determined by the anharmonicities of the interatomic forces, and this is difficult to deduce from other data. Van Vleck (1941 a) has treated a similar but somewhat simpler problem in connection with paramagnetic relaxation in the alums ; namely the transfer of energy between lattice oscillators at the same position in space but at different temperatures. The anharmonicity was derived from compressibility data and the temperature was low enough for U-processes to be neglected. In this case thermal equilibrium is restored by processes represented by eqns. (2) and (3) ; as has been mentioned before, however, these processes alone do not lead to a thermal resistance. Even if a similar calculation could be made for thermal conductivity it would be difficult to obtain the necessary experimental data from which the anharmonicity could be derived for crystals as hard as sapphire and diamond but it may be possible in the case of solid helium, which is very compressible.

It will be seen that the absolute value of the conductivity of dielectric crystals can be very high, yet in discussions of the Wiedemann–Franz law it is assumed that the contribution of the lattice conductivity to the measured conductivity of monovalent metals, such as copper and sodium, is negligible. The justification for this is that the presence of free electrons in metals provides an extra mechanism for scattering phonons so that even in a pure metal the lattice conductivity is small at all temperatures, regardless of the degree of anharmonicity of the atomic forces.

3.2. *Boundary Scattering*

In his original paper Peierls drew attention to the conductivity of diamond which according to Eucken's measurements appeared (erroneously) to be almost independent of temperature. Since the characteristic temperature is very high, the measurements extended to lower values of T/θ than for other crystals. Peierls suggested that under these conditions, where U-processes are very rare, reflection of the waves at the crystal boundaries is all-important so that the conductivity, if defined in the usual way, would depend on the crystal size.

In their first experiments to test Peierls' theory at low temperatures, de Haas and Biermasz (1935) found that the thermal resistance of a quartz crystal increased with decreasing temperature in the liquid helium region. It was realized that impurities in the crystal would give rise to a thermal resistance additional to that caused by Umklapp processes, but Peierls had shown that this resistance too should fall off at low temperatures.

Casimir (1938) worked out the consequences of Peierls' suggestion that scattering of the lattice waves at the boundaries of a crystal becomes important at low temperatures. By assuming that the interaction

between the waves can be completely neglected Casimir compared a crystal to a hollow space filled with electromagnetic radiation. He calculated the flow of heat in a crystal under these conditions by considering the case to be similar to the flow of radiation down a tube with diffusely reflecting walls. Diffuse reflection was to be expected because in the crystals which had been measured the irregularities of the walls were certainly larger than the wave-lengths of the lattice waves dominant in heat conduction at the temperatures considered. (If the reflection were specular the heat flow would be independent of length, which is not in agreement with experiments.) There will then be a temperature gradient along the walls when there is a flow of heat along the crystal.

On the assumption that all phonons behave in the same way on reflection Casimir deduced that the flow of heat is proportional to the temperature gradient, to the cube of the absolute temperature and to the cube of the radius of the crystal (or to the cube of the length of side for a crystal of square cross-section). If a heat conductivity is defined from this relation it will evidently be proportional to the radius of the crystal, but it must be emphasized that this is not a true conductivity.

On the more exact theory of Klemens account is taken of the interaction between the lattice waves, even when these are not of the Umklapp type. Since such collisions alone do not give rise to thermal resistance the effect of boundary scattering is the same as that calculated by Casimir.

Casimir's result is that the conductivity is given by

$$\kappa = 2{\cdot}31 \times 10^3 RpA^{2/3}T^3 \text{ Watts/cm deg}, \quad . \quad . \quad . \quad . \quad (7)$$

where R is the radius of the crystal and p is a dimensionless quantity equal to the ratio $\left(\overline{\Sigma \frac{1}{v_j^2}}\right) \Big/ \left(\overline{\Sigma \frac{1}{v_j^3}}\right)^{2/3}$; $(\overline{\ })$ denotes the mean value over all directions. A is the constant in the expression $c_v = AT^3$, for the specific heat per unit volume at low temperatures according to Debye's theory. The factor p occurs because different mean velocities are required for evaluating the specific heat and the energy flow. For a crystal of square cross-section of side d, R is replaced by $0{\cdot}56d$.

It is very convenient to discuss the effect of boundary scattering by expressing the conductivity in terms of the phonon mean free paths, as has been done previously. If the conductivity is equated to $\frac{1}{3}cvl$, then it is possible to calculate the value of l which will give the same conductivity as that derived by Casimir and given by eqn. (7). From Debye's theory both the specific heat and, therefore, the mean wave velocity can be expressed in terms of θ, M and ρ, where M is the mean atomic weight in the crystal and ρ is the density. If p is taken as $1{\cdot}4$ (which, as Casimir shows, is about the value it has for most crystals) then l is almost exactly equal to $2R$, the diameter of the crystal.

It will be noticed that for boundary scattering, acting alone, it is possible to calculate the absolute magnitude of the conductivity since, unlike Umklapp processes, the strength of coupling between the waves is not involved.

3.3. *The Combined Effect of Umklapp Processes and Boundary Scattering*

For an ideal crystal Umklapp processes are dominant in determining the conductivity at high temperatures and boundary scattering is dominant at low temperatures. Over a certain range of temperature both processes must be considered, but this range is small as both types of resistance vary rapidly with temperature. In order to calculate the conductivity when more than one scattering process is important it is necessary to insert into eqn. (6) the value of the mean free path l_{Kj} (for phonons Kj) resulting from the combined scattering processes, and then to carry out the summation, over all values of K and j. Simple addition of the thermal resistances due to each scattering process, considered as acting separately, will in general only lead to the same result if all scattering processes are independent of K and j.

Klemens has in this way derived a combination formula which gives the conductivity when Umklapp processes and boundary scattering are both important. The results calculated for ideal sapphire crystals are shown in fig. 1, together with the values which would be obtained by adding the resistances which the two processes would produce if they acted separately. In the neighbourhood of the maximum the difference can amount to about 30%.

3.4. *Other Factors which may affect the Conductivity*

Measurements have been made of the thermal conductivity of some dielectric solids in the region of specific heat anomalies. Eucken and Schröder (1939), Gerritsen and van der Star (1942) and v. Simson (1951) have measured HBr, CH_4 and NH_4Cl respectively, in each of which the anomalies in the solid state are associated with the rotational energies of the molecule or parts of the molecule. Corresponding anomalous increases in the measured heat conductivities have been found, but no detailed theoretical work has been carried out on this subject.

The contribution of the spins in a paramagnetic salt to heat conductivity has been treated theoretically by Fröhlich and Heitler (1936) and by Akhieser and Pomeranchuk (1944). Pomeranchuk (1941 c) has also discussed the effect of the magnetic spectrum on the phonon conductivity. An excited ionic level is considered not localized in the lattice but the excitation energy is exchanged with other ions. The thermal conductivity associated with the motion of the excitations is determined at low temperatures by their mutual scattering and also by the effect of impurities. Both calculations show that if only mutual scattering is important this ' exciton ' conductivity increases with decreasing temperature. At sufficiently low temperatures it should therefore become greater than the phonon conductivity which decreases as the cube of the temperature. Akhieser and Pomeranchuk estimate that in potassium chrome alum the two contributions would be about equal at 0·02° K. The calculation only gives the order of magnitude of the ratio of the two contributions (e.g., in the expression for the lattice specific heat

$C_v = 464(T/\theta)^3$ cal/mole the numerical factor is omitted) but as the ratio varies as T^4 the calculation will certainly give the order of magnitude of the temperature at which they become equal.

The only experiments in which the contribution of the spins might have been noticeable are those of Garrett (1950) on potassium chrome alum. Even here, however, the lowest temperature at which measurements were made is about ten times larger than that at which Akhieser and Pomeranchuk estimate that this contribution would be equal to the phonon conductivity, and, indeed, no effect was found.

§4. The Theory of Imperfect Crystals

As can be seen from fig. 1, even the dielectric crystal with the highest conductivity so far measured, synthetic sapphire, has a conductivity which, near the maximum, is only about one eighth of that to be expected for a perfect crystal. This can be attributed to imperfections in the crystal, which will produce extra scattering of the phonons. Various types of imperfections may occur and mention will be made here of the effects of mosaic structure and of small scale defects, such as impurity atoms or displaced atoms.

4.1. *Small Scale Defects*

A single defect alters the elastic properties of the crystal over a region of the order of size of a unit cell ; for long waves the scattering will obey Rayleigh's law and the mean free path of a phonon is proportional to $1/K^4$. If there were no coupling between waves the mean free path of the longest waves would tend to infinity, giving rise to an infinite conductivity. Peierls showed that the anharmonic coupling leads to a finite conductivity because it effects the transfer of energy away from these long waves by processes represented by eqns. (2) and (3). As a result, the thermal resistance due to small defects is proportional to the absolute temperature at low temperatures. This result is also obtained by Klemens.

For short waves or for defects of large extent Rayleigh's law is not applicable ; the scattering is less frequency dependent and becomes almost frequency independent at the highest frequencies. Hence the resistance due to defects is proportional to the temperature only at low temperatures.

4.2. *Mosaic Structure*

From x-ray observations it is evident that the alignment of the atomic planes is not perfect even in single crystals. A broadening of the diffraction pattern indicates that the crystal is divided into small regions which are inclined at very small angles (of the order of seconds) to neighbouring regions. Pomeranchuk (1942) has calculated the phonon mean free path when it is limited by such disorientations and has shown that it is proportional to $1/K^2$. At low temperatures the thermal resistance due to this cause is proportional to $1/T$.

§5. Experimental Work on Thermal Conductivity of Pure Crystals

Many authors have reported measurements on particular crystals at various temperatures and instead of discussing these in chronological order it would seem to be more useful to describe them according to the information they yield when considered in the light of present knowledge about thermal conductivity.

5.1. *The Umklapp Process*

It is now known that it is necessary to measure thermal conductivity at temperatures between $\theta/20$ and $\theta/10$ in order to observe the exponential variation of conductivity predicted by Peierls for low temperatures. This exponential rise should be observable at still lower temperatures in ideal crystals with diameters of the order of a millimetre, but seems to be masked by lattice imperfections at temperatures somewhat higher than those at which boundary scattering should be appreciable.

For the crystals measured by Eucken the temperature of liquid air is too high for the conductivity to deviate appreciably from the $1/T$ law, except for diamond. Although the values differed considerably from crystal to crystal Eucken found the average value of κ_{83}/κ_{273} to be of the order of 3–4. A few measurements were made at the boiling point of liquid hydrogen and for rock salt and for quartz the ratio κ_{22}/κ_{88} was greater than 10, but was only about 3 for sylvin.

The diamond specimen which Eucken used in his experiments (1911 c) was not large enough for the temperature gradient to be determined in the usual way and the overall resistance which was measured included some contact resistance at either end of the crystal. He showed that this could lead to considerable error in the conductivity at low temperatures by measuring a rock-salt crystal in the same way and comparing the values found with the results of his more accurate method. Although it could be seen that the conductivity of diamond must be very great at room temperature it was not evident how the conductivity varied with temperature.

Although some of the results obtained by Eucken provided data for comparison with Peierls' theory, systematic measurements at low temperatures were very necessary. De Haas and Biermasz started their series of experiments in 1935 by measuring the conductivity of a quartz crystal. Although they verified Eucken's ratio of κ_{22}/κ_{88} and found that the rise in conductivity continued certainly down to 15° K, they subsequently concentrated their attention on the unexpected variation of conductivity which they found to occur at liquid helium temperatures. For the alkali halides which de Haas and Biermasz measured (1937) the conductivity did not increase faster than inversely proportional to the temperature down to 15° K but they again found that the conductivity decreased in the liquid helium region.

It is probable that the conductivity of the alkali halide crystals does not rise rapidly with decreasing temperature in a way similar to quartz because of the effect of small quantities of impurities. In view of the recent papers of Krishnan and Roy (1951, 1952), in which it is shown that the cubic anharmonicities in these crystals are absent, owing to the symmetry of the lattice, it would be very interesting if measurements were made on crystals sufficiently pure for the conductivity to be limited only by mutual scattering of the phonons at temperatures where the exponential rise of conductivity would be expected. The relatively large thermal conductivity of KCl at room temperature, where the effect of impurities is small, also suggests a small anharmonicity ; the phonon mean free path, calculated from eqn. (5) is several times greater than in quartz at the same temperature.

De Haas and Biermasz also measured the conductivity of diamond (1938 a) ; most of the measurements were at temperatures below 20° K, but they also measured one crystal at liquid air temperature to see whether the apparent temperature independence suggested by Eucken's results held. Below 20° K the variation of conductivity showed that boundary scattering was the chief cause of thermal resistance but the value at 89° K was the same as the extrapolated value at 24° K. This value was nearly ten times greater than Eucken's and de Haas and Biermasz attributed this to a difference in the quality of the stones. They concluded that between 24 and 90° K the conductivity is independent of temperature. Although the values of de Haas and Biermasz and of Eucken differed by a large factor, so that the two sets of results could not be combined, the impression left by these experiments seems to have been that the thermal conductivity of diamond is independent of temperature between 24 and 340° K. Recently measurements have been made on a specimen of gem quality between 2° K and room temperature (Berman, Simon and Wilks 1951) and it has been found that the conductivity is not independent of temperature over the large range of temperature, as previously assumed. There is certainly a smaller variation, over a much narrower temperature range (20–100° K), than would be expected for an ideal crystal and this can be explained in terms of the effect of a very small concentration of clusters of impurities or other defects (Klemens 1952).

As all the earlier measurements of thermal conductivity had only been made at fairly widely spaced temperatures or over small temperature ranges and had in many cases led to inconclusive results, it was considered necessary to make measurements over a considerably larger range. For this purpose an apparatus was designed (Berman 1951) to cover the temperature range from 2 to 90° K. For some substances the measurements have also been extended up to room temperature. Measurements have been made on single crystals of quartz, synthetic sapphire and diamond of various cross-sections ; the conductivities of the largest crystal measured in each case are shown in fig. 3.

Recently extensive measurements have been carried out on the thermal conductivity of solid helium at different pressures (Wilkinson and Wilks 1951, Webb, Wilkinson and Wilks, 1952) and some of the results are shown in fig. 4. Solid helium is very compressible and, unlike other substances, lends itself to the formation of crystals of substantially different density and θ values by using quite moderate pressures.

As has been discussed previously, the variation of conductivity with temperature is determined by the ratio T/θ. The crystals which have been measured represent a wide range of θ values, varying from about 25° for solid helium at the lowest pressures to over 2000° K for diamond, so that the measurements provide a considerable amount of data for comparison with Peierls' theory. This comparison has recently been

Fig. 3

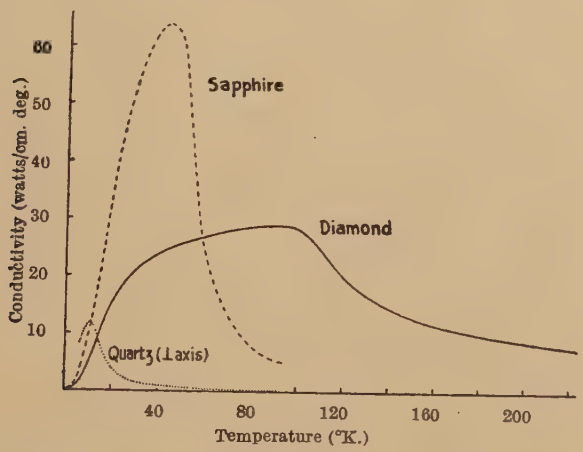

Thermal conductivities of quartz, synthetic sapphire and diamond. (Berman, Simon and Wilks 1951.)

made (Berman, Simon and Wilks 1951) and figs. 3 and 4 are taken from the paper. It can be seen that the thermal conductivities of these pure crystals behave in the same general way. Between temperatures equivalent to roughly $\theta/20$ and $\theta/10$ the conductivity fits a relation of the form $\kappa \propto T^{\nu} \exp(\theta/bT)$. If θ is taken as the Debye characteristic temperature corresponding to the specific heat per mean gram atomic weight then b has a value close to 2 for each crystal. Since the exponential factor is so strong it is not possible to decide the power of T from the experiments. Over the relatively small temperature ranges for which this relation holds, the experimental results can be fitted equally well by different values of ν and corresponding values of b not very different from 2. Since it was only shown by Peierls that b should be of the order of 2 and since none of the crystals has a specific heat which exactly follows

Debye's law, the precise value of θ/b which is found to give the best fit with the conductivity measurements is not a crucial test of Peierls' theory.

The mean free paths for U-processes have been calculated from the relation $\kappa=\frac{1}{3}cvl$ and are shown in fig. 5. The mean free paths can be expressed by relations of the form

$$l=A\exp(\theta/b'T) \quad . \quad . \quad . \quad . \quad . \quad . \quad . \quad . \quad (8)$$

where the values of b' are 2·3 for solid helium, 2·7 for diamond and 2·1 for sapphire and A varies from 6×10^{-8} cm for helium to $1{\cdot}4\times10^{-6}$ cm for diamond. Values for quartz have not been derived as the crystal is strongly anisotropic and the conductivity is difficult to treat theoretically.

Fig. 4

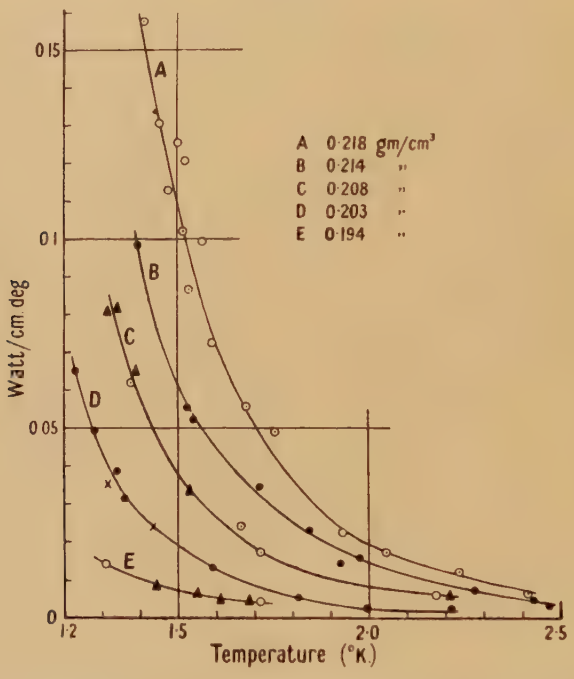

Thermal conductivity of solid helium at constant density.
(Berman, Simon and Wilks 1951.)

For each crystal the probability of a U-process, as measured by the mean free path, is a function of θ/T, but the absolute number of collisions depends on the values of A, which must therefore be a measure of the anharmonicity of the inter-atomic forces. It is interesting to observe that the value of A is the same for solid helium crystals having the wide range of density and conductivity shown in fig. 4.

It can be seen from fig. 3 that the maximum conductivity occurs for each crystal for a value of θ/T of about 20–25. If the conductivity

maximum were determined by the onset of appreciable boundary scattering alone then at the maximum the mean free path due to U-processes should be of the order of the crystal diameter. However, for all the crystals so far measured the mean free path at the maximum is an order of magnitude lower than this and possible explanations of the discrepancy will be discussed in § 5.3. Efforts are being made to obtain crystals of other substances in order to make further measurements in the tempera-

Fig. 5

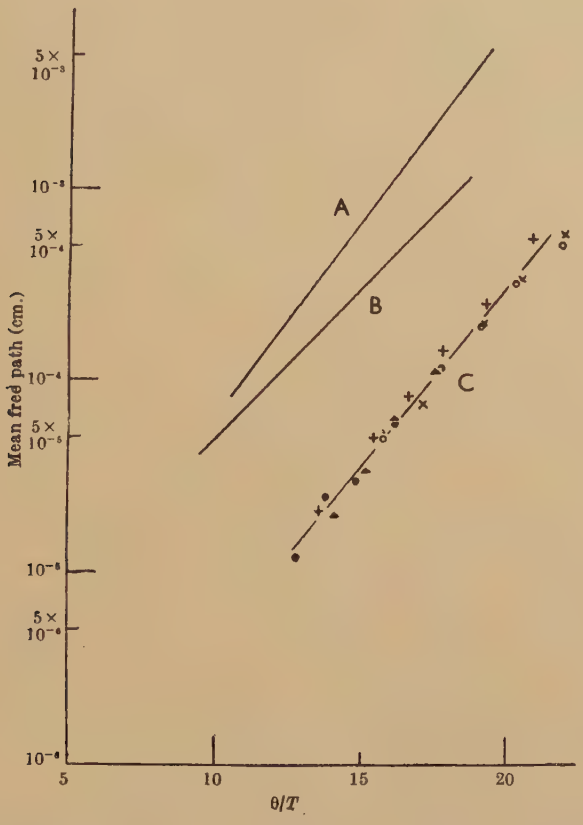

Mean free path for U-collisions as a function of θ/T. A: synthetic sapphire ($\theta \simeq 980$); B: diamond ($\theta \simeq 1{,}840$); C: solid helium (θ, 22–35). For solid helium the densities are: 0·218 (×); 0·214 (○); 0·208 (+); 0·203 (▲); 0·194 (●) g/cm³. (Berman, Simon and Wilks 1951.)

ture range where the exponential variations of conductivity should be found. The combination of requirements is however rather exacting: great purity, freedom from strains, simple structure and sufficient size (particularly length) for accurate measurements.

The simple expression (8) for the mean free path does not hold at temperatures greater than about $\theta/10$ since the other temperature dependent terms become important. It is evident however that the mean free path

continues to decrease and measurements at high temperatures suggest that it would eventually reach the order of atomic dimensions. In potassium chloride, for example, at 0° C, ($\theta/T=0{\cdot}8$) the value of the mean free path calculated from the thermal conductivity is only of the order of twenty lattice spacings.

5.2. *Boundary Scattering*

5.2.1. *Single Crystals*

De Haas and Biermasz carried out many experiments on the size effect at liquid helium temperatures but did not find for any crystal even at the lowest temperatures (2° K) that the conductivity is proportional to T^3, as given by Casimir's formula. For diamond and quartz the highest power of T reached was about 2·5 while for KCl and KBr the power of T was less than 2. The deviation from the expected relation can be

Fig. 6

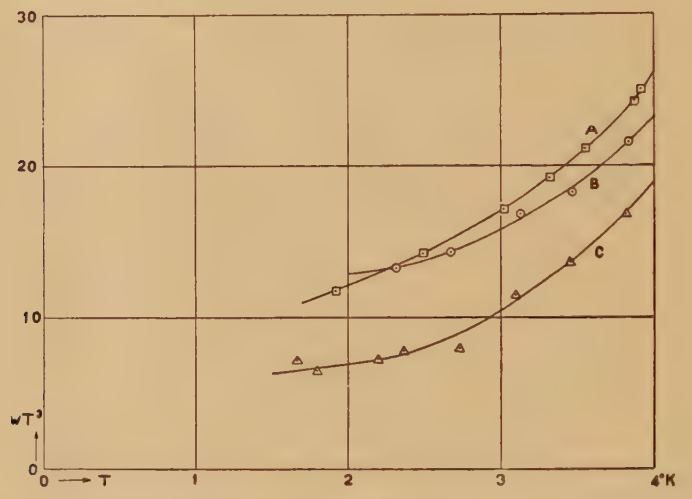

WT^3 versus T. A: KCl, d =0·252 cm; B: SiO_2, R =0·227 cm; C: SiO_2, R=0·108 cm; (the ordinates of C have been diminished by 20). (Casimir 1938.)

clearly seen by plotting T^3/κ against T, when a horizontal line should be obtained. Figure 6 shows such a plot made by Casimir. (In the figure $W=1/\kappa$.) This behaviour can be explained by assuming that there is present in all these crystals some additional source of scattering and that the resistance due to it does not vary rapidly with temperature, so that it is still important down to the lowest temperatures of the measurements.

In accord with the idea that deviations from the T^3 law are caused by imperfections in the crystals, de Haas and Biermasz found that at a given temperature the conductivity is not strictly proportional to the diameter of the crystal and, in fact, seems to approach a limiting value for large diameters. This is shown by plotting the conductivity at constant

temperature against the diameter and fig. 7 is taken from the work of de Haas and Biermasz. They suggest that the deviations from the T^3 law are due to a mosaic structure in the crystals ; this has also been suggested by Klemens (1951) for quartz. As has been discussed earlier, scattering by a mosaic structure would lead to a thermal resistance inversely proportional to the temperature, so that if mosaic scattering alone were important the conductivity would be proportional to the temperature. At liquid helium temperatures the resistance due to U-processes in quartz is extremely small, so that for an infinitely large crystal the conductivity would only be limited by mosaic scattering. From fig. 7 it can be seen that the limiting values of the conductivities for large diameters are roughly proportional to the temperature, in agreement with the relation which should hold for mosaic scattering.

Fig. 7

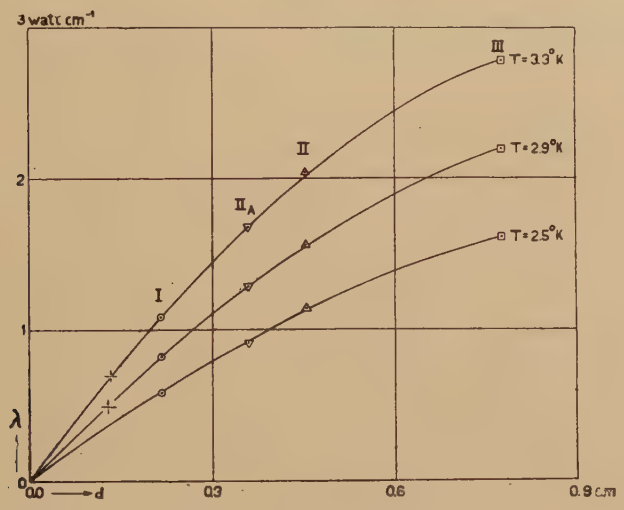

Thermal conductivity of SiO_2 ⊥ as a function of the thickness.
(de Haas and Biermasz 1938 b.)

Klemens suggests that the departures from ideal behaviour in the alkali halides, both above and below the temperature of the conductivity maximum, are due to impurities and has shown that very small concentrations can explain the results (as will be discussed in § 6.1).

If this explanation of deviations from Casimir's formula is correct, then at sufficiently low temperatures boundary scattering would be the only important cause of thermal resistance and the T^3 law would be obeyed. Few measurements on single crystals have been made, however, at lower temperatures. From the rate of temperature equalization of the ends of paramagnetic crystals demagnetized from inhomogeneous fields, Kurti, Rollin and Simon (1936) deduced values for the conductivity of potassium chrome alum at 0·18° K and of iron ammonium alum at

0·07 and 0·10° K. Although the accuracy of the experiments was not sufficient for the temperature variation of the conductivity to be deduced with great certainty, the ratio between the values of the conductivities of iron ammonium alum was about 3, while the cubes of the temperatures are in the ratio of about 3 too. If we take Duyckaerts' values of the lattice specific heat (1942) and assume a value of 2×10^5 cm/sec for the phonon velocity (see van Vleck 1941 b), then the mean free path calculated from eqn. (5) is about quarter of a millimetre, which is less than one twentieth of the crystal diameter.

Potassium chrome alum has also been measured by Bijl (1949) and by Garrett (1950). Bijl used a conventional heating method and determined the temperature gradient, when a steady state had been reached, by measuring the mutual inductance between a primary coil and two secondary coils wound round the ends of the specimen. The measurements were made between 1·4 and 3·9° K and in this region the conductivity was found to be proportional to a power of the temperature of about 2·3. Bijl found that the conductivity depended on the rate at which the specimen was cooled below 70° K, an effect which has not yet been fully explained (see Eisenstein 1952).

Garrett used a method similar to that of Kurti *et al.*, but a temperature gradient was produced in the crystal by magnetizing the specimen non-uniformly after the adiabatic demagnetization. The conductivity was measured at temperatures between 0·16 and 0·29° K and in this range the conductivity was found to be proportional to the cube of the temperature within the experimental accuracy and seems to fit on to the 'slow cooling' curve of Bijl, as shown in fig. 8. The phonon mean free path calculated from Garrett's measurements, taking the value of the lattice specific heat given by Casimir (1940) and a value of 2×10^5 cm/sec for the phonon velocity, is about $\frac{1}{2}$ mm while the diameter of the crystal was 15 mm. Such a large discrepancy suggests that there are boundaries within the crystal sufficiently definite to scatter phonons independently of their wave-number and so to limit the mean free path to $\frac{1}{2}$ mm even at these low temperatures.

It is evident that in order to find whether Casimir's formula is correct for the case where only boundary scattering is important, it is necessary to measure the conductivity at temperatures which are only a small fraction of the temperature at which the conductivity maximum occurs. Except for diamond, for which the limitation has been the size of crystals available, the measurements have not been carried out at low enough temperatures by conventional methods and the methods relying on temperature equalization in a paramagnetic salt are too difficult to carry out for many experiments to have been made at sufficiently low temperatures. Recently artificial sapphire crystals (θ 900° K) of great purity have become available in suitable sizes for measurement. Also a diamond of sufficient length and of regular cross-section has been obtained. For these two crystals the conductivity maxima occur at temperatures

approximately 4 and 10 times that of quartz, so that measurements down to liquid helium temperatures extend correspondingly further into the region where boundary scattering is the dominant factor in determining the conductivity.

The measurements on diamond have not yet been made on specimens of sufficiently different cross-section, but the results obtained so far seem to agree with those on artificial sapphire. For both crystals the conductivity does not vary with a power of T greater than 2·7 to 2·8, although

Fig. 8

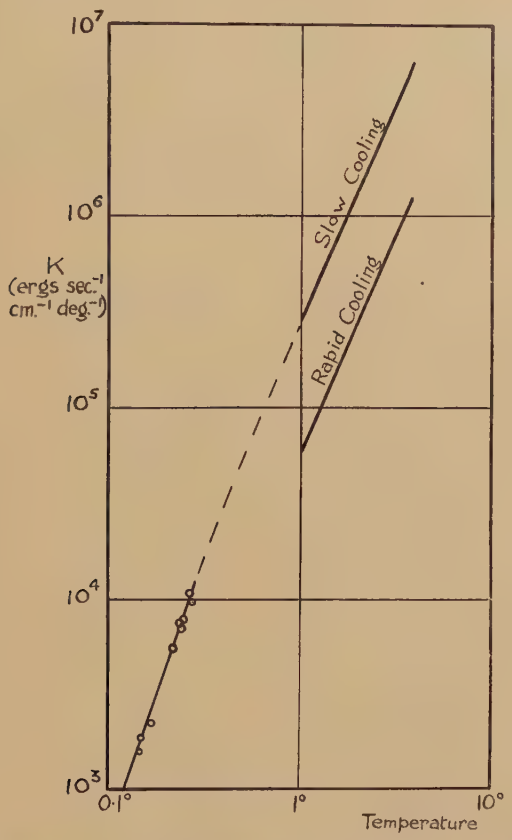

The thermal conductivity of Potassium Chrome Alum. (Garrett 1950.)

the lowest temperature of the measurements, 2° K, corresponds to about 1/50 of the temperature of the maximum for diamond. At 2° K, however, the phonon mean free path in diamond, calculated from eqn. (5), is slightly greater than the length of side of the square cross-section. According to Casimir's theory, the conductivity for a crystal of square cross-section, should correspond to a mean free path 1·1 times the length of the side.

The values found for the conductivity of diamond at helium temperatures are about three times as great as those found by de Haas and Biermasz.

They used crystals of triangular cross-section, the linear dimensions of which must have been of the order of one millimetre ; the original side of the crystal now measured was 4 mm.

The measurements on sapphire have so far been made on a crystal 3 mm diameter, which was later ground to a diameter of 1·5 mm ; measurements on specimens of both larger and smaller diameter will also be made. The results are shown in fig. 1. The main features are in agreement with theory, namely that at high temperatures the conductivity is independent of the diameter but that at the lowest temperatures, below 10° K, the conductivity is proportional to the diameter. However the mean free path at 10° K is only one third of the diameter of each specimen and increases with decreasing temperature, reaching 0·8 of the diameter at 2° K. Strict proportionality of conductivity to diameter suggests that only boundary scattering is important, but in that case Casimir's theory leads to a conductivity proportional to T^3 and a mean free path equal to the diameter of the crystal. There does not seem to be a simple explanation of these results and the measurements made so far on diamond indicate a similar behaviour.

One explanation would be that, although the evidence suggests that at sufficiently low temperatures Casimir's relation would be valid, at the temperatures of the present measurements the resistance due to boundary scattering is not proportional to T^3. If the power of the temperature is considered to be an unknown factor to be derived from experiments of the type discussed, then if boundary resistance is taken as being inversely proportional to the diameter, the total resistance at low temperatures due to imperfections as well as boundary scattering can be represented by $x/R+B$, where x and B are functions of the temperature and the two terms represent boundary scattering and the size-independent defector Umklapp-resistance. For crystals of two different diameters we have then the equations

$$x/R_1+B=1/\kappa_1 \quad \text{and} \quad x/R_2+B=1/\kappa_2$$

at a given temperature. If these simultaneous equations are solved for the conductivities of the two sapphire specimens for temperatures between 2 and 45° K, then it is found that x is proportional to $T^{2\cdot6}$ and B is nearly independent of temperature. This cannot be considered as a proof that boundary resistance departs from a T^{-3} variation and it is clear that further experiments are necessary.*

5.2.2. *Polycrystalline Solids*

It is evident that at low temperatures a crystal of very small diameter would have a very low thermal conductivity but measurements have not been made on single crystals with a diameter less than the order of a millimetre. Several authors have, however, reported values for the

* More recent experiments on still thinner diamond and sapphire crystals show conductivities departing only very little from the T^3 law below 4 K.

conductivity of compressed powders of paramagnetic salts, composed of grains from 10^{-3} cm upwards. Kurti, Rollin and Simon (1936) mentioned that the conductivity of a compressed powder of iron ammonium alum was about 1/10 of the conductivity of a single crystal of 7 mm diameter. The dependence of conductivity on size was not known at the time and there was therefore no reason to think that the difference was due to a cause other than the porosity ; neither the density of the specimen nor the grain size were stated.

Van Dijk and Keesom (1940) deduced the relation $\kappa = 0{\cdot}00312\ T_m^3$ calories/cm sec deg for the conductivity of a compressed powder of the same salt in the temperature range 0·04 to 0·3° K (T_m being the magnetic temperature). This would give a value at 0·1° about one sixth of the single crystal value of Kurti *et al.* Again the grain size is not given, but the density is stated to be very close to the single crystal value.

Hudson (1949) obtained some mean conductivity values between 0·10 and 0·22° K for a compressed powder of iron ammonium alum of nearly single crystal density, consisting of crystallites estimated to be between 10^{-3} and 10^{-2} cm in size. At 0·10° K the conductivity was about fifty times less than the single crystal value of Kurti *et al.* although from the relative diameters alone the ratio would be expected to be several hundred. Hudson attributes this discrepancy to an increase of the phonon mean free path above the size of the crystallites, which is made possible by the good contact between the crystallites. However, as has been pointed out above, the mean free path calculated from the single crystal conductivity is about one twentieth of the crystal diameter, so that Hudson's results actually suggest that the mean free path in the polycrystalline material is of the order of size of the crystallites.

Recently some other polycrystalline solids have been measured (Berman 1952) and for specimens of alumina and beryllia which had nearly the single crystal density the calculated mean free path becomes slightly greater than the estimated crystallite size at low temperatures. For graphite specimens with a density of about 70% of the single crystal there is no evidence that the phonon mean free path does increase above the crystallite size. The interpretation of the results is made difficult by the absence of measurements on the corresponding single crystals, except in the case of alumina, although even for this it is not certain that the crystal form was exactly the same as the artificial sapphires which have been measured.

The sintered alumina had a density equivalent to 95% of the single crystal value and at temperatures above the conductivity maximum had a conductivity about half that of a single crystal. This difference can be ascribed to the fact that the crystallites do not touch over their whole surface, so that even if there is no actual contact resistance the overall conductivity is less than that of the individual crystallites. Below the maximum the conductivity decreases proportionally to $T^{2{\cdot}7}$, which indicates that the mean free path is still increasing slowly, and is about

20 μ at 3° K, compared with direct measurements of the crystallite size from a photomicrograph which showed crystallites ranging in size from about 5 to 30 μ. This suggests that the mean free path does increase slightly above the crystallite size and it is interesting to estimate the crystallite size from the position and value of the conductivity maximum. The maximum conductivity occurs at 75° K and the mean free path due to Umklapp processes at this temperature can be obtained from the single crystal measurements, and is about 3 μ. As the maximum would be expected to occur at a temperature such that the Umklapp mean free path is of the order of size of the crystallites, this gives a value for the crystallite size. The actual value of the conductivity at the maximum also suggests this order of size of the crystallites.

The sintered beryllia was only measured up to about 90° K and over this whole range the conductivity increases with temperature so that the maximum must occur at a considerably higher temperature than for alumina. Although the boundary resistance is about the same for the two substances, much higher values of conductivity at room temperature and above have been reported for sintered beryllia (e.g. Norton and Kingery 1952) so that its resistance due to Umklapp processes must be lower and the maximum conductivity should occur at a higher temperature than for alumina.

Many samples of graphite have been measured above room temperature by Powell and Schofield (1939) who found that some specimens at room temperature had very high conductivities. For example, some samples had conductivities similar to that of copper, even though measurements of the electrical conductivity show that less than 1% of the heat conductivity can be ascribed to free electrons.

Samples having mean crystallite sizes of 300, 1000 and 2000 Å have now been measured (Berman 1952) from 2° K up to room temperature and the general behaviour is similar to that of the sintered alumina. However, the conductivity is much lower at low temperatures, corresponding to the much smaller crystallite size, and for the specimen with the smallest crystallite size the mean free path seems to be restricted to about 300 Å even at the lowest temperatures. Graphite is an extremely anisotropic solid and has a specific heat which departs considerably from Debye's theory, being proportional to a power of T between 2 and 2·5 at low temperatures, so that the interpretation of the conductivity results is uncertain. It may be significant that the conductivity at low temperatures varies as a power of T which is about 2·2 for the specimen of smallest crystallite size and is about 2·7 in the largest case.

These graphite specimens are very good heat insulators at low temperatures; at 2° K, for example, the thermal conductivity of the 300 Å graphite is one twelfth of that of ordinary glass, which would generally be considered a good heat insulator. It is not certain how the conductivities would compare at lower temperatures, since the conductivity even of glass would eventually be limited by boundary scattering,

while the conductivity of graphite might not continue to fall off so rapidly below 1° K if the electronic heat conductivity becomes more important than the lattice contribution.

Although the results on microcrystals are, in general, more difficult to interpret than those in single crystals it does appear that they conform more closely to the simple theoretical picture of an ideal crystal with only two causes of thermal resistance, Umklapp processes and boundary scattering. Presumably as the phonon mean free path is always restricted to a very small length by these two processes the effect of imperfections in the crystal lattice is not noticeable at any temperature.

5.3. *The Conductivity near the Maximum*

The conductivity to be expected when both boundary scattering and U-processes are important has been discussed in § 3.3. For single crystals of the size usually measured, the conductivity at the maximum should be about 20–30% less than would be given by simple addition of the resistances due to the two processes, considered to act separately. Since the resistances due to both processes vary rapidly with temperature the conductivity on either side of the maximum should very soon be determined by one process alone.

For all the pure single crystals which have so far been measured the maximum conductivity is less than the value calculated for an ideal crystal, even when this is calculated according to the combination formula given by Klemens. The absolute value of the Umklapp resistance in the neighbourhood of the maximum cannot at present be calculated from other properties of the crystal, but it can be estimated by extrapolation from higher temperatures where it is the dominant factor.

A small difference between the calculated and experimental values of the maximum conductivity could be ascribed to uncertainty as to the dependence of Umklapp scattering on temperature at temperatures below those at which its effects alone are important. However, for solid helium in a tube of $\frac{1}{2}$ mm diameter the discrepancy is about a factor 2, for the 3 mm diameter sapphire it is a factor 8 and for a diamond of 4 mm square cross-section it is a factor of over 20.

The simplest explanation is to postulate a sufficient number of defects to account for the discrepancies ; it is then necessary to decide the type of defect which would give the extra thermal resistance observed. For both sapphire and diamond the differences between the calculated and observed thermal resistances increase with decreasing temperature ; in the case of sapphire the extra resistance is roughly inversely proportional to the temperature, while for diamond the variation with temperature is much less. For the two sizes of sapphire the extra resistance is the same at the conductivity maximum, but increases more rapidly with decreasing temperature for the smaller crystal, a fact which is connected with the departures from Casimir's law discussed earlier. The equality of the extra resistances at the maxima confirms the belief that these are due to some defect in the crystal and not merely to an error in the theory

and the experiments made so far on diamond also suggest that the extra resistance at the maximum does not depend on the size. As the extra resistance must actually be the main resistance at the maximum the value of the maximum itself should be little changed by altering the diameter of the crystal, which only alters a small component of the total resistance. From fig. 1 it can be seen that the maximum conductivities for the two sapphires should occur at about 30° K and should be about 500 and 300 watt units, whereas the actual maxima are at a higher temperature, of much smaller magnitude and are only about 12% different from each other. Experiments will be made when the crystal is further reduced in diameter.

An extra thermal resistance which increases slowly with decreasing temperature could be due either to the effect of a mosaic structure or to impurities (or other small scale defects). Impurities would have to be grouped together in clusters which are of such a size that Rayleigh scattering does not occur for the wavelengths which are important at the temperatures concerned. At lower temperatures Rayleigh scattering might occur, but here the boundary resistance is great enough to mask the effect of defects.

Only one experiment has been made to find the effect of a mosaic structure : this was performed on an artificial sapphire selected, by X-ray examination, to have a mosaic structure much more pronounced than in most specimens. Although this structure was certainly more marked than in the sapphire on which the other experiments have been carried out, the thermal conductivity was no different even in the region of the conductivity maximum, where any extra source of resistance would be most noticeable (Berman, to be published).

Klemens (1952) has pointed out that Ahearn (1951) postulates the presence of clusters of defects in diamond to explain the electrical properties which he has measured. Such clusters could also account for a thermal resistance which is nearly independent of temperature. The strong effect of defects in diamond would also explain the differences between the values measured by de Haas and Biermasz and those shown in fig. 3. At liquid helium temperatures the two sets of measurements are in agreement when account is taken of the different cross-sectional areas used, but at liquid air temperature the single measurement of de Haas and Biermasz gives a value of the conductivity one half of the recent value. As has been explained, reduction of the cross-section has very little effect on the conductivity in this temperature region, so that the difference in conductivities here can be ascribed to the different qualities of the stones.

The purity of the diamond which is being used for the present measurements will be determined at the end of the experiments and it is hoped that it will be possible to obtain a stone of different purity. Artificial sapphires can be prepared with a wide range of suitable impurities and one series of measurements on an impure crystal will be described in the next section.

The relative smallness of the discrepancy between the calculated and measured conductivity maximum for solid helium would be expected both from the purity of the crystal, which must result from the way in which it is formed in the apparatus (Webb *et al.* 1952) and also from the small diameter of the crystal measured. It would be interesting to find whether the discrepancy increases with increasing diameter as for diamond and sapphire.

§ 6. Measurements of the Effects of Lattice Imperfections

6.1. *Impurities*

There have not been many measurements designed to determine the effect of lattice imperfections on thermal conductivity. Eucken and Kuhn (1928) measured a series of mixed crystals of KCl–KBr at room temperature and at liquid air temperature. The thermal conductivity was greatest for crystals of either of the pure components and for any intermediate concentrations the relative decrease in conductivity was greater at the lower temperature. This occurs because the resistance due to impurities is weakly dependent on temperature at these temperatures while the Umklapp resistance is roughly proportional to the temperature in this range. The importance of these experiments is that quantitative deductions can be made as to the effect of impurities, whereas in later experiments the impurity concentration is not known so accurately.

De Haas and Biermasz found that above the conductivity maximum the thermal conductivities of KCl and KBr crystals are inversely proportional to the temperature and the absolute values are smaller than those for quartz. The conductivity of KCl is about one quarter of that of quartz in the region of the maxima but becomes greater at temperatures above about 60° K. The values for KBr are smaller at all temperatures at which measurements were made. This strongly suggests that the absence of the exponential variation of conductivity at low temperatures is not observed for the alkali halides on account of impurity scattering. For these ionic crystals there is a simple mechanism by which impurity atoms can enter the lattice, whether they are of the same or different valency from the other atoms. The scattering can then be due either to the effect of the presence of an atom of different atomic weight or to the combined effect of an impurity atom and the corresponding hole created to preserve the electrical neutrality of the crystal as a whole. The latter cause would be expected to give the greater scattering.

In the KCl crystal measured by de Haas and Biermasz the concentration of sodium and magnesium impurities were both estimated to be less than 10^{-4}. Since magnesium is divalent there must be a potassium atom missing from the lattice for each magnesium atom present. Klemens (1951) has calculated the thermal resistance to be expected on the assumption that the effect of an impurity atom and the associated vacant site is the same as would be produced by the presence in the crystal of a

spherical hole of radius equal to X times the lattice constant. If ϵ is the impurity concentration then he shows that for KCl $\epsilon X^6 = 6{\cdot}4 \times 10^{-5}$. If X is of the order of unity, then the impurity concentration calculated this way is not inconsistent with the estimated purity of the crystal. Comparison at liquid air temperature of the resistance of the crystal measured by de Haas and Biermasz with that of a mixed crystal containing 10% KBr shows that the scattering caused by an atom of wrong valency is at least 100 times greater than the scattering produced by an atom of different mass but of the same valency.

In the case of KCl and KBr Klemens has also accounted for the low power of the temperature variation of the conductivity below the maxima by the presence of impurites. The resistance due to impurities is proportional to the temperature and therefore dies away much more slowly than that due to Umklapp processes. Measurements would have to be made at much lower temperatures for boundary scattering alone to be important.

An experiment has been made to determine the effect of impurities directly, as a function of temperature (Berman, to be published). Measurements were made on an artificial ruby, which is an artificial sapphire with chromium impurity. Scattering is caused by the replacement of a few aluminium atoms by chromium atoms, which have the same valency but double the atomic weight. The thermal resistance of a pure sapphire of the same diameter has been subtracted from the resistance of the ruby and the resulting resistance is practically independent of temperature between about 20 and 70° K.

This indicates that it is possible for impurities to give an extra thermal resistance which varies with temperature in a way similar to the variation of extra resistance calculated in diamond and sapphire. From this experiment it would be assumed that in the ruby the impurity atoms are to a certain extent clustered together so that the scattering deviates from Rayleigh's law. It is not certain how significant it is that at the surface there was a concentration of chromium atoms not in homogeneous solution in the crystal.

The exact concentration of chromium is not yet known as this can only be determined by analysis of the crystal, being less than the concentration of chromium in the powder from which the crystal is made. It is estimated to be of the order of $\frac{1}{2}$%, which is considerably more than the maximum divalent impurity which could have been present in the KCl crystal measured by de Haas and Biermasz. The relative increase in resistance is, however, small, in agreement with the small increase of thermal resistance found, by Eucken and Kuhn, to result from impurities of the correct valency.

It is not certain how the results of Estermann and Zimmerman (1951) on the conductivity of pure and impure germanium should be interpreted. There are no measurements in the neighbourhood of the conductivity maximum and also the two specimens had very different diameters.

6.2. *Displaced Atoms*

Experiments have been made to determine the effect of displaced atoms on the thermal conductivity of a quartz crystal (Berman, Klemens, Simon and Fry 1950, Berman 1951). One crystal was given three successive periods of neutron irradiation in the Harwell pile and a second crystal, which originally had the same conductivity, was later given a very small irradiation. As the conductivities of the two original crystals

Fig. 9

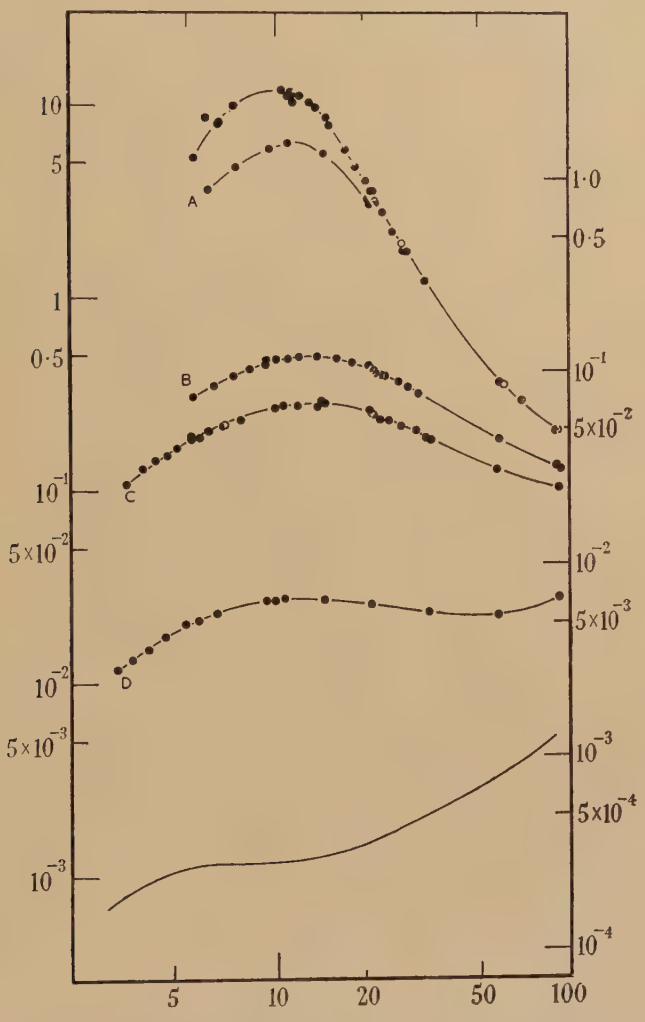

Thermal conductivity of quartz crystal ⊥ axis, irradiated quartz crystal and quartz glass. Approximate cumulative irradiation doses :—A : 0·03 units; B : 1 unit ; C : 2·4 units ; D : 19 units.
Thermal neutron dose for 1 unit : $1{\cdot}8\times10^{18}/\text{cm}^2$.

were the same we may consider the series as four successive irradiations of one crystal.

The conductivity–temperature curves after each irradiation are shown in fig. 9, but in order to interpret the results it is simpler to consider the extra thermal resistance induced. The thermal resistance of the original crystal has been subtracted from the resistance of the crystal subsequently, to give the resistance–temperature curves shown in fig. 10. It is justifiable to assume that the thermal resistance is additive in a simple

Fig. 10

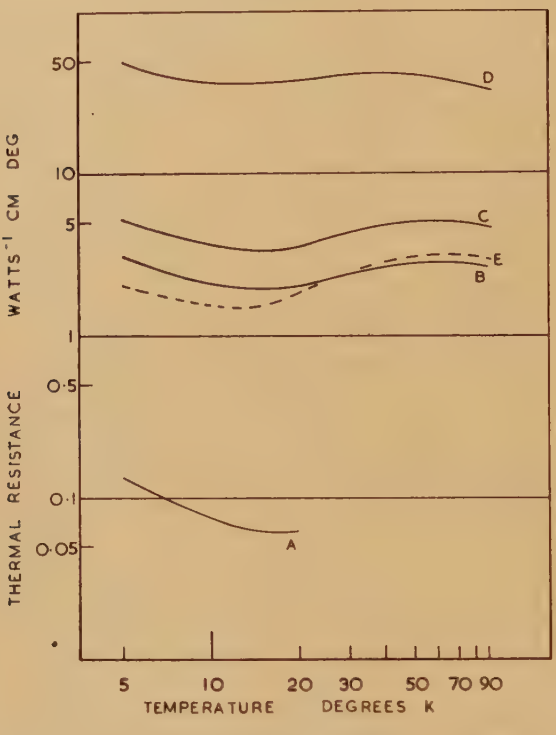

THERMAL RESISTANCE INDUCED IN QUARTZ CRYSTAL BY NEUTRON IRRADIATION

For irradiation doses see fig. 9.

way as the resistance of the crystal after the irradiation is always considerably greater than the original resistance. This assumption is also confirmed by the fact that all the extra resistance–temperature curves have a similar shape.

Above 15° K the resistance varies in the manner to be expected for small defects and by comparison with the calculations made for the alkali halides it is possible to estimate the defect concentration ; this agrees with the order of magnitude estimated from the irradiation doses. It is necessary, however, to assume that large defects are also present to explain the increasing resistance at lower temperatures. These could be

clusters of interstitial atoms and vacant sites, formed in accordance with the processes discussed by Seitz (1949). The scattering by clusters of defects would be less dependent on the phonon frequency than the scattering by single defects and if they were large enough would act in a similar way to boundary scattering but with a much smaller mean free path.

Some support for the conclusion that there are clusters of defects present is provided by the measurements of conductivity made after various periods of heating following the last irradiation. The crystal was heated for periods usually of about 6 hours, and the thermal resistance extra to that of the original crystal again determined. The simplest comparison between the resistance left after any of these heatings and the resistance induced by irradiation can be made for treatments which resulted in nearly the same resistance. After the crystal had been heated at 700° C the conductivity was restored to roughly the value it had after the second irradiation, as can be seen by comparing curves E and B of fig. 10. The shapes of the curves of extra resistance against temperature are, however, different ; the similarity of the two curves at the higher temperatures suggests that after this particular heating there were present about as many defects as were produced after the second irradiation, but the difference at the lower temperatures suggests that the scattering by the clusters is less for the defects left after heating. As the irradiation effects are cumulative the size of the clusters and the ratio of their number to the total number of defects remains the same for any period of irradiation. On heating, however, the size or density of the clusters must decrease so that when the total number of defects has been reduced to a given amount the relative effect of clusters is less.

An unirradiated crystal, which originally had the same conductivity as the crystals which were later irradiated, was given the same heating as the irradiated crystal in order to find whether heat treatment alone had any effect on the conductivity. De Haas and Biermasz (1935) carried out a similar experiment and found that the conductivity at liquid hydrogen temperatures was reduced by 10–15% after the crystal had been heated to 570° C and then allowed to cool slowly. In the present experiments no difference was found even after heating a crystal to 800° C. It is possible that this difference of behaviour can be explained by the difference between the rates of heating and cooling ; on the other hand, de Haas and Biermasz do not give any indication of the reproducibility of their results if a specimen is merely removed from the apparatus and then set up again. However, after this present crystal had been heated to 850° C its conductivity was considerably reduced and turned out to be almost the same as that produced in the other crystal by the first irradiation. A comparison of the extra resistances suggests that heating produces fewer clusters than irradiation.

The main purpose of the annealing experiments was to find whether the irradiation effects are reversible. They were not complete enough, as regards the influence of both time and temperature for a value of the

activation energy of the recovery process to be derived. It is evident, however, that measurements of the thermal conductivity could be used for this purpose, although the effort involved in making measurements at the low temperatures which are necessary for appreciable sensitivity would be considerable.

6.3. *Mosaic Structure*

There have been several suggestions that comparatively low values of thermal conductivity, at temperatures where boundary scattering might be expected to be the chief cause of resistance, can be attributed to scattering due to a mosaic structure (de Haas and Biermasz 1938 b, Garrett 1950, Klemens 1951). It has already been mentioned that de Haas and Biermasz' results for quartz do suggest that for a crystal of sufficiently large diameter the conductivity would be limited by mosaic scattering. It is to be noted, however, that Klemens has shown that for the KCl crystal measured by these workers the observed conductivity can be explained without assuming mosaic scattering.

Garrett found that the conductivity of potassium chrome alum between 0·16 and 0·29° K is proportional to T^3 but that the phonon mean free path calculated from the conductivity is only about 1/10 of the crystal diameter. Although Garrett suggests that this can be ascribed to a mosaic structure Pomeranchuk's treatment leads to scattering by mosaic structure which is frequency dependent, resulting in a conductivity proportional to the temperature. The boundaries within the crystal must therefore be more definite in order to give a scattering which is independent of frequency and a conductivity proportional to the cube of the temperature.

The measurements on artificial sapphire could also possibly be explained by the effect of a mosaic structure but, as has been mentioned, a crystal which was found to have a more marked mosaic character showed no difference in its thermal conductivity. This would seem to be the only set of measurements intended to test the effect of mosaic scattering directly. It cannot be considered conclusive as to the effect of a mosaic structure as this crystal was very short and the accuracy of the measurements was not as high as for other crystals. Any effect could not, however, be greater than 2–3%, so that if a mosaic structure accounts for the great reduction found in the maximum thermal conductivity of the crystals so far measured, it must be at its maximum effectiveness even in crystals of good quality. It is clearly desirable that further experiments should be made on this effect.

§ 7. Amorphous Solids

7.1. *Theoretical*

In his original paper Debye (1914) explained the great difference between the thermal conductivities of crystals and of amorphous solids in terms of the difference in the mean free paths of the lattice waves. In a crystal

the scattering arises from the density fluctuations associated with the thermal vibrations and these fluctuations decrease with the temperature, so that the mean free path increases with decreasing temperature. In an amorphous solid, however, the mean free path is restricted by the disordered structure to a length of the order of the interatomic distance and Debye assumed that it would be independent of temperature. Using eqn. (1) it is evident that the thermal conductivity should be proportional to the specific heat.

It was pointed out by Kittel (1949) that it could be deduced from several measurements which had been made below liquid air temperatures that the phonon mean free path in various glasses does increase with decreasing temperature at sufficiently low temperatures. He suggested that this would be expected to occur for temperatures such that the dominant phonons correspond to wavelengths greater than the size of the ' unit cell ' in the glass ; for such phonons the scattering by the disorder in structure decreases with increasing wavelength. For quartz glass, in which the unit cell may be taken to be 7 Å (the size of the oxygen tetrahedron surrounding each silicon atom) the temperature below which the mean free path should increase is about 200° K.

Klemens (1951) has developed a detailed theory of heat conduction in glass. As for a crystal, the thermal motion can be resolved into normal modes of vibration, but as the structure is irregular these normal modes are not plane waves. The instantaneous displacements can still be resolved into plane waves but there is now an interchange of energy between them leading to ' structure scattering '. Klemens assumes that short waves are attenuated by this process with a constant mean free path. In order to find the mean free path of long waves he considers their energy in two parts : the energy pertaining to the overall motion of a large region and the energy pertaining to relative motion of neighbouring atoms. The energy of overall motion is assumed to belong to a normal mode which is almost identical to the plane wave and this energy is retained by the wave. The energy of relative motion belongs to high frequency modes and is attenuated in the same way as high frequency plane waves. It is thus shown that the mean free path of long waves is inversely proportional to the square of the wave-number.

As in the treatment of crystals, it is necessary to consider the effect of processes in which momentum is conserved, represented by eqn. (2) and (3), and the mean free path for such processes is assumed to be the same as in crystals, as has been calculated by Pomeranchuk (1941) and by Landau and Rumer (1937).

Klemens obtains the thermal conductivity in terms of three empirical constants which can be found by comparison with the experimental results. At high temperatures the conductivity is mainly determined by the mean free path of transverse waves and is proportional to the specific heat, but at low temperatures the conductivity is determined by longitudinal waves and is proportional to the absolute temperature. The contributions of the

two types of waves is equal, for quartz glass, at about 25° K. The comparison between theory and experiment is shown in fig. 2; κ_I and κ_{II} denote the contributions of the longitudinal and transverse phonons respectively. It can be seen that the main features of the theoretical curve which are not dependent on the determination of the constants are in agreement with experiment and by choosing the constants suitably very close quantitative agreement is obtainable over the whole range of temperature.

7.2. *Experimental*

The measurements by Eucken (1911 a) on quartz glass and by Stephens (1932) on Pyrex glass showed that the conductivity varies roughly as the specific heat down to liquid air temperature. Measurements have been made at lower temperatures by Bijl (1949) Wilkinson and Wilks (1949) and Berman (1951) and there is an isolated measurement at 1·3° K by Keesom (1944).

Bijl measured four types of glass between 1·5 and 3·0° K, using a method similar to that which he used for potassium chrome alum. The temperature gradient along the rods was measured by measuring the temperature of two specimens of a paramagnetic salt which were enclosed in glass vessels attached to the glass rod. The geometrical factor for calculating the conductivity could not be determined to better than about 30% but, by making all the specimens of the same size, Bijl was able to compare the conductivity of the various types of glass. It was found that the conductivities of all four glasses were of the same order of magnitude and varied approximately as $T^{1\cdot3}$.

Wilkinson and Wilks measured the conductivity of Phoenix glass by determining the rate at which a rod conducted heat into a vessel of liquid helium. By varying the temperature of the 'warm' end of the rod, it was shown that the conductivity is nearly independent of the temperature between 10 and 20° K.

Quartz glass and Phoenix glass were measured between 2 and 90° K by Berman and a soft glass was measured between 2 and 5° K. The absolute values are in agreement with those of Wilkinson and Wilks for Phoenix glass and the variation with temperature at liquid helium temperatures is similar to that found by Bijl. Comparison with the absolute values found by Bijl cannot be made for any one glass, but the most similar in composition are the Thuringian glass measured by Keesom and Bijl and the G. E. C. Wembley X 8 glass measured by Berman. An extrapolation of Bijl's curve gives a value 30% higher than that found by Keesom at 1·3° K and at liquid helium temperatures his results are also about 30% higher than those of Berman. This difference is the same as the uncertainty in absolute values which Bijl states is due to the difficulty in determining the geometrical factor necessary in calculating the conductivity in his experiments.

Some work has been carried out on plastics: a temperature variation of conductivity similar to that of glass has been found for Perspex (Berman

1951), which was measured between 2 and 20° K. Also an attempt was made to find whether there is any difference in conductivity between stretched and unstretched Nylon threads, associated with the different degree of crystallinity. Up to now only some preliminary measurements have been made on a stretched sample below 20° K. The conductivity can be represented roughly by $\kappa = 2{\cdot}5 \times 10^{-5}\, T^{1{\cdot}2}$ watt units. Until further measurements are made it is not certain whether this temperature variation is related to the similar variation found in glasses below about 4° and which may also hold for Perspex below 2° K.

Fig. 11

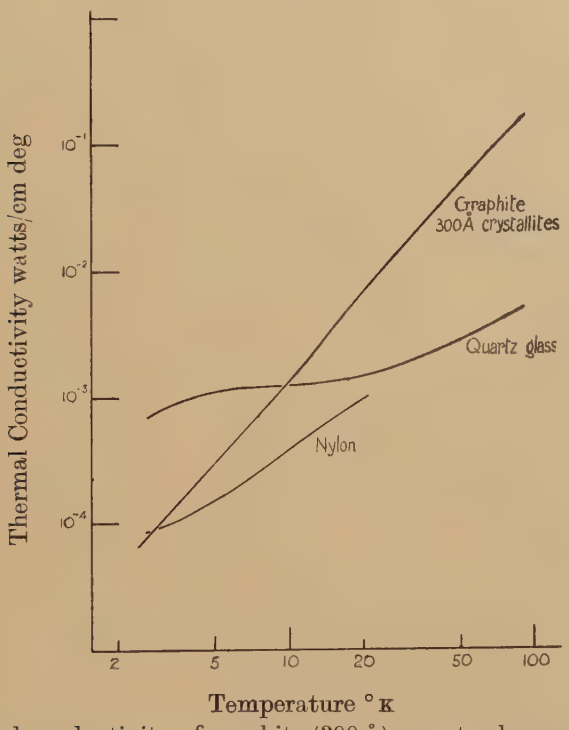

Thermal conductivity of graphite (300 Å), quartz glass and nylon.

It has been pointed out in § 5.2.2, that although glasses are poor heat conductors at normal temperatures, microcrystalline solids may have much lower conductivities at low temperatures. In fig. 11 are shown, for comparison, the conductivities of quartz glass, Nylon and of the graphite specimen with the smallest crystallite size which was measured.

§ 8. Summary

The main features of the conductivity-temperature relation for pure dielectric crystals can be explained in terms of Peierls' theory, supplemented by the calculation by Casimir of the influence of the crystal size at low temperatures. The Umklapp processes postulated by Peierls give

rise to a thermal resistance which decreases with decreasing temperature—at low enough temperatures the decrease follows an exponential law. The thermal resistance remains finite, however, and, in fact, increases again owing to scattering of the phonons at the boundaries of the crystal; this increasing resistance is no longer an intrinsic property of the crystalline material but depends on the diameter of the crystal measured.

The exponential rise in conductivity has recently been observed for several crystals and boundary scattering has been studied for a considerable time, but there are considerable difficulties in explaining the details of the temperature variation of conductivity actually found for single crystals. The greatest discrepancy between the theoretical values, based on the two sources of resistance mentioned, and the experiments is found in the neighbourhood of the conductivity maximum. Here the resistance of the ideal crystal would be very small, so that any extra source of resistance would be shown up most clearly.

Experiments on the dependence of the maximum conductivity on crystal diameter suggest that the discrepancy is due to defects in the crystals, since it is found that the discrepancies are smaller for crystals of smaller diameter: for sufficiently small crystals, such as exist in some polycrystalline solids, the resistances due to Umklapp processes and to boundary scattering are at all temperatures large enough to mask the effect of imperfections.

It was found that only about 3 displaced atoms per million (produced by neutron bombardment) in a quartz crystal halved the value of the maximum conductivity, so that it might be expected that crystals of high purity, having the same diameter, would accidentally have sufficiently different imperfections to show differences in their maxima. However, three natural quartz crystals were measured in the course of the experiments and there was no difference between the values of the maxima (the experimental accuracy was 1–2%). Also, no difference was found between two artificial sapphire crystals, one of which had a much more pronounced mosaic structure than the other. Only in the case of diamond is there some evidence that the maxima may be different for different crystals, and further measurements will be made on pure crystals near the maxima to look for small differences.

From the temperature dependence of the extra thermal resistance which is present near the maximum it is possible to deduce the grouping of imperfections which would give rise to it. Single defects, defects grouped together in either clusters or linear arrays (such that all dimensions are not small compared with the dominant lattice wavelengths) and a mosaic structure have been suggested to explain the results for various crystals. There is, however, only meagre experimental evidence as to the temperature variation of the resistance which each of these groupings of imperfections actually produces.

There are discrepancies between theory and experiment at lower temperatures which cannot be explained simply in terms of imperfections;

these are observed in the region where only boundary scattering would be expected to be important. The conductivity should be proportional to T^3 and should correspond to a phonon mean free path equal to the diameter of the crystal. These two characteristics of boundary scattering have not been found together for the conductivity of any crystal. The T^3 variation of conductivity has only been observed in measurements of potassium chrome alum below 0·3° K and a phonon mean free path equal to the theoretical value has been derived only from measurements on diamond at about 2° K. In both cases the temperatures correspond to about $\theta/1000$. At higher temperatures the conductivity is still found to be proportional to the crystal diameter, which suggests that only boundary scattering is important, but it is proportional to a smaller power of the temperature than 3 and the mean free path is less than the diameter.

Although the thermal conductivities of dielectric crystals do not reach the very high values calculated for the ideal case, the values can be of the order of magnitude associated with metallic conductors. It is commonly stated that metals are better conductors than dielectrics on account of the electronic conductivity. The conductivity of dielectrics is much more temperature dependent than that of metals and it happens that at room temperature the conductivities are generally well below the maximum and are, consequently, lower than the good metallic conductors. For diamond, however, room temperature is still a relatively low temperature and the thermal conductivity is higher than that of any metal yet measured. At the other extreme it has been shown that, as a result of boundary scattering, dielectric solids with sufficiently small crystallites can have conductivities much smaller than amorphous solids, such as glass.

It is hoped that some of the experiments which are planned, particularly those on the ' size effect ', will throw more light on the discrepancies still existing between theory and experiment ; they should suggest ways in which the theory needs further development.

Acknowledgment

I should like to thank Prof. F. E. Simon, F.R.S., Dr. J. Wilks and Dr. P. G. Klemens for many valuable suggestions and criticisms.

References

Ahearn, A. J., 1951, *Phys. Rev.*, **84,** 798.
Akhieser, A., and Pomeranchuk, I., 1944, *J. Phys. U.S.S.R.*, **8,** 216.
Berman, R., 1951, *Proc. Roy. Soc.* A, **208,** 90 ; 1952, *Proc. Phys. Soc.* A, **65,** 1029.
Berman, R., Simon, F. E., Klemens, P. G. and Fry, T. M., 1950, *Nature, Lond.*, **166,** 277.
Berman, R., Simon, F. E., and Wilks, J., 1951, *Nature, Lond.*, **168,** 277.
Bijl, D., 1949, *Physica*, **14,** 684.
Casimir, H. B. G., 1938, *Physica*, **5,** 595 ; 1940, *Magnetism and Very Low Temperatures* (Cambridge University Press).

Debye, P., 1914, *Vorträge über die Kinetische Theorie der Materie und der Elektrizität*, pp. 19–60 (Berlin: Teubner).
van Dijk, H., and Keesom, W. H., 1940, *Physica*, **7**, 970.
Duyckaerts, G., 1942, *Thesis*, Liége.
Eisenstein, J., 1952, *Rev. Mod. Phys.*, **24**, 74.
Estermann, I., and Zimmerman, J. E., 1951, *Technical Report* 6, O. N. R. Carnegie Institute of Technology.
Eucken, A., 1911 a, *Ann. Phys. Lpz.* (4), **34**, 185; 1911 b, *Phys. Z.*, **12**, 1005; 1911 c, *Verh. der Deutschen Phys. Gesellschaft*, **13**, 829.
Eucken, A., and Kuhn, G., 1928, *Z. Phys. Chem.*, **134**, 193.
Eucken, A. and Schröder, E., 1939, *Ann. Phys.*, **36**, 609.
Fröhlich, H., and Heitler, W., 1936, *Proc. Roy Soc.* A, **155**, 640.
Garrett, C. G. B., 1950, *Phil. Mag.*, **41**, 621.
Gerritsen, A. N., and van der Star, P., 1942, *Physica*, **9**, 503.
de Haas, W. J., and Biermasz, Th., 1935, *Physica*, **2**, 673; 1937, *Ibid.*, **4**, 752; 1938 a, *Ibid.*, **5**, 47; 1938 b, *Ibid.*, **5**, 621.
Hudson, R. P., 1949, *Thesis*, Oxford.
Keesom, P. H., 1944–5, *Physica*, **11**, 339.
Klemens, P. G., 1951, *Proc. Roy. Soc.* A, **208**, 108; 1952, *Phys. Rev.*, **86**, 1055.
Kittel, C., 1949, *Phys. Rev.*, **75**, 972.
Krishnan, K. S., and Roy, S. K., 1951, *Proc. Roy. Soc.* A. **207**, 447; 1952, *Ibid.*, **210**, 481.
Kurti, N., Rollin, B. V., and Simon, F., 1936, *Physica*, **3**, 266.
Landau, L., and Rumer, G., 1937, *Phys. Z. Sowjet*, **11**, 18.
Norton, F. H., and Kingery, W. D., 1952, *U.S.A.E.C.* NYO–601.
Peierls, R., 1929, *Ann. Phys. Lpz.*, **3**, 1055; 1935, *Ann. Inst. Poincaré*, **5**, 177.
Pomeranchuk, I., 1941 a, *J. Phys. U.S.S.R.*, **4**, 259; 1941 b, *Phys. Rev.*, **60**, 820; 1941 c, *J. Phys. U.S.S.R.*, **4**, 357; 1942, *Ibid.*, **6**, 237.
Powell, R. W., and Schofield, F. H., 1939, *Proc. Phys. Soc.*, **51**, 153.
Seitz, F., 1949, *Disc. Faraday Soc.*, (No. 5) 271.
v. Simson, Cl., 1951, *Naturwiss.*, **38**, 559.
Stephens, R. W. B., 1932, *Phil. Mag.*, **14**, 897.
van Vleck, J. H., 1941 a, *Phys. Rev.*, **69**, 730; 1941 b, *Ibid.*, **59**, 724.
Webb, F. J., Wilkinson, K. R., and Wilks, J., 1952, *Proc. Roy. Soc.* A, **214**, 546.
Wilkinson, K. R., and Wilks, J., 1944, *J. Sci. Instrum.*, **26**, 19; 1951, *Proc. Phys. Soc.* A, **64**, 89.

The Scientific Work of René Descartes

(1596—1650)

By

J. F. SCOTT, B.A., M.Sc., Ph.D.

With a foreword by H. W. TURNBULL, M.A., F.R.S.

This book puts the chief mathematical and physical discoveries of Descartes in an accessible form, and fills an outstanding gap upon the shelf devoted to the history of philosophy and science.

There is to be found in this volume the considerable contribution that Descartes made to the physical sciences, which involved much accurate work in geometrical optics and its bearing upon the practical problem of fashioning lenses, as also the deeper problems of light and sight and colour. The careful treatment that Dr. Scott has accorded to this work of Descartes is welcome, is well worth reading and will be an asset to all libraries. Publication is recommended and approved by the Publication Fund Committee of the University of London.

212 *pages*, 7″ × 10″, *amply illustrated.*

Price £1 - 0 - 0 net **Published July 1952**

Printed & Published by

TAYLOR & FRANCIS, LTD.

RED LION COURT, FLEET STREET, LONDON, E.C.4

FILED IN STACKS

Another Taylor & Francis Publication

Atomic Scientists' News

Journal of the Atomic Scientists' Association

President . . . . . Professor M. H. L. PRYCE, F.R.S.
Executive Vice-President . . . . . Professor KATHLEEN LONSDALE, F.R.S.

Vice-Presidents:
Sir WALLACE AKERS.
Professor The Rt. Hon. LORD CHERWELL, P.C., F.R.S.
Professor H. S. W. MASSEY, F.R.S.
Professor N. F. MOTT, F.R.S.
Professor R. E. PEIERLS, F.R.S.
Professor F. A. PANETH, F.R.S.
Professor H. W. B. SKINNER, F.R.S.
Professor P. M. S. BLACKETT, F.R.S.
Sir JOHN COCKCROFT, F.R.S.
Sir CHARLES DARWIN, F.R.S.
Professor P. B. MOON, F.R.S.
Professor M. L. E. OLIPHANT, F.R.S.
Professor F. E. SIMON, F.R.S.
Professor Sir GEOFFREY TAYLOR, F.R.S.
Professor Sir GEORGE THOMSON, F.R.S.
Professor C. F. POWELL, F.R.S.

General Sec.: Dr. J. L. MICHIELS.
Treasurer: Dr. L. E. J. ROBERTS.

- The Atomic Scientists' Association is an association of scientists whose work has given them special knowledge of the consequences for the world of the use and misuse of atomic energy. To make known the true facts about atomic energy and its implications, it publishes every two months the **Atomic Scientists' News.**

- Full membership of the Association is open to all scientists able to put before the public an informed opinion upon some aspect of atomic energy. Others interested in its work may become associate members. Enquiries c/o Professor J. Rotblat, Physics Department, St. Bartholomew's Hospital, London, E.C.1.

Vol. 2 NOVEMBER 1952 No. 2

CONTENTS

Price to non-members 6/– *(plus postage)* **Annual subscription £1 12s. 6d.** *(post free)*

Non-members apply to the Printers and Publishers:—

Messrs. TAYLOR & FRANCIS, LTD.
Red Lion Court, Fleet Street, London, E.C.4